This meeting is supported by the National Institute of Arthritis and Musculoskeletal and Skin Diseases (NIAMS) and the National Institute on Aging (NIA) of the National Institutes of Health under Award Number R13AR070644. The content is solely the responsibility of the authors and does not necessarily represent the official views of the National Institutes of Health.

GENERAL MEETING INFORMATION

Registration

Registration desks will be open for new registrants in the Colorado Convention Center in the Registration Hall, Lobby A Foyer on **Thursday, September 7 from 7:00 am – 6:00 pm.**

Speaker Ready Room

Speakers must check into the Speaker Ready Room in advance of their presentation. At that time, speakers may review their slides. The Speaker Ready Room is located in Room 206 in the Colorado Convention Center. The Speaker Ready Room will be open on **Thursday, September 7 from 7:00 am – 5:00 pm**

Organizing Committee

Mary L. Bouxsein, Ph.D.
Claus-C Glüer, Ph.D.
Marjolein C.H. van der Meulen, Ph.D.

Support

This activity is supported by educational funding donations provided by:

AMGEN
Lilly, USA, LLC
Scanco Medical

CONTINUING MEDICAL EDUCATION

JOINTLY ACCREDITED PROVIDER™
INTERPROFESSIONAL CONTINUING EDUCATION

This activity has been planned and implemented by Creighton University Health Sciences Continuing Education (HSCE) and The American Society for Bone and Mineral Research (ASBMR) for the advancement of patient care. Creighton University Health Sciences Continuing Education is accredited by the American Nurses Credentialing Center (ANCC), the Accreditation Council for Pharmacy Education (ACPE), and the Accreditation Council for Continuing Medical Education (ACCME) to provide continuing education for the healthcare team.

AMA PRA Statement

Creighton University Health Sciences Continuing Education designates this live activity for a maximum of 6.5 *AMA PRA Category 1 Credit(s)* ™. Physicians should claim only the credit commensurate with the extent of their participation in the activity

AAPA accepts AMA category 1 credit for the PRA from organizations accredited by ACCME.

Online Evaluation to Receive CME

The online evaluation to receive CME will be available beginning Friday, September 15. You will receive an email from ASBMR with instructions on how to claim credit.

Target Audience

This meeting will bring together national and international investigators currently working in the field of bone fragility as well as young and established investigators, industry scientists, NIH intramural scientists and program staff, clinicians, endocrinologists and basic and translational researchers.

Learning Objectives

Upon returning home from the meeting, participants should be able to:

1. Provide attendees with state of the art knowledge regarding current concepts in skeletal fragility
2. Discuss our understanding has progressed of both the mechanisms underlying skeletal fragility and the methods to assess bone strength and fracture risk in patients.
3. Discuss novel image anaylsis methods for clinical imaging data, including in vivo imaging of bone microarchitecture

ASBMR Expectations of Authors and Presenters

Through ASBMR meetings, the Society promotes excellence in bone and mineral research. Toward that end, ASBMR expects that all authors and presenters affiliated with the ASBMR Symposium on Current Concepts in Bone Fragility: From Cells to Surrogates will provide informative and fully accurate content that reflects the highest level of scientific rigor and integrity.

ASBMR depends upon the honesty of the authors and presenters and relies on their assertions that they have had sufficient full access to the data and are convinced of its reliability.

Furthermore, ASBMR expects that:

- Authors and presenters will disclose any conflicts of interest, real or perceived.
- Authors of an abstract describing a study funded by an organization with a proprietary or financial interest must affirm that they had full access to all the data in the study. By so doing, they accept complete responsibility for the integrity of the data and the accuracy of the data analysis.
- The content of abstracts, presentations, slides and reference materials must remain the ultimate responsibility of the author(s) or faculty.
- The planning, content and execution of abstracts, speaker presentations, slides, abstracts and reference materials should be free from corporate influence, bias or control.
- All authors and presenters (invited and abstracts-based oral and poster presenters) should give a balanced view of therapeutic options by providing several treatment options, whenever possible, and by always citing the best available evidence.

Disclosure Policy

The ASBMR is committed to ensuring the balance, independence, objectivity and scientific rigor of all its individually sponsored or industry-supported educational activities. Accordingly, the ASBMR adheres to the requirement set by ACCME that audiences at jointly-sponsored educational programs be informed of a presenter's (speaker, faculty, author, or planner) academic and professional affiliations, and the disclosure of the existence of any significant financial interest or other relationship a presenter or their spouse has with any proprietary entity over the past 12 months producing, marketing, re-selling or distributing health care goods or services, consumed by, or used on patients, with the exemption of non-profit or government organizations and non-health care related companies. When an unlabeled use of a commercial product, or an investigational use not yet approved for any purpose, is discussed during the presentation, it is required that presenters disclose that the product is not labeled for the use under discussion or that the product is still investigational. This policy allows the listener/attendee to be fully knowledgeable in evaluating the information being presented. The On-Site Program book will note those speakers who have disclosed relationships, including the nature of the relationship and the associated commercial entity.

Disclosure should include any affiliation that may bias one's presentation or which, if known, could give the perception of bias. This includes relevant financial affiliations of a spouse or partner. If an affiliation exists that could represent or be perceived to represent a conflict of interest, this must be reported in the abstract submission program by listing the name of the commercial entity and selecting the potential conflict(s) by clicking in the box next to the relationship type. Disclosures will be printed in the program materials. These situations may include, but are not limited to: (1) Grant/Research Support; (2) Consultant; (3) Speakers' Bureau; (4) Major Stock Shareholder; (5) Other Financial or Material Support.

Copyright

mechanical, or other means, or intended use, is prohibited without the express written permission of the American Society for Bone and Mineral Research.

Disclaimer

All authored abstracts, findings, conclusions, recommendations, or oral presentations are those of the author(s) and do not reflect the views of the ASBMR or imply any endorsement. No responsibility is assumed, and responsibility is hereby disclaimed, by the American Society for Bone and Mineral Research for any injury and/or damage to persons or property as a matter of products liability, negligence or otherwise, or from any use or operation of methods, products, instructions, or ideas presented in the materials herein (2017 Abstracts). Independent verification of diagnosis and drug dosages should be made. Discussions, views, and recommendations as to medical procedures, choice of drugs, and drug dosages are the responsibility of the authors.

Audio and Video Recording

ASBMR expects that attendees respect each presenter's willingness to provide free exchange of scientific information without the abridgement of his or her rights or privacy and without the unauthorized copying and use of the scientific data shared during his or her presentation. In addition, ASBMR expects that attendees will respect exhibitors' desires not to have their products or booths photographed or video-recorded.

The use of cameras, audio-recording devices, and video-recording equipment is strictly prohibited within all Scientific Sessions, the Exhibit Halls, and Poster Sessions without the express written permission of both the ASBMR and the presenter/exhibitor. Unauthorized use of the recording equipment may result in the confiscation of the equipment or the individual may be asked to leave the session or Exhibit Hall. These rules are strictly enforced.

Meeting Evaluation

An online evaluation form for the ASBMR Symposium on Current Concepts in Bone Fragility: From Cells to Surrogates will be available on the ASBMR Website at www.asbmr2017.org after the meeting and sent to you via email. Your participation in this evaluation is extremely important to us. Please take a moment to complete the evaluation of this meeting to aid in planning future meetings. Thank you in advance for your feedback.

Use of ASBMR Name and Logo

ASBMR reserves the right to approve the use of its name in all materials disseminated to the press, public and professionals. The ASBMR name, meeting name, and meeting logo may not be used without permission. Use of the ASBMR logo is prohibited without the express written permission of the ASBMR Executive Director. All ASBMR corporate supporters and exhibitors should share their media outreach plans with the ASBMR before release.

No abstract presented at the ASBMR Symposium may be released to the press before its official presentation date and time. Press releases must be embargoed until one hour after the presentation.

Future ASBMR Annual Meeting Dates

ASBMR 2018 Annual Meeting
Palais des Congrès de Montréal, Montreal, Quebec, Canada
September 28 – October 1, 2018

ASBMR 2019 Annual Meeting
Orlando Convention Center, Orlando, FL, USA
September 20-23, 2019

THURSDAY, SEPTEMBER 7, 2017

CONTINENTAL BREAKFAST

7:00 am – 8:00 am **Lobby B**

CURRENT CONCEPTS IN BONE FRAGILITY

8:00 am – 9:30 am **Room 205/207**

Co-Chairs:
Galatia Kazakia, Ph.D., University of California, San Francisco, USA
Claus Gluer, Ph.D., Christian Albrechts Universitaet zu Kiel, Germany

8:00 am **Hierarchical Material in Nature: How Bone is Tough**
Peter Fratzl, Ph.D., Max Planck Institute of Colloids and Interfaces, Germany
Disclosures: None

8:30 am **Interaction of Skeletal Traits Determines Long Bone Fragility**
Karl Jepsen, Ph.D., University of Michigan, USA
Disclosures: None

9:00 am **Beyond Whole Bone Strength**
Chris Hernandez, Ph.D., Cornell University, USA
Disclosures: None

BREAK AND POSTER VIEWING

9:30 am – 10:00 am **Lobby B**

MULTI-SCALE CHARACTERIZATION ON BONE STRENGTH

10:00 am – 11:40 am **Room 205/207**

Co-Chairs:
Matt Allen, Ph.D., Indiana University School of Medicine, US
Virginia Ferguson, Ph.D., University of Colorado, USA

10:00 am **Multiscale Characterization of Human Bone: The Osteocyte Network**
Bjorn Busse, Ph.D., University Medical Center Hamburg-Eppendorf, Germany
Disclosures: None

10:20 am **Beyond Bone Mineral: Contributions of Collagen and Noncallagenous Proteins to Bone Strength**
Lamya Karim, Ph.D., University of Massachusetts Dartmouth, USA
Disclosures: None

10:40 am **Contribution of Cortical vs Trabecular Bone to Whole Bone Strength**
Bert van Rietbergen, Ph.D., Eindhoven University of Technology, The Netherlands
Disclosures: None

11:00 am **Mechanical Loading, Structural Heterogeneity and Bone Strength**
Elise Morgan, Ph.D., Boston University, USA
Disclosures: None

11:20 am **Effect of Osteoporosis Therapies on Bone Mechanical Properties: Preclinical Studies**
Paul Kostenuik, Ph.D., Phylon Pharma Services, USA
Disclosures: None

LUNCH AND POSTER VIEWING

11:40 am – 1:00 pm **Lobby B**

BEYOND AREAL BMD

1:00 pm – 2:20 pm **Room 205/207**

Co-Chairs:
Fj6la Johannesdottir, Ph.D., Harvard Medical School; Beth Israel Deaconess Medical Center, USA
Sharmila Majumdar , Ph.D., University of California, San Francisco, USA

1:00 pm **Extending Beyond BMD**
Bill Leslie, M.D., MSc, FRCs, University of Manitoba, Canada
Disclosures: None

1:20 pm **Contribution of Bone Microarchitecture to Fracture Risk**
Steven Boyd, Ph.D., University of Calgary, Canada
Disclosures: None

1:40 pm **Bone Structure: Beyond Standard Metrics**
Andrew Burghardt, Ph.D., University of California, San Francisco, USA
Disclosures: Research Grant, Ultragenyx Pharmaceuticals

2:00 pm **Identifying Patients with Fragile Bone via QCT-based FEA**
Tony Keaveny, Ph.D., University of California, Berkeley, USA
Disclosures: None

BREAK

2:20 pm – 2:50 pm **Lobby B**

CLINICAL CONUNDRUMS

2:50 pm – 3:50 pm **Room 205/207**

Co-Chairs:
Marjolein van der Meulen, Ph.D., Cornell University, USA
Joy N. Tsai, M.D., Masschusettes General Hosptial, USA

2:50 pm **Atypical Femoral Fractures: Clinical Risk Factors**
Angela Cheung, M.D., Ph.D., University of Health Network University of Toronto, Canada
Disclosures: None

3:10 pm **Atypical Femoral Fractures: Tissue Level Contribution?**
Eve Donnelly, Ph.D., Cornell University, USA
Disclosures: None

3:30 pm **Skeletal Fragility in T2D**
Robert Fajardo, UT Health Science Center, San Antonio, USA
Disclosures: None

BREAK

3:50 pm – 4:00 pm **Lobby B**

IS NOW THE TIME FOR SURROGATE ENDPOINTS IN OSTEOPOROSIS?

4:00 pm – 5:00 pm **Room 205/207**

Co-Chairs:
Gayle Lester, Ph.D., National Institutes of Arthritis, Musculoskeletal & Skin Disease, USA
Mary Bouxsein, Ph.D., Beth Israel Deaconess Medical Center, Harvard Medical School, USA

4:00 pm **Introduction**
Gayle Lester, Ph.D., National Institutes of Arthritis, Musculoskeletal and Skin Disease, USA
Disclosures: None

4:15 pm **The FNIH Bone Quality Study**
Dennis Black, Ph.D., UC San Francisco, USA
Disclosures: None

4:30 pm **Clinical Perspective: What Do We Need?**
Sundeep Khosla, M.D., Mayo Clinic College of Medicine, USA
Disclosures: None

4:45 pm **Panel Discussion**
Dennis Black, Ph.D., UC San Francisco, USA
Disclosures: Consulting, Merck

Theresa Kehoe, M.D., CDER, FDA, USA
Disclosures: None

Sundeep Khosla, M.D., Mayo Clinic College of Medicine, USA
Disclosures: None

CLOSING REMARKS

5:00 pm- 5:15 pm **Room 205/207**

RECEPTION AND POSTER VIEWING

5:15 pm- 6:15 pm **Lobby B**

POSTER
S

All posters presented at the ASBMR Symposium on Current concepts in Bone Fragility From Cells to Surrogates will also be presented at the ASBMR 2017 Annual Meeting, September 8-11, 2017, in the Colorado Convention Center.

**Denotes Presenting Author*

P01
Relating Cortical Bone Mechanics to Intracortical Pore Morphology, Distribution and Remodeling History within the Fibula Diaphysis. Lydia Bakalova*[1], Christina Andreasen[2], Jesper Thomsen[3], Annemarie Bruel[3], Ellen Hauge[3], Birgitte Kiil[3], Jean-Marie Delaisse[3], Thomas Andersen[2], Mariana Kersh[1]. [1]University of Illinois at Urbana-Champaign, United States, [2]University of Southern Denmark, Denmark, [3]Aarhus University, Denmark

During aging and osteoporosis, the cortical bone becomes more porous, making it more fragile and susceptible to fractures. The aim of this study was to investigate the intracortical compression-induced strain energy distribution, and determine whether the intracortical pores associated with high strain energy density (SED) in the surrounding bone have a different morphology, distribution and remodeling history than pores with low SED. The study was conducted on fibula diaphysis specimens from 20 patients undergoing a jaw reconstruction (age range 43-75 years, 14 men and 6 women). Specimens were plastic embedded, mCT-scanned and sectioned for histology. Pore size, circularity, and location with respect to the bone edges was quantified. Three-dimensional micro-finite element models of each specimen were tested in compression using a linearly elastic analysis, and the SED of the bone immediately surrounding the pores was calculated within a plane of interest corresponding to the histological sections. The statistical distribution of the SED of all pores, per sample, was used to identify high SED pores (SED > 1.5 times the interquartile range from the 75th percentile) and the remaining low SED pores. Pores with high SED were larger (p 0.0001), less circular (p 0.0001), and were located closer to the endosteal edge of the cortex (p 0.0001) than low SED pores (Figure 1A-C). A detailed histological analysis of the remodeling events generating the pores revealed that the high SED pores compared to low SED pores had 13.3-fold higher odds of being a resorptive (70%) or formative (11%) pore rather than a completely remodeled pore (p 0.0001). Compared to the low SED pores, the resorption space associated with the high SED pores had 5.9-fold higher odds of overlapping with the pore of a preexisting osteon (type 2 pore - 91%) than having no overlap (type 1 pore – 9%) (p 0.0001). Collectively, these data show that the high SED pores are enlarged irregular pores positioned closer to the endosteal surface of the cortex. These pores tend to be resorptive and overlap with the pore of a preexisting parent osteon, suggesting that these pores may originate from resorption within preexisting pores rather than from penetrative resorp- tions generating new pores. Overall, the study demonstrates a strong relationship al bone mechanics and pore morphology, distribution and remodeling history in the human fibula.

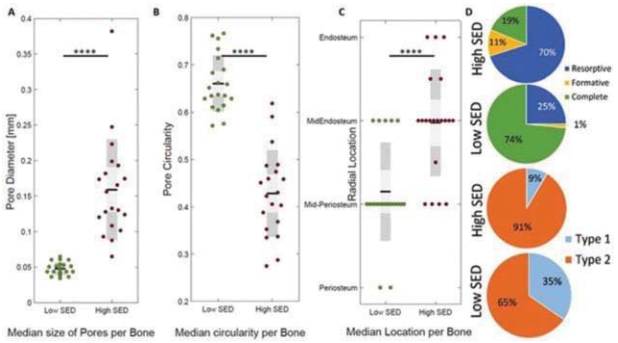

P02
Exploring the Associations between Bone Composition and Clinical Measures of Fragility Fracture Risk: a Pilot Transcutaneous *in vivo* Raman Study. Hao Ding*, Andrea Baker, Ping Wang, Philip Orlander, William Ip, James Kellam, Catherine Ambrose, Nahid Rianon, Xiaohong Bi. University of Texas Health Science Center, United States

The fracture resistance of bone is determined by its quantity and quality. Bone tissue composition, as a key component of bone quality, has been investigated extensively in vitro. However, the relation between composition and the fracture risk is still unclear. The goal of the current study is to investigate the association between compositional bone quality indicators and fragility fracture risk in an aging population. We conducted a cross-sectional clinical study examining the relationship among bone composition using Raman spectroscopy (noninvasively determined) and clinical risk factors assessed by the Fracture Risk Assessment Tool (FRAX) and bone mineral density (BMD) in patients with or without fragility fracture. A total of 17 patients were recruited to our pilot study including 9 with acute fracture (fragility fracture within the past 3 months) and 8 age-matched controls (no history of fracture). Raman spectra were collected transcutaneously from the mid-shaft of anterior tibia for each patient using a custom-designed in vivo Raman spectroscope.

Raman signatures of bone were differentiated from that of the soft tissue using independent component analysis. Composition variables that were previously reported indicative of bone quality, including mineral-to-collagen ratio, carbonate content, and mineral crystallinity were calculated. All variables were compared between fractured and non- fractured groups using standard t- test. Spearman's correlation test was employed to determine the relationship between composition and clinical measures.

The fracture group demonstrated decreased mineral-to-collagen ratio and mineral crystallinity. No significant difference was observed between groups in carbonate con- tent, BMD of spine or femoral neck, or T-score of spine. The mean T-score of femoral neck was -2.48 and -1.6 for fracture and non-fractured groups respectively with p=0.053. The FRAX score for hip fracture and major osteoporosis-related fracture didn't show significant difference when the acute fracture was excluded, but was significantly higher after factoring in the fracture. There was no significant correlation between tissue composition and any of the clinical indices examined, indicating that tissue composition could be an independent risk factor for fragility fracture. The results from this study suggest the necessity of including compositional bone quality indicators for fracture risk prediction.

P03

Alendronate Treatment Does Not Influence Resistance to Damage Accumulation in Femoral Cortical Bone in Hound Dogs.

Daniel Brooks*[1], Dimitrios Psaltos[1], Katherine Lo[1], Robert Urban[2], Sephanie McCarthy[2], Deborah Hall[2], Thomas Turner[2], Mary Bouxsein[1]. [1]Beth Israel Deaconess Medical Center, United States, [2]Rush University Medical Center, United States

Although the mechanisms underlying atypical femoral fractures (AFF) are unknown, clinicians and patients are concerned about long-term use of bisphosphonates (BP) and their possible association with AFF. There is a common hypothesis that BPs reduce the ability of cortical bone to resist damage accumulation and subsequently increase the risk of AFF. To test this hypothesis, we determined the effect of 12 or 18 months alendronate (ALN) treatment on bone microarchitecture and mechanical prop- erties of femoral cortical bone in large dogs. Skeletally-mature male hound dogs (29.7 3.3 kg, range: 24 to 36 kg) were assigned (n=10 /gr) to: 1) Control, 12 mo; 2) Control, 18 mo, 3) ALN, 12 mo, or 4) ALN, 18 mo. Dogs received daily ALN-filled gelatin capsules at a clinically relevant dose (0.2mg/kg/day) or identical capsules filled with lactose. At study end, cortical beams (2 x 2 x 30 mm) were cut from the cranial, medial and lateral aspect of the femoral diaphysis of each dog and assessed using: 1) monotonic 4-pt bending, 2) cyclic damage accumulation testing, and 3) reference point indentation (RPI, 10 N for 20 cycles, Biodent, ActiveLife Scientific). For the damage accumulation testing, we cyclically loaded the beams in 4-pt bending with incrementally greater displacements (from 75% to 200% yield displacement in 25% increments) to induce tissue damage. Following each damage cycle, we computed the secant stiffness and calculated the percent stiffness degradation relative to baseline stiffness (Tommasini et al 2005). We used two-way ANOVA and unpaired t-tests to test for effects of ALN treatment. Results: Treatment duration did not influence the outcomes, thus results are presented for both time points combined (Table 1).ALN treatment did not alter any 4-pt bending properties (apparent bending modulus, strength, post-yield displacement, or toughness). ALN treatment also did not significantly influence the ability of cortical bone to resist stiffness degradation during cyclic damage accumulation testing. There were also no differences in the tissue level mechanical properties that were measured with RPI. In conclusion, we found that treatment of adult male hound dogs with clinically relevant doses of ALN did not influence the tissue level mechanical properties of femoral cortical bone nor alter the ability of cortical bone to resist damage accumulation.

Table 1. Effect of ALN treatment on femoral cortical bone tissue-level mechanical properties in hound dogs (mean ± SD)

	ALN (n = 19)	CON (n = 20)	p-value
Monotonic 4-pt Bending (Cortical beam from medial aspect)			
Bending Modulus (GPa)	17.66 ± 1.59	17.71 ± 1.45	0.930
Flexural Strength (MPa)	132.8 ± 10.7	129.6 ± 10.9	0.369
Post-yield Displacement (mm)	2.572 ± 0.787	2.659 ± 0.597	0.702
Toughness to maximum force (mJ/mm^3)	0.788 ± 0.359	0.762 ± 0.338	0.822
Toughness to yield (mJ/mm^3)	0.097 ± 0.027	0.093 ± 0.022	0.558
Toughness to fracture (mJ/mm^3)	1.100 ± 0.359	1.056 ± 0.279	0.672
Post-yield toughness to fracture (mJ/mm^3)	1.003 ± 0.363	0.963 ± 0.278	0.706
Reference Point Indentation (Cortical beam from cranial aspect)			
Total Indentation Distance (μm)	86.58 ± 3.79	89.15 ± 5.68	0.101
Indentation Distance Increase (μm)	12.18 ± 1.17	12.90 ± 1.24	0.066
Average Creep Indentation Distance (μm)	1.51 ± 0.09	1.57 ± 0.11	0.092
Average Energy Dissipated (μJ)	35.3 ± 2.16	36.61 ± 3.1	0.128
Average Unloading Slope (N/μm)	0.54 ± 0.05	0.55 ± 0.05	0.417
Average Loading Slope (N/μm)	0.42 ± 0.03	0.42 ± 0.03	0.712
Damage Accumulation Testing (Cortical beam from lateral aspect)			
Stiffness degradation (%) after 100% Yield loading	12.4 ± 4.4	11.9 ± 4.5	0.737
Stiffness degradation (%) after 150% Yield loading	46.3 ± 11.4	40.3 ± 13.1	0.146
Stiffness degradation (%) after 200% Yield loading	79.1 ± 9.2	77.3 ± 16.7	0.688

P04

Parathyroid Hormone (PTH) increased rod-shaped trabeculae and maintained modulus of cancellous bone before fatigue failure.

Julia T. Chen*[1], Remy Walk[1], Shefford Baker[1], G. Elizabeth Pluhar[2], Adele Boskey[3], Christopher Hernandez[1], Marjolein van der Meulen[1]. [1]Cornell University, United States, [2]University of Minnesota, United States, [3]Hospital for Special Surgery, United States

Clinically parathyroid hormone (PTH), the only-FDA approved anabolic osteo- porosis treatment, decreases fracture risk by 10% [Neer et al. 2001]. In animal models, PTH increases cancellous bone volume [Jike et al. 1999], but its effect on bone tissue composition and mechanics is unknown, particularly under cyclic loading experienced during normal function. We hypothesized that PTH would increase compressive strength and preserve mechanical properties during cyclic fatigue loading through architectural and compositional changes. To produce osteopenia, 13 mature ewes underwent ovariectomy and were fed a meta- bolic acidosis diet for one year. In the second year, sheep were injected with PTH (PTH, n=7, 5mg/kg/day SQ) or saline (VEH, n=6). In each animal two cancellous samples were taken from the distal femur: one for monotonic loading and one for cyclic fatigue loading. Samples were

submitted to microCT scanning to evaluate microarchitecture. The number and volume fraction of rod- and plate-like trabeculae were determined using individual trabecular segmentation [Liu et al. 2008]. Then specimens were failed in compression to determine cancellous bone strength. Cyclic loading (max. normalized stress=0.004) was applied to failure (2.5% apparent strain). Energy dissipation and modulus reduction were evaluated during cyclic loading, and fatigue life was determined (Nf, number of cycles of failure). Cancellous tissue mechanics and composition were analyzed by nanoindentation and Raman spectroscopy.

Compressive strength and fatigue life were not different between PTH and VEH. However, PTH-treated samples experienced less energy dissipation and reduction in modulus before fatigue failure than VEH (Fig 1). PTH increased the number and volume fraction of rod-type trabeculae and decreased the volume fraction of plate-like trabecu- lae. The increased fraction of rods explained 50% of the variation in cyclic energy dissipation. In addition, mineralization decreased, while nanoindentation modulus and mineral crystallinity increased with PTH. Considering both alterations in architecture and composition, the increased fraction of rods and decreased mineralization explained 74% of the variation in energy dissipation. Not all osteoporosis-related fractures are caused by a single overload. Our finding show that PTH alters microarchitecture and material rove maintenance of mechanical properties following cyclic loading.

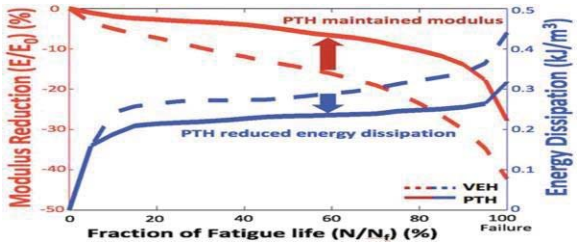

P05

Micrograv ity exposure diminishes trabecular microarchitecture and cortical bone morphology in skeletally mature mice.

Jennifer C. Coulombe*[1], Alicia M. Ortega[1], Eric W. Livingston[2], Ted A. Bateman[2], Louis S. Stodieck[1], Samuel M. Cadena[3], Virginia L. Ferguson[1]. [1]University of Colorado, United States, [2]University of North Carolina at Chapel Hill, United States, [3]Novartis Institutes for Biomedical Research, Inc., United States

Microgravity causes bone loss in humans at rates that are greater than in postmeno- pausal osteoporosis. Spaceflight studies utilizing rodents have historically been of lim- ited duration (~2 weeks), and many of these experiments utilized young mice where the influence of bone formation and resorption were not readily separated. Here we evaluate bone changes in skeletally mature mice flown for 21 days on the International Space Station (ISS) on Rodent Research-1, SpaceX-4. Tibiae were collected from a separate study of skeletal muscle in wild type (WT) and muscle RING-finger protein-1 (MuRF1) knockout (KO) mice, a gene associated with skeletal muscle degradation. Thirty-two week-old female C57BL/6, WT and MuRF1 KO mice (n=10/group), were equally distributed into ground control (GC) and space- flight (SF) groups. SF mice were housed on the ISS for 21 days, at which point they were euthanized and hindlimbs were removed. GC mice were maintained under matched conditions. Microcomputed tomography (microCT; 10mm; Scanco mCT80) was used to evaluate trabecular microarchitecture and cortical bone morphology within the prox- imal tibia. Two-way ANOVA indicated no effect of MuRF1 deficiency on any microCT out- come measures (a=0.05), thus WT and MuRF1 KO groups were pooled to subsequently compare GC vs. SF. Microgravity significantly reduced trabecular (Tb.) bone volume fraction Tb.BV/TV (-42.3%, $p<0.01$), thickness Tb.Th. (-24.0%, $p<0.0001$), and volu- metric bone mineral density Tb.vBMD (-43.2%, $p<0.01$); however, no differences were observed in trabecular number and separation, connectivity density, or structure model index. In cortical (Ct.) bone, SF significantly reduced Ct.BV/TV (-5.4%, $p<0.0001$), thickness Ct.Th. (-15. 9%, $p<0.01$), and polar moment of inertia (-13.7%, $p<0.05$). Correspondingly, porosity Ct.Po (+27.2%, $p<0.0001$) increased significantly in SF. Overall, 21 days of microgravity exposure resulted in significantly decreased trabe- cular microarchitecture and cortical bone morphology in skeletally mature mice. As bone formation rates are low in skeletally mature bone, resorption is implicated as the dominant mechanism underlying these microgravity-induced changes. This phenom- enon is similar to that which is observed in astronauts, where bone resorption outpaces formation. These results motivate the need for further study of bone changes following long-duration spaceflight and sup y bone loss and potential countermeasures in microgravity.

	GC-WT	GC-KO	SF-WT	SF-KO	P-value
Tb.BV/TV	0.042 ± 0.008	0.045 ± 0.016	0.023 ± 0.008	0.027 ± 0.009	<0.01
Tb.Th (mm)	0.051 ± 0.003	0.053 ± 0.002	0.043 ± 0.008	0.036 ± 0.002	<0.0001
Tb.vBMD (mg HA/cm^3)	66.7 ± 17.4	74.2 ± 24.9	36.1 ± 13.8	43.9 ± 14.3	<0.01
Ct.BV/TV	0.83 ± 0.02	0.84 ± 0.02	0.79 ± 0.01	0.79 ± 0.02	<0.0001
Ct.Th (mm)	0.14 ± 0.01	0.13 ± 0.01	0.12 ± 0.04	0.11 ± 0.02	<0.01
Ct.Po (%)	16.6 ± 1.8	16.4 ± 1.6	20.6 ± 1.5	21.3 ± 2.1	<0.0001
pMOI (mm^4)	1.05 ± 0.14	1.06 ± 0.13	0.89 ± 0.03	0.93 ± 0.16	<0.05

Table 1: Bone microarchitecture is diminished with flight but not MuRF1 deficiency. P-values from 2-way ANOVA comparing Ground (GC) and Spaceflight (SF).

P06

The Decrease in Fracture Resistance with Aging in BALB/c Mice Involves Alterations to the Bone Matrix. Amy Creecy*[1], Sasidhar Uppuganti[2], Mathilde Granke[3], Madeline Girard[4], Siegfried Schlunk[4], Paul Voziyan[5], Jeffry Nyman[6]. [1]Vanderbilt University, VA Tennessee Valley Healthcare System, United States, [2]Vanderbilt University Medical Center, VA Tennessee Healthcare System, United States, [3]Vanderbilt University Medical Center, VA Tennessee Valley Healthcare System, United States, [4]Vanderbilt University, United States, [5]Vanderbilt University Medical Center, United States, [6]Vanderbilt University, VA Tennessee Valley Vanderbilt University Medical Center, United States

The age-related increase in fracture risk is disproportionate to the loss in areal bone mineral density. Thus, a decrease in bone quality with aging is thought to contribute to increased fracture risk among the elderly. To elucidate mechanisms by which deleterious changes in the bone matrix lowers fracture resistance, there is a need for a validated preclinical model that mimics the aging effects on human bone. After euthanizing BALB/c mice from a NIA colony, we analyzed bones from 6-mo adult males (n=20) and females (n=20) and 20-mo agedmales (n=18) and females (n=18). Following mCT evaluations of the mid-shaft to determine structural properties and tissue mineral density (Ct.TMD), each hydrated femur was broken in 3pt bending (3 mm/min) to assess fracture resistance. Bound water was measured with non-destructive 1H-NMR followed by crosslink measurements with HPLC on hydrolysates. Protein extracts from the left tibiae were analyzed by mass spectrometry. As expected, moment of inertia was higher at 20-mo than at 6-mo (male: p=0.002 and female: p<0.0001). Unexpectedly, cortical thickness decreased with age inmales (p<0.0001), while it increased with females (p<0.0001). Tissuemineral density was higher for oldermice, irrespective of sex (p<0.0001 for each). Independent of geometry, bending strength was lower with advanced aging for both males (p=0.0008) and females (p=0.003)(Fig. 1). Moreover, toughness was significantly less for the aged cortical bone (p<0.0001 for both sexes). Within the matrix, hydroxylysl-pyridinoline concentration (PYD) was higher for 20-mo than for 6-mo cortical bone (p<0.0001), and the pentosidine concentration (an AGE crosslink) was also higher with aging (p=0.0003). As for other post-translation modifications, significant age-related differences were found in the collagen a1 chain and in matrix-bound osteopontin. These included higher carboxy-methyl-modifications (CML) at specific lysine residues (p=0.015 and p=0.03, respectively) in old than in young bone. Bound water within the bone matrix was lower in older mice (p<0.0001). The increases in CML, PYD, and pentosidine with aging, along with the decrease in bound water, suggest that lower fracture resistance with aging in mice could be the result of changes to the organic matrix of bone, though an age-related increase in mineralization may also contribute. With similarities to human aging, the BALB/c mouse is suitable for studies into the agerelated decrease in bone quality.

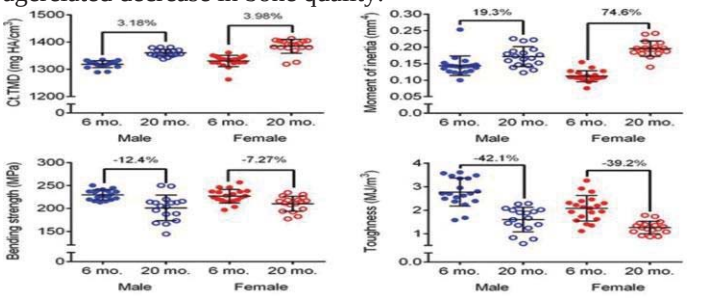

Figure 1: TMD and I_{min} are shown to be higher in aged mice for males (blue) and females (red), while bending strength and toughness are shown to be lower. Brackets indicate statistical differences between age groups. Numbers above brackets indicate the percent change from 6 mo. aged mice

P07

Influence of Microcracks and Compositional Heterogeneity on Fracture Resistance of Cortical Bone. Ahmet Demirtas*, Ani Ural. Villanova University, United States

Several recent studies demonstrated an association between atypical femoral fracture and long-term bisphosphonate (BP) use for osteoporosis treatment. Due to BP treatment, bone undergoes mechanical alterations including reduced tissue composition heterogeneity and increased microcrack density. The aim of this study is to investigate the effects of microcracks and tissue composition heterogeneity on the crack propagation behavior in human cortical bone by using finite element (FE) analysis. A transverse microscopy image of cortical bone from the mid-diaphysis of a 58-yearoldmale donor tibia was converted to a 3DFE model (Fig 1a, 1b). The fracture behavior of the model was investigated by modeling compact tension specimen tests (Fig. 1c) incorporating cohesive extended finite element method in the osteons and interstitial bone and by cohesive interface elements at the cement lines. Twelve simulations were performed on the model including homogeneous (HM) and heterogeneous (HT) material compositions, and four differentmicrocrack distributions which were composed of 5 and 10 randomly distributed microcracks per unit area and 10 clustered microcracks per unit area. Fracture resistance was assessed by comparing the crack volume between the models. The simulation results (Fig. 1d) showed that the crack volume was the highest in the model with no microcrack for both HM and HT material properties. Increasing the microcrack density resulted in lower crack volume in all models. The microcracks reduced the crack volume more in HM models compared to the HT ones (Fig. 1d-f). Comparison of the two different random distribution of microcracks demonstrated the influence of the location and size of microcracks on the crack growth behavior in cortical bone (Fig. 1d). In addition, clustered microcracks were not as effective in contributing to the fracture resistance as distributed microcracks (Fig. 1d, 1g, 1h). In summary, the results showed that the microcracks enhance the fracture resistance of bone, however, their distribution and location significantly affect the fracture behavior. Microcracks influence the fracture resistance

less when the tissue composition is more heterogeneous. These results provide new information on the interaction of microcracks, tissue heterogeneity and fracture resistance and may improve the understanding of the influence of mechanical changes due to prolonged bisphosphonate use on the fracture behavior of cortical bone.

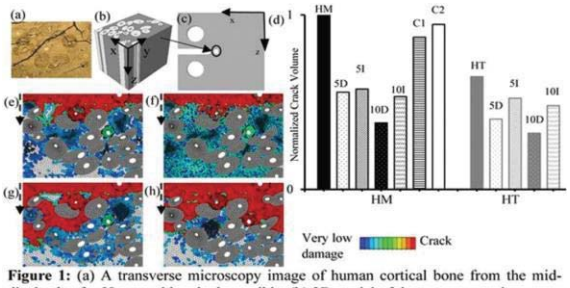

Figure 1: (a) A transverse microscopy image of human cortical bone from the mid-diaphysis of a 58-year-old male donor tibia. (b) 3D model of the transverse microscopy image in (a). (c)Finite element model of the CT specimen. The marked region shows the location where the microstructure cell was inserted. (d)Normalized crack volume of the models where the values are grouped by material composition as homogeneous (HM) with black color and heterogeneous (HT) with gray color. "5" and "10" shows the microcrack density. "D" and "I" represent the two different random distributions of microcracks. C1 and C2 represent the clustered MC models that are located around the edge and the center of the model, respectively. Representative planar crack growth views of (e) 10HMI, (f) 10HTI, (g) HM-C1 and (h) HM-C2.

P08

Fracture toughness and geometry-independent microscale material properties are improved with exercise for male but not female rats in diet-induced obesity. Chelsea Heveran*[1], Rebecca Foright[2], Ginger Johnson[2], Virginia Ferguson[1], Paul MacLean[2], Vanessa Sherk[2]. [1]Department of Mechanical Engineering, University of Colorado, United States, [2]Department of Medicine, Division of Endocrinology, Metabolism & Diabetes, University of Colorado Anschutz Medical Campus, United States

Obesity increases bone fracture risk, yet combined effects of obesity, exercise, and sex differences on fracture toughness (Kc) are not understood. This study assessed whether diet-induced obesity (DIO) impairs Kc and microscale bone quality, and whether exercise can mitigate negative effects of DIO. The study also tested whether DIO and/or exercise are sex-specific. Female and male Wistar rats (N = 31) were fed an ad libitum high fat diet (HFD) for 10 weeks, starting at 5 weeks of age. Within sex, obese and lean groups were defined as the highest and lowest tertiles of weight and fat gain. Obese and lean rats were randomized to exercise (EX) or sedentary (SED) controls for the last 4 weeks of HFD (n = 4/ group; except female obese EX: n = 3). EX was treadmill running at 15 m/min, 60 min/ day, 5 days/week. Kc was evaluated in notched femurs. Post-fracture, femurs were dehydrated, embedded, and polished to a 0.1 mm finish. Nanoindentation was performed with 25 indents each for lamellar and woven bone in the medial quadrant. Nanoindentation modulus (E) and plastic work (W, hysteresis of unloading curve) were averaged per lamellar/woven region. Three-way ANOVA evaluated how Kc, E, and W depended on sex, obesity status, and exercise status. Bone radii and thickness were 36.0% ($p < 0.01$) and 28.5% ($p < 0.01$) larger, respectively, in males than females but did not differ with exercise or obesity. Male lean EX rats had 21% tougher (i.e., higher Kc) bone than male lean SED ($p = 0.05$). Male obese EX rats had 22% tougher bone than male obese SED ($p = 0.04$). Female rats had less tough bone than males (-12.6%, $p = 0.05$), and did not improve Kc with exercise. Diminished Kc in SED males corresponded to decreased microscale bone material quality, but the location of lower quality bone depended on obesity status. Obese SED rats may have lower E in woven bone compared with obese EX (-9.1%, $p = 0.07$). Lean SED rats may have lowerWin lamellar bone compared with lean EX (-13.0%, $p = 0.06$). For all lean EX rats, increased heterogeneity (i.e., variance) of E in lamellar bone correlated with greater Kc ($r2 = 0.57$). Meanwhile, variance in E did not change Kc in obese or SED rats. In summary, Kc was preserved with EX for both lean and obese male rats fed HFD, but not for females. Lower Kc in male SED rats corresponded with decreased microscale bone quality. These findings may help explain the effects of sex and exercise on obesity related bone fragility.

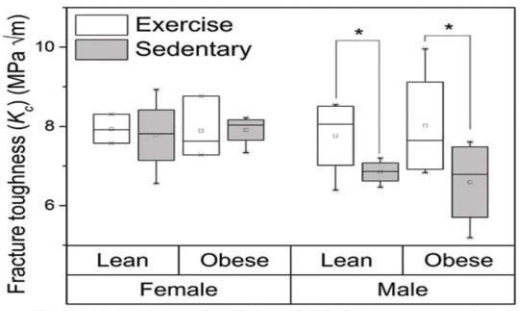

Fig 1: K_c is higher for EX vs SED for male rats. * $p \leq 0.05$

P09

Effects of Progressive Glycemic Derangement on Bone Tissue Composition in Postmenopausal Women. Jared Pearl*[1], Nicholas Miller[1], Jing Han Zhang[1], Heather Hunt[1], Kendall Moseley[2], Eve Donnelly[1]. [1]Cornell University, United States, [2]Johns Hopkins University School of Medicine, United States

Individuals with type 2 diabetes mellitus (T2DM) have 10-year hip fracture risks greater than those of non-diabetics despite comparable bone mineral density (BMD). This observation suggests that progressive glycemic derangement may cause BMDindependent changes in bone quality. In this study, our objective was to assess the association between different states of glucose intolerance and bone tissue composition. Iliac crest biopsies were collected from postmenopausal women ages 55-80 years allocated to three groups based on oral glucose tolerance testing: normal glucose tolerance (NGT, n=32), impaired glucose tolerance (IGT, n=12), and T2DM n=13) (Table 1). Three cortical and three trabecular regions of ~400 mm x 400 mm on each of three sections per biopsy were scanned using Fourier transform-infrared imaging. The distribution of pixel values within each image was assessed for four parameters: mineral: matrix, carbonate:phosphate, collagen maturity, and crystallinity. Tissue mineral content increased with progressive states of glycemic derangement, as evidenced by greater mean values of mineral:matrix in the IGT group. Specifically, cortical bone had greater mean mineral:matrix in the IGT vs. the NGT group (+6.5%, p = 0.0226; Fig. 1a). Furthermore, the distributions of trabecular mineral:matrix were narrower in the T2DM vs. the NGT group (-11.7%, p = 0.0457; Fig. 1d). Cortical and trabecular tissue from the T2DM group had wider distributions of crystallinity vs. that from the NGT group (+16.3%, p = 0.0168, Fig. 1c; +11.8%, p = 0.0219, Fig. 1d, respectively). The distributions of crystallinity values in the IGT group were also wider vs. the NGT group in trabecular bone (+16.8%, p = 0.0317), and trended toward being wider in cortical bone (+15.9% p = 0.0843). No other differences in tissue properties were observed. Greater cortical mineral content, as well as narrower distributions of trabecular mineralization, were observed in bone tissue from individuals with worsening glycemic derangement. Because bone mineral content increases with tissue age (time since bone formation), these observations support prior observations that T2DM inhibits bone remodeling. However, the wider distributions in crystallinity in the IGT and T2DM groups compared to the NGT group are inconsistent with this interpretation; these more complex effects of impaired glycemic control on mineral properties require further investigation.

Table 1: Patient demographics.

Characteristic	NGT (n=32)	IGT (n=12)	T2DM (n=13)	IGT % difference vs. NGT	T2DM % differe vs. NGT
Age (years)	64.3 ± 6.9	65.6 ± 4.2	64 ± 5.1	2.02	-0.47
Height (cm)	161.0 ± 6.77	166.3 ±5.58	156.6 ± 13.8	3.29	-2.73
Weight (kg)	77.7 ± 14.1	94.1 ± 19.1	92.5 ± 16.1	**21.1**	**19.05**
BMI (kg/m^2)	30.01 ± 5.51	33.75 ± 5.00	34.1 ± 12.18	12.46	**13.63**
HbA1c	5.75 ± .27	6.02 ± .30	9.22 ± 2.03	4.7	**60.35**
Fast GLC (mg/dL)	90.1 ± 12.2	94.2 ± 9.86	N/A	4.55	N/A
120 Min GLC (mg/dL)	103.7 ± 24.5	158.5 ± 26.0	N/A	**52.84**	N/A

Values shown as means ± standard deviation. Significant differences (p<0.05) by ANOVA with Tukey post hoc are bolded.

Figure 1: FTIR properties (MinMatrix = mineral:matrix, CP = carbonate:phosphate, XLR = collagen maturity, XST = crystallinity) reported as image pixel distribution (a) means for cortical bone, (b) means f trabecular bone, (c) full widths at half maximum (FWHM) for cortical bone, and (d) full widths at half maximum for trabecular bone; * p < 0.05, # p < 0.1. Bar heights and error bars indicate raw mean and 9 confidence intervals, respectively.

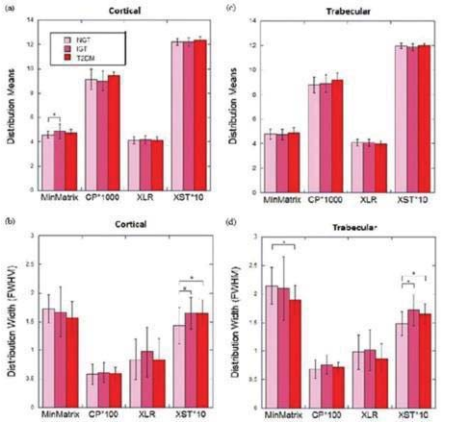

P10

Sex-Related Differences in Endplate Porosity and its Correspondence to Vertebral Strength. Elise Morgan*, Timothy Jackman, Amira Hussein, Cameron Curtiss. Boston University, United States

Epidemiological data suggest that the pathogenesis of vertebral fractures may not be the same between men and women. Recent evidence from biomechanical studies indicates that the vertebral endplate is critically involved in the mechanisms of vertebral fracture: the onset of endplate deflection during mechanical loading coincides with a pronounced drop in the ability of the vertebra to support loads and is associated with the local microstructure of the endplate region. The goal of this study was to investigate sex- related differences in the endplate microstructure and its correspondence to vertebral strength. Cadaveric, spine segments (T7-T9; 16 male, 12 female; mean+/-stdev in age = 72+/-11 years) were imaged via quantitative computed tomography to measure integral BMD (In.BMD) and micro-computed tomography tomeasure endplate porosity and microstructural properties of the 5mmthick layer of

trabecular bone immediately underlying the endplate. The spine segments were compressed to failure in axial compression (n=14) or axial compression with anterior flexion (n=14). Eachmicrostructural parameterwas compared between sexes via a t-test and analysis of covariance (ANCOVA) with age and In.BMD as covariates.Regression analysiswas used to examine the potential sex- dependence of a correspondence between vertebral compressive strength on endplate porosity. We found that endplate porosity was 19.3% higher (p=0.012), and that the trabecular degree of anisotropy (DA) was 5.0%higher (p=0.050), in female than in male vertebrae. The difference in endplate porosity between sexes persisted even after adjustment for In.BMD and age (Figure. 1), whereas the difference in trabecularDAdid not. No sex differences in any other microstructural parameters (including trabecular BV/TV) were found (p>0.110). We found a strong trend towards a dependence of compressive strength of the vertebra on endplate porosity for both sexes (r2=0.507, p=0.060); however, the dependence tended to be stronger in female than male vertebra (p=0.060 for the interaction between sex and endplate porosity). In contrast, the dependence of vertebral compressive strength on In.BMD did not differ between sexes (p=0.670). These results indicate a sexdependent, BMD-independent difference in microstructure specifically in a region that is biomechanically critical in the process of vertebral failure. Endplate porosity may be associated with the higher rates of vertebral fracture in women vs. men.

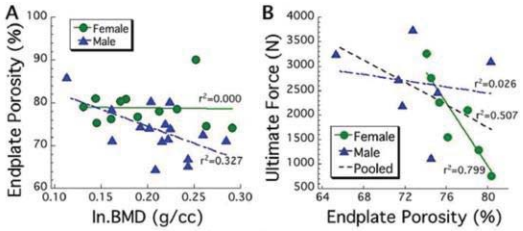

Figure 1. Endplate porosity is (A) higher in women than in men, even after adjustment for In.BMD and (B) more strongly associated with vertebral strength in women than in men.

P11

Sequential antiresorptive and anabolic treatment maintains cortical bone quality in an ovariectomized rat model. Erik Taylor*[1], Xiaomei Yao[2], Yong Wang[2], Don Kimmel[3], Mark Johnson[2], Eve Donnelly[1], Nancy Lane[4]. [1]Cornell University, United States, [2]University of Missouri-Kansas City, United States, [3]University of Florida, United States, [4]University of Davis, United States

Antiresorptive and anabolic agents are used sequentially to treat osteoporosis, but their effects on bone quality are incompletely understood. Therefore, in this study, we compared cortical bone tissue composition from ovariectomized rats treated with multiple sequential treatment regimens. Six-month-old female Sprague-Dawley rats were ovariectomized (OVXd) (N=40) or sham-OVXd (Sham, N=6). After 2 months, OVXd rats were given varying treatment sequences every 3 months for 9 months that included vehicle (V, saline 1 ml/kg/dose, 3x/ wk SC), h-PTH 1-34 (P, 25 mg/kg/ 5x/wk SC), alendronate (A, 25 mg/kg/ dose, 2x/wk SC), and raloxifine (R, 5 mg/kg/dose 3x/wk by oral gavage) in groups corresponding to 6 treatments: VVV (N=6), AAA (N=4), RRR (N=5), PVV (N=5), AVA (N=5), APA (N=5), and RPR (N=4). After euthanasia, a mid-frontal section through the proximal third of the tibia was prepared, and 48-80 Raman spectra per tibia were collected within 20 mm of lacuni. Four parameters were calculated: the mineral:matrix ratio, carbonate: phosphate ratio, crystallinity, and collagen maturity. Cortical tissue mineral content decreased in animals treated with PVV compared to that of the VVV control (-17.2%, $p < 0.05$; Fig. 1A). The cortical collagen maturity increased in the RRR group relative to the VVV control (+10.5%, $p < 0.01$; Fig. 1D). Cortical bone from the APA group had lower collagen maturity relative to RRR, AAA, and PVV (-12.0%, $p<0.01$; -9.8%, $p<0.05$; and -9.1%, $p<0.05$ respectively). Overall, estrogen-deficient osteopenic female mature rats exposed to osteoporosis treatment sequences with both anti-resorptive and anabolic agents at 3-month intervals resulted in cortical tissue with lower mineral content relative to the VVV control. Suppression of resorption can increase tissue age, reflected by increased secondary mineralization and collagen maturity. The decrease in tissue mineral content in the PVV group reflects younger tissue age arising from recent bone formation. The decrease in collagen maturity with sequential anabolic and antiresorptive treatments in the APA group relative to monotherapies suggests that this treatment regime can decrease collagen maturity without increasing tissue mineral content. These results suggest that sequential anti-resorptive and anabolic treatments may improve cortical bone quality relative to monotherapies. Studies should be extended to human cortical bone biopsies to determine if these results can be translated to clinical care.

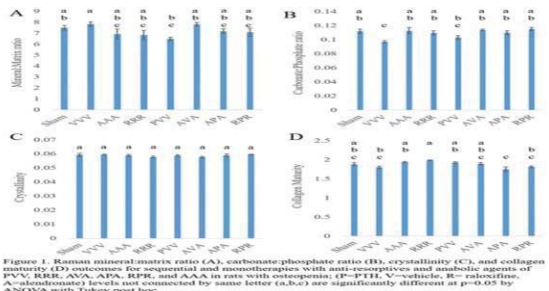

Figure 1. Raman mineral:matrix ratio (A), carbonate:phosphate ratio (B), crystallinity (C), and collagen maturity (D) outcomes for sequential and monotherapies with anti-resorptives and anabolic agents of PVV, RRR, AVA, APA, RPR, and AAA in rats with osteopenia; (P=PTH, V=vehicle, R= raloxifine, A=alendronate) levels not connected by same letter (a,b,c) are significantly different at p=0.05 by ANOVA with Tukey post hoc.

P12

A novel Raman parameter correlates with the fracture toughness of human cortical bone. Mustafa Unal*[1], Selin Timur[2], Sasidhar Uppuganti[1], Ozan Akkus[2], Jeffry S. Nyman[1]. [1]Vanderbilt University Medical Center, United States, [2]Case Western Reserve University, United States

Although age- and disease-related deterioration in bone matrix is an important contributor of impaired bone fracture resistance, there is currently no clinical tool that assesses the matrix. Raman spectroscopy (RS) is well suited to address this need, but to date, only one study showed RS parameters, namely crystallinity, significantly correlate with mechanical properties (tensile) of human cortical bone. Recently, we identified a new RS parameter, 1670/1640, as being sensitive to denatured collagen and related to toughness of bovine cortical bone. To establish the potential for RS in assessing the contribution of the matrix to the fracture resistance, we hypothesized that i) the new RS parameter correlates with fracture toughness of human cortical bone and ii) more importantly, RS adds value helping volumetric BMD (vBMD) and age predict fracture toughness properties. Cadaveric femurs (28M/30F, age = 21- 101 yrs) were machined into single-edge notched beam specimens. The intended crack path region was scanned by mCT and corresponding vBMD was determined. A non-linear fracture mechanics approach (Rcurve testing) was used to determine crack initiation (KJc), crack growth toughness (_Kj/_a) and overall J-integral (J-int). Thirty-two Raman spectra per sample were each acquired by 12 accumulations (5 s), and distributed throughout the entire surface of bone (785 nm confocal RS, 20x obj). From the average spectrum per donor, we calculated traditional RS parameters (mineral to matrix ratios (MMRs), carbonate substitution, and crystallinity) as well as matrix maturity ratio (1670/1690) and the new 1670/1640 and 1610/1670 ratios (the intensities of Amide I shoulders were identified by the local maxima, not by band-fitting as guided by second derivative spectra) (Fig 1). Matrix maturity and v1PO4/Pro did not correlate with any of the fracture toughness properties. Other traditional RS parameters and 1610/1670 only explained up to 18% of the variance for the fracture toughness properties (Table 1). The new parameter, 1670/ 1640, explained 48% of the variance in J-int and 35% of the variance for KJc (R2). After including age and vBMD in multilinear regressions as covariates, 1670/1640 significantly improved the prediction of J-int (from adj-R2= 12.35 to 46.55) and the prediction of Kjc (from adj-R2= 40.73 to 50.49), suggesting RS assessment has potential to assist existing clinical tools in assessing an individual's fracture risk.

Figure 1. A representative Raman spectrum showing the major peaks in bone spectrum.

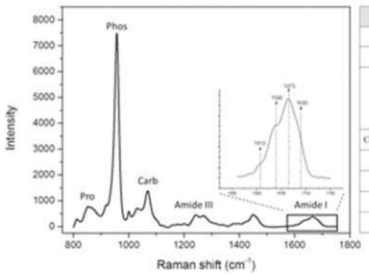

Table 1. Significant linear correlation coefficients (R^2) in bold and corresponding p-values below (in italics) as calculated from bootstrapped data.

Characteristic Property		Age	Fracture Toughness		
			K_{Jc}	K_{max}	J-int
Age		1	**0.21** *(0.0007)*	**0.17** *(0.003)*	**0.13** *(0.004)*
Bone mineral density	vBMD	NS	**0.23** *(<0.001)*	NS	**0.05** *(0.046)*
Mineral-to-matrix (MMR)	v_1PO_4/Amide I	NS	**0.16** *(0.002)*	**0.11** *(0.020)*	**0.38** *(<0.001)*
	v_1PO_4/Amide III	**0.10** *(0.016)*	**0.15** *(0.003)*	**0.08** *(0.045)*	**0.11** *(0.009)*
	v_1PO_4/Proline	**0.15** *(0.002)*	NS	NS	NS
Carbonate substitution	CO_3/v_1PO_4	**0.35** *(<0.001)*	**0.16** *(0.002)*	**0.09** *(0.036)*	**0.08** *(0.015)*
Crystallinity	1/FWHM(v_1PO_4)	**0.17** *(0.001)*	NS	**0.13** *(0.011)*	NS
Matrix Maturity	1670/1690	**0.14** *(0.003)*	NS	NS	NS
Collagen Denaturation	1670/1640	**0.29** *(<0.001)*	**0.32** *(<0.001)*	**0.18** *(0.001)*	**0.48** *(<0.001)*
Conformation Change of Collagen	1610/1670	**0.40** *(<0.001)*	**0.15** *(0.004)*	**0.19** *(0.026)*	**0.18** *(<0.001)*

P13

Effect of Mineralized Collagen Fibril Orientation on Cortical Bone Fracture Resistance. Yaohui Wang*, Ani Ural. Villanova University, United States

Bone is a hierarchically structured composite material which exhibits different fracture mechanisms at each length scale. At the submicroscale, the bone is composed of mineralized collagen fibrils. At this scale, the fracture processes in cortical bone have not been extensively studied in the literature. In this study, a novel approach to simulate the submicroscale fracture response in cortical bone was developed incorporating finite element models of unit cells of mineralized collagen fibrils. The models with varying fibril orientations were utilized to assess the influence of the fibril network pattern on the fracture behavior in cortical bone at the submicroscale. Four sets of fibril networks were generated using a MATLAB script with a plywood structure incorporating fibril orientations of 0_/90_, _15_, _30_, _45_ (Fig. 1a). A fibril diameter distribution of 100_5 nm was used in all models. Both longitudinal and transverse tensile loading with respect to simmain fibril direction were applied to each model. Interfacial separation between the fibrils was represented by cohesive interface elements. Extended finite element (XFEM) cohesive fracture approach was applied to individual fibrils to account for fibril fracture. The material properties used in all the simulations were adapted from recent experimental data reported in the literature. The simulation results showed that the interfacial separation dominates transverse loading as the interfaces are mostly perpendicular to the loading direction (Fig. 1b, 1d). The fibril fracture dominates longitudinal loading since the loading direction is approximately along the fibril direction (Fig. 1c, 1e). The yield and ultimate strength in longitudinal loading is higher than the transverse direction because the interface is much weaker than the fibril. With larger fibril orientation angles, fibrils deviate further from the main loading direction leading to an increase in the elastic modulus and strength in transverse loading (Fig. 1d) and a decrease in longitudinal loading (Fig. 1e). In conclusion, this study introduced a new modeling method to simulate the submicroscale fracture behavior of bone using a novel model generation approach and fracture mechanics-based finite element modeling. The results demonstrate the importance of the orientation of mineralized collagen fibrils with respect to the loading direction in determining cortical bone fracture behavior at the submicroscale.

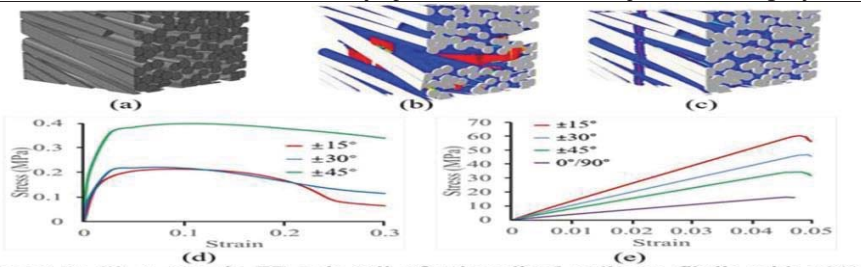

Figure 1: (a) A sample FE unit cell of mineralized collagen fibrils with ±30° plywood fibril orientation. (b) Deformed shape of the model in (a) under transverse loading demonstrating fibril separation (denoted by red color). (c) Deformed shape of the model in (a) under longitudinal loading demonstrating fibril fracture (denoted by red color). Stress-strain curves for various fibril orientations under (d) transverse loading and (e) longitudinal loading.

P14

Prediction of Distal Radius Failure Load Using Finite Element Modeling of Peripheral Quantitative Computed Tomography (pQCT-FE): A Validation Study. Hongyuan Jiang*[1], Dale L Robinson[1], Saija Kontulainen[2], James D Johnston[2], Peter VS Lee[1], John D Wark[1], Matthew McDonald[3]. [1]The University of Melbourne, Australia, [2]University of Saskatchewan, Canada, [3]Department of Engineering, College of Engineering, University of Saskatchewan, Canada

BACKGROUND Finite element (FE) modeling based on peripheral quantitative computed tomography (pQCT-FE) has potential to estimate distal radius failure load non-invasively due to the volumetric and density distribution information acquired by pQCT. The objective of this study was to compare distal radius failure loads derived from biomechanical testing using cadaveric forearms with pQCT-FE estimates of bone mechanical properties. METHODS Forty fresh-frozen cadaveric forearms were scanned at the distal end of radius (4% of length) using pQCT (Stratec XCT 3000). Specimens were then loaded to failure with either 15^{o} inclination (n=21), which simulated bending and compressive loading experienced during a fall onto the outstretched hand, or no inclination (n=19), which simulated pure compressive loading. Peripheral QCT images were used to estab- lish a cross-sectional FE model. Stiffness and strength of three loading cases were obtained from the FE models, including: compression, torsion and bending. Axial compression was simulated by a 0.01 mm displacement of the superior surface towards the inferior surface. Torsion was simulated by a 0.01^{o} rotation of the inferior surface about the z- axis. Bending was simulated by a 0.01^{o}rotation of the inferior surface about a bending axis aligned with inclination rotation axis. RESULTS In specimens with 15^{o} inclination, bone strength derived from FE analy- sis correlated well with experimental failure load (Scompression: r^2 0.452; Storsion: r^2 0.570; Sbending: r^2 0.615). In specimens with no inclination, moderate correlations were observed (Scompression: r^2 0.264; Storsion: r^2 0.23; Sbending: r^2 0.339). DISCUSSION Our pQCT-FE model offered reasonable predictions of distal radius failure load acquired using experimental mechanical testing simulating a fall onto the outstretched hand associated with Colles' fracture. Future research will compare failure load with pQCT-FE analyses of the radial mid-shaft (radial diaphysis).

Table 1. Correlations between experimental failure load and pQCT-FE bone strength

	With 15° inclination		With no inclination	
	R^2	p	R^2	p
$S_{bending}$	0.615	<0.001	0.339	0.006
$S_{compression}$	0.452	<0.001	0.264	0.01
$S_{torsion}$	0.57	<0.001	0.230	0.02
$S_{bending}$+$S_{compression}$	0.616	<0.001	0.341	0.04
$S_{bending}$+ $S_{torsion}$	0.621	<0.001	0.394	0.02
$S_{compression}$+ $S_{torsion}$	0.568	0.001	0.268	0.09
$S_{bending}$+$S_{compression}$+ $S_{torsion}$	0.625	0.001	0.406	0.06

P15

Bone quality and mechanical competence during pediatric skeletal growth. Elizabeth Zimmermann*[1], Christoph Riedel[1], Kilian Stockhausen[1], Yuriy Chushkin[2], Eric Schaible[3], Felix Schmidt[1], Bernd Gludovatz[4], Eik Vettorazzi[5], Frederico Zontone[2], Klaus Püschel[6], Michael Amling[1], Robert Ritchie[7], Björn Busse[1]. [1]Department of Osteology and Biomechanics, University Medical Center Hamburg, Germany, [2]European Synchrotron Radiation Facility, Grenoble, France, [3]Advanced Light Source, Berkeley, United States, [4]Lawrence Berkeley National Laboratory, United States, [5]Department of Medical Biometry and Epidemiology, University Medical Center Hamburg, Germany, [6]Department of Forensic Medicine, University Medical Center Hamburg, Germany, [7]Department of Materials Science and Engineering, University of California, Berkeley, United States

Thirty percent of children/adolescents experience a bone fracture. High fracture incidence was linked initially to cortical porosity (1); however, recent clinical studies find no correlation between cortical bone volume fraction and fracture risk (2,3). Thus, transitions in *bone quality* (*i.e.*, structure, composition) may explain pediatric fracture risk. Here, bone quality was quantitatively investigated in a cross-sectional cohort between 22 weeks of gestation and 14 years from the mid-femoral diaphysis, allowing comparison between ages. Autopsy samples were separated into groups consisting of primary bone (fetal -

1 year, n=4) or remodeled osteonal bone (2-14 years, n=4). The study was approved by the local Institutional Review Board. Histological sections were used to image bone structure, mineral distribution was measured with quantitative backscattered electron imaging (qBEI), collagen fiber orientation was imaged with polarized light microscopy and mechanical tests evaluated bone strength. The *primary bone* consisted of a porous scaffold of woven tissue (Fig. 1a,b). Comparatively, *remo- deled bone* consisted of osteons with highly organized lamellae (Fig. 1c,d). Remodeled bone exhibited 29% greater cortical bone volume fraction (primary BV/TV = 0.73 0.06, osteonal BV/TV = 0.95 0.03, p=0.03) and 10% higher mineralization relative to pri- mary bone (qBEI: primary CaMean = 22.3 1.2 CaWt%, osteonal CaMean = 24.5 0.5 CaWt%, p=0.03). These structural and compositional differences are associated with 160% larger stiffness (primary stiffness = 5.1 2.0 GPa, osteonal stiffness = 13.2 1.9 GPa, p=0.05) and 83% higher strength (primary strength = 73.5 18.1 MPa, osteonal strength = 134.3 20.4 MPa, p=0.05) in remodeled osteonal *vs* primary bone. Thus, higher bone volume fraction, osteonal organization and mineralization in *remodeled* bone enhance mechanical resistance. The limitations to the study include its cross- sectional design and unknown inter-individual differences, which may influence some observed differences. The implications of this study are that primary bone is inherently weaker than remodeled bone. As primary bone is present in the fetal/infant ile skeleton and near sites of growth (i.e., growth plate), our results suggest primary bone quality during growth contributes to high fracture incidence in children/adolescents. (1) Parfitt, AM, Osteoporos Int, 3:382, 1994. (2) Määttä M, et al., Osteoporos Int, 26:1163, 2015., JBMR, 29: 2193, 2014.

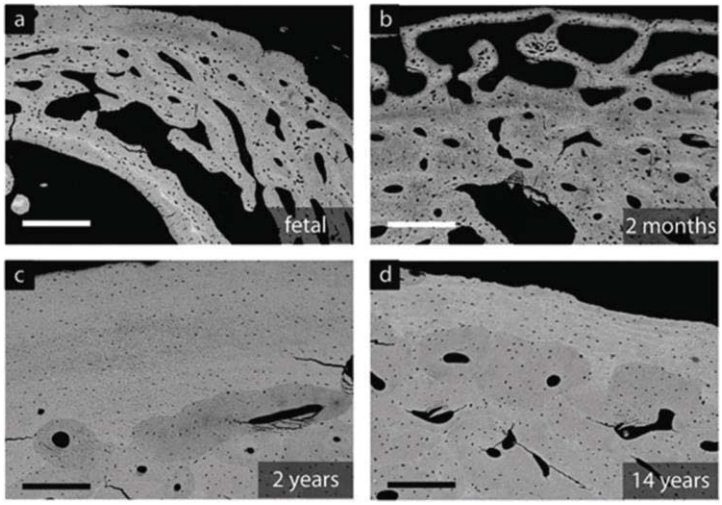

P16

Lumbar Spine Trabecular Bone Score: a Potential Screening Tool for the First Year Post-menarche?. Jodi Dowthwaite*[1], Renaud Winzenrieth[2], Tamara Scerpella[3]. [1]SUNY Upstate Medical University, United States, [2]Med-Imaps, France, [3]University of Wisconsin, Madison, United States

Trabecular bone score (TBS) grades lumbar spine trabecular texture from gray-scale DXA images. Silva et al. (2014) recommended TBS thresholds for post-menopausal women to be 1.35 (normal microarchitecture), >1.2 to <1.35 (partially degraded) and 1.2 (degraded). Numerous studies have evaluated pubertal lumbar spine BMC and BMD, but no studies have evaluated factors in TBS variation at initial reproductive maturity. Thus, for the first year post-menarche, we aimed to evaluate: 1) whether "normal" adult TBS (1.35) has been reached; 2) the role of maturational timing (menarcheal age) and status (gynecological age) in TBS. Participants were derived from a longitudinal DXA study of bone growth in healthy girls. For inclusion, a lumbar spine scan (LS: L1-L4), whole body scan and anthropo- metry were required between menarche and 1 year post-menarche. For some girls, 2 DXA sessions qualified; the scan closest to 0.5 years post-menarche was used. Custom software adjusted for soft tissue thickness (TBS iNsight, Med-Imaps, France). We used linear and quadratic regressions to evaluate menarcheal age and gynecological age as factors in LS TBS, BMC and BMD, reporting beta semi-partial correlation coefficients (spcc) and significance. Table 1 presents descriptive statistics. The lowest observed TBS was 1.362. For TBS, there were no significant linear or quadratic correlations with gynecological age, height, weight, BMI or fat mass (p>0.15); a significant negative linear correlation persisted with menarcheal age (spcc= -0.36, p=0.015), after accounting for gynecological age (spcc= +0.23, p= 0.111). In contrast, gynecological age correlated positively with LSBMC and LSBMD (spcc= +0.37, +0.38; p < 0.015), while menarcheal age did not (spcc= -0.09, -0.19; p> 0.18). TBS linear correlations with both LSBMC and LSBMD were significant (r= +0.47, +0.63; p< 0.001). "Normal" adult TBS appears to be achieved by menarche in healthy girls. Accordingly, TBS during the initial post-menarcheal year could assess trabecular struc- ture to screen at-risk girls for intervention prior to "peak bone mass". TBS may reflect risk factors in trabecular structural development that are not reflected by lumbar spine BMC or BMD. Assessments may be particularly important in girls with delayed menarche; current gynecological age should be taken into account. Further longitudinal study is needed to ascertain whet er initial post- menarcheal TBS is a significant pre- dictor of TBS at peak bone mass.

Table 1: Descriptive Statistics for Post-menarcheal Study Participants (n= 46)				
Variables	Mean	Standard Deviation	Minimum	Maximum
Age (years)	12.7	0.6	11.2	13.7
Menarcheal Age (years)	12.2	0.5	10.8	13.4
Gynecological Age (years)	0.50	0.25	0.03	0.93
Height (m)	1.61	0.06	1.49	1.72
Weight (kg)	52.2	8.3	40.8	83.3
Body Mass Index (kg/m^2)	20.2	2.8	15.3	30.1
Lean Mass (kg)	35979.9	3828.2	25142.0	43623.0
Fat Mass (kg)	14471.2	5454.4	6799.0	37321.0
Whole Body Bone Mineral Content (BMC, g)	1939.2	218.63	1476.0	2437.0
Sub-head BMC (g)	1547.8	196.2	1088.0	2001.0
Lumbar Spine BMC (g)	46.05	7.34	32.4	67.0
Lumbar Spine Bone Mineral Density (g/cm^2)	1.016	0.100	0.800	1.200
Lumbar Spine Trabecular Bone Score (TBS)	1.495	0.054	1.362	1.577

P17
Frequency of vigorous physical activity predicts bone strength accrual during adolescence. Leigh Gabel*[1], Lindsay Nettlefold[1], Heather Macdonald[1], Heather McKay[2]. [1]Centre for Hip Health and Mobility, Canada, [2]University of British Columbia, Canada

Purpose: The link between physical activity (PA) and bone strength is irrefutable; however, we do not know the precise PA prescription (i.e., frequency and total volume) for optimal accrual of bone strength during growth. Thus, we aimed to examine the influence of vigorous PA (VPA) bout frequency on bone strength accrual across adoles- cence, independent of total volume of VPA Method: We acquired high-resolution peripheral quantitative computed tomogra- phy scans of the distal tibia (8% site) and applied finite element analysis to estimate bone strength in compression (failure load, F.Load, N) in 309 adolescents (9–20 years at baseline) over a maximum of 4 years. We measured VPA [total volume (min/day) and bout frequency < 5 min in duration (bouts/day)] annually using accelerometers (ActiGraph GT1M). We aligned participants on maturity offset (years from age at peak height velocity) and fit a mixed effects model adjusting for maturity, sex, ethnicity, tibia length, lean body mass and VPA (volume and bout frequency). Results: Average volume of VPA (min/day) and VPA bout frequency (# bouts per day of VPA < 5 min in duration) declined across adolescence, from approximately 14 and 20 min/ day and 35 and 42 bouts/day in girls and boys, respectively, at 2 years prior to APHV to 6 and 8 min/day and to 8 and 11 bouts/day in girls and boys, respectively, at 7 years post-APHV. Both VPA total volume and bout frequency were positively associated with F.Load across adolescence. However, VPA volume did not predict F.Load after accounting for VPA bout frequency. Participants in the upper quartile of VPA bout frequency (~33 bouts/day) had 10% (500 N; 95% CI: 112 to 889; $p = 0.012$) greater F.Load across adolescence compared with participants in the lowest quartile (~9 bouts/day) (Figure). Each additional daily bout of VPA was associated with 21 N greater F.Load, independent of total volume of VPA.Conclusion: Consistent with results from classic animal loading models, VPA bout frequency was a stronger predictor of bone strength at the distal tibia in adolescent girls and boys as compared with total volume of VPA. Further, despite significant declines in VPA in girls and boys, our findings suggest the influence of VPA bout frequency on F. Load is consistent across adolescence. Public health guidelines for bone strength may be ng frequent, short bouts of VPA.

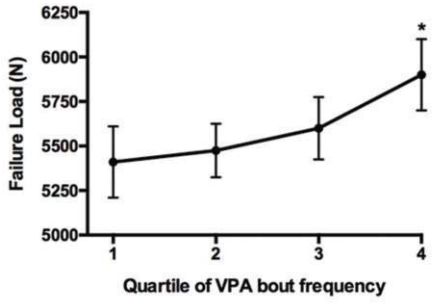

Figure. Relationship between failure load (N) and quartiles of vigorous physical activity (VPA) bout frequency. Estimated marginal means (95% confidence interval) from mixed effects model adjusted for maturity offset, sex, ethnicity, tibia length, lean body mass and total volume of VPA. Cut points for quartiles were 9, 20 and 33 bouts/day. *$p = 0.012$ compared with quartile 1.

P18
Plate-like trabeculae increase with age and lean mass in healthy girls at the distal tibia. Deborah Mitchell* [1], Signe

Caksa[2], Amy Yuan[2], Mary Bouxsein[2], Madhusmita Misra[3], Sherri-Ann Burnett-Bowie[2]. [1]Pediatric Endocrine Unit, Massachusetts General Hospital, United States, [2]Endocrine Unit, Massachusetts General Hospital, United States, [3]Pediatric Endocrine and Neuroendocrine Units, Massachusetts General Hospital, United States

Background: Childhood is a critical window for bone accrual and microarchitecture development. Previous data suggest that changes in trabecular bone parameters are relatively modest across late childhood and adolescence in girls. We hypothesized that trabecular morphology would change across this period, becoming more plate-like and thereby conferring increased strength and fracture resistance. We further hypothesized that trabecular morphology would correlate with body composition. Design and methods: We conducted a cross-sectional study of 86 healthy girls ages 9-18 years. Skeletal maturity was assessed with bone age x- ray. We measured body composition by DXA and used HR-pQCT to measure volumetric bone density and microarchitecture at the distal tibia. Individual trabecula segmentation (ITS) was used to assess trabecular morphology. Results: Trabecular bone volume fraction (BV/TV) tended to increase with bone age (R=0.20, p=0.065). In comparison, plate-like BV/TV increased significantly (R=0.41, p<0.001), while rod-like BV/TV decreased significantly (R=-0.28, p=0.008) with bone age. The increase in plate BV/TV was driven by increases in plate number (R=0.24, p=0.026) as well as by plate size including both thickness (R=0.52, p<0.001) and surface area (R=0.43, p<0.001). To examine the associations of body composition with trabe-cular morphology, we used multivariable modeling with bone age, lean mass, and fat mass as predictors. In this model, lean mass was positively correlated with plate BV/TV (partial R=0.24, p=0.028) and plate thickness (partial R=0.28, p=0.010), while fat mass was negatively correlated with plate thickness (partial R=-0.23, p=0.039) and surface area (partial R=-0.26, p=0.019). In addition, fat mass positively correlated with rod BV/TV (partial R=0.31, p=0.004) and rod number (partial R=0.33, p=0.002) and negatively correlated with rod length (partial R=-0.41, p<0.001). Conclusions: Between the ages of 9 to 18, despite only modest increases in BV/TV, trabecular morphology changes significantly in healthy girls, with an estimated 61% increase in plate BV/TV and 21% decrease in rod BV/TV at the distal tibia. Lean mass independently correlates with plate parameters, expected to confer strength, while fat mass correlates with smaller plates and more numerous and shorter rods. These data suggest that increased lean mass in youth promotes bone strength while increased fat may be associated with maladaptive microarchitecture.

P19

Limitations Associated with Bone Assessment by Dual-Energy X-ray Absorp- tiometry at the Distal Femur in Children with Cerebral Palsy. Chuan Zhang*[1], Daniel Whitney[1], Benjamin Conner[1], Freeman Miller[2], Christopher Modlesky[1]. [1]University of Delaware, United States, [2]A.I duPont hospital for children, United States

Background: Children with cerebral palsy (CP) have a high fracture rate at the distal femur. Studies examining the pattern of bone architecture suggest that the deficit in children with CP becomes more pronounced with increased distance proximally from the growth plate within the metaphysis. However, whether the same pattern is observed for areal bone mineral density (aBMD) and bone mineral content (BMC) from dual- energy X-ray absorptiometry (DXA) is unknown. Methods: 32 children with CP (4 - 13 y; 18 M and 14 F; I-V on Gross Motor Function Classification System) and 32 sex- and age-matched typically developing children parti- cipated in this study. A lateral distal femur scan of the more affected side in children with CP and the non-dominant side in controls was acquired using DXA. The region of interest (ROI) was a 14 mm height box starting 2 mm above the growth plate. To determine the pattern of bone mineral and size, the ROI was evenly divided into 7 subregions. aBMD, BMC and bone area of the total ROI and each subregion were determined. Twenty magnetic resonance images (MRI; 0.7 mm thick per image) were used to assess bone area, the medial-lateral (ML) width and the anterior-posterior (AP) width of the distal femur at the same approximate ROI. Results: Children with CP compared to controls had lower aBMD (26.9 %), BMC (32.7 %) and bone area (9.4 %) from DXA and lower bone area from MRI (21.5 %) (all $p < 0.05$). Linear random coefficients analysis indicated all four measurements decre- ased as distance from the growth plate increased (all $p < 0.05$). However, the rate of the decline was less steep for aBMD and BMC in children with CP than controls (both $p < 0.05$). While the rate of decline for bone area from DXA was not different ($p = 0.897$), the rate of decline for bone area from MRI was less steep in the children with CP ($p = 0.011$). Children with CP had a lower ML bone width and a lower ratio of ML to AP bone width (both $p = 0.001$). Although AP bone width was lower in children with CP, the difference was not significant ($p = 0.068$). Conclusion: The decline in aBMD and BMC with distance from the growth plate in the distal femur is less pronounced in children with CP compared to their typically developing peers. The unusual pattern may be the result of the 2-D bone area data yielded by DXA in the AP plane, which failed to capture the more robust deficit in bone width in the ML plane in children with CP.

P20

Parathyroid Hormone Rescues Bone Loss and Marrow Fat Expansion Induced by Calorie Restriction. David Maridas*[1], Elizabeth Rendina-Ruedy[1], Ron Helderman[1], Anyonya Guntur[1], Victoria DeMambro[1], Beate Lanske[2], Daniel Brooks[3], Mary Bousxein[3], Clifford Rosen[1]. [1]Maine Medical Center Research Institute, United States, [2]Harvard School of Dental Medicine, United States, [3]Beth Israel Deaconess Medical Center, United States

Recently, parathyroid hormone (PTH) receptor deletion in mice has been shown to result in the accumulation of marrow fat, whereas PTH prevents this expansion *in vitro*. Thus, we postulated that PTH could prevent the increase in marrow fat reported in the calorie-restricted mouse model of anorexia nervosa. Eight-week-old female C57BL/6J mice were fed either a control (AIN93M) diet (CTRL) or a 70% calorie restricted (CR) diet. The CR diet was formulated to have matching nutrients and minerals to the CTRL diet. At 12 weeks of age, CR and CTRL mice were injected daily with PTH (80mg/kg, CR/PTH or CTRL/PTH) or vehicle (CR/VEH or CTRL/VEH) for 4 weeks. An additional two cohorts of 8-week-old mice were CR and simultaneously injected (CR+PTH or CR+VEH)

for 4 weeks. CR mice lost considerable amount of body weight compared to the CTRL mice with significant decreases in fat proportion, lean mass, aBMD and aBMC after 4 weeks of CR. Histological sections of tibias showed an increase in marrow fat in CR compared to CTRL. PTH injections significantly increased aBMD and aBMC in both CR/PTH and CTRL/ PTH mice as well as in CR+PTH mice when compared with their respective controls. Interestingly, simultaneous injections had a much stronger effect on aBMD and aBMC than injections after calorie restriction. PTH did not affect fat proportion and lean mass when compared with VEH in any of the cohorts. mCT revealed that BV/TV from CR/VEH mice was not different from CTRL/VEH mice, yet PTH significantly increased BV/TV in CR/ PTH and CR+PTH mice. Cortical fraction was considerably decreased in CR/VEH com- pared to CTRL/VEH. PTH injections also increased the cortical fraction in both CR/PTH and CR+PTH. Bone marrow fat was analyzed on histological sections of proximal tibias stained with hematoxylin-eosin. We observed increases in adipocyte density and size in CR mice compared to CTRL mice. Surprisingly, PTH did not change adipocyte density although there was a trending decrease in adipocyte size in CR/PTH. The opposite effect was observed in CR+PTH with a trending decrease in adipocyte density but no

change in adipocyte size. Our results show that PTH can rescue bone loss in CR mice. Furthermore, our data suggest that PTH may reduce adipocyte size after CR. However, when PTH tes indicating both a differentia- for PTH depending on the time of treatment.

P21

Beyond the Skeletal Effects of PTH: Energy expenditure, body composition, gene expression and bone mass in PTH treated mouse models. Victoria DeMambro*[1], David Maridas[1], Elizabeth Rendina-Ruedy[1], Beate Lanske[2], Clifford Rosen[1]. [1]Maine Medical Center Research Institute, United States, [2]Harvard University, United States

Several *in vitro* studies have demonstrated that PTH can stimulate lipolysis in primary adipocytes and 3T3-L1 cells. More recently PTH1R (PPR) activation has been shown to lead to 'beiging' of white inguinal adipocytes (iWAT). Remarkably no clinical trials with PTH or abaloparatide have reported changes in total fat mass or compartmental fat. Notwithstanding we noted that PTH altered marrow stromal cell fate in mice and humans by reducing bone marrow adipose tissue (BMAT). Taken together we hypothesized that activation of the PPR might lead to changes in body composition and fat mass. To test this hypothesis we studied C57BL6J (B6) female and male mice treated with daily intermittent PTH (1-34) (80ug/kg/d) or vehicle 4 weeks after ovariectomy (OVX) or 4 weeks after calorie restriction (CR) (n=8/group). As expected, OVX'd, 20 wk old B6 mice treated with PTH had a 100% increase in femoral aBMD and a similar increase in femoral trabecular BV/TV ($p<0.0001$ vs vehicle). Fat mass increased in the vehicle group by 40% while in the PTH treated group there was a remarkable decline of 7% ($p<0.0001$ vs vehicle). Gene expression in the iWAT revealed a reduction in *AdipoQ* and *Pparg* with PTH ($p<0.05$), as well as a 40% decline in lysosomal acid lipase A (*Lal*). Gonadal (g)WAT also demonstrated a 50% reduction in *Lal* and a similar reduction in hepatic lipase (*Lipc*). Perilipin 2, a lipid-droplet protein, was markedly reduced in both iWAT and gWAT, while *Ucp1* and *DiO2*, markers of beiging, were increased 20 fold respectively ($p<0.05$ vs vehicle). As expected, body weight, fat mass, and resting energy expenditure (REE) declined significantly in the CR model without PTH. Areal BMD also declined significantly in the CR group. Of note, the change in both total body weight and % fat mass was greater with PTH than control ($p<0.01$ and $p<0.06$ respectively). Moreover, the PTH treated CR animals had higher REE than the vehicle treated CR albeit lower than control mice fed a regular diet. Activity levels did not differ between control and vehicle treated mice. Multivariate analysis controlling for body weight, PTH had a positive effect on energy expenditure. In conclusion activation of PPR has significant effects on bone mass and body composi- tion, likely through activation of the beige transcriptional network in adipocytes. Further studies are needed both in humans and in mice to define the translational importance in respect to anabolic therapies.

P22

Genetic Variation of Inbred Mouse Strains Uncovers Differences in Femur Strength Distinctly Influenced by Bone Matrix Composition. Michael-John Beltejar*[1], Jun Zhang[2], Dana A. Godfrey[1], Renata Rydzik[3], Olivia Hart[3], Douglas J. Adams[3], Cheryl L. Ackert-Bicknell[1]. [1]Center for Musculoskeletal Research, University of Rochester Medical Center, United States, [2]Department of Orthopedics, Zhejiang Provincial People's Hospital, China, [3]Department of Orthopaedic Surgery, University of Connecticut Health, United States

Osteoporosis is a disease characterized by progressive reduction in bone quantity and alterations in bone matrix quality. This often culminates in fractures that significantly alter quality of life and increase mortality risk. Although bone mineral density (BMD) is the current basis for surveillance, diagnosis, and therapy, it only captures 50% of fracture resistance because it minimally reflects contributions from bone shape and composition. Understanding the contributions of composition is necessary to develop novel and more comprehensive screening and treatment. The goal of this work was to determine how defined genetic variations in bone matrix quality results in altered bone strength. To accomplish this, we leveraged the genetic diversity of 7 inbred mouse strains. Three-point bending was used to measure flexural strength of femurs from 20-week old male mice. Moments of inertia for diaphyseal cross sections of femurs were measured using microCT. Tissue modulus and strength were calculated using beam theory. Areal BMD of the whole body was measured using DXA. Finally, matrix composition of humeri was assessed using Fourier-Transform Infrared Spectroscopy (FTIR). Differences among strains were determined by one-way ANOVA with a Student's T post hoc test with a Bonferroni correction. All of these determi- nants were highly reproducible within a strain, yet differed among strains, suggesting high heritability for these phenotypes. Multiple regression using parameters of composition (BMD, mineral: matrix, carbonate:phosphate, crystallinity) and geometric properties (I and I/c about ML axis) confirmed that whole-bone mechanical strength is predominantly determined by I/c, crystallinity and the mineral to matrix ratio (min:matrix). Tissue modulus is predominantly determined by crystallinity and min:matrix. Poignantly, contributions of aBMD to whole- bone strength is redundant. We then identified the main determinants of strength for each strain. For example, despite having lower BMD and geometrically smaller bones than B6, CAST femora have greater tissue strength, tissue modulus, and a mineral to matrix ratio, resulting in greater structural strength than B6 mice. This suggests that

genetically regulated matrix properties might be involved in offsetting deficiencies of size and shape to produce femurs of similar structural strength. These genetic differences can now be exploited to identify the molecular pathways involved in governing structural bone strength.

P23

Phenomic analysis of zebrafish type I collagen mutants reveals a spectrum of skeletal phenotypes mimicking the clinical variability in human brittle bone disease. Charlotte Gistelinck*[1], Ronald Y. Kwon[1], Fransiska Malfait[2], Sofie Symoens[2], Petra Vermassen[2], Hanna De Saffel[2], Katrin Henke[3], Matthew P. Harris[3], Anne De Paepe[2], MaryAnn Weis[1], David R. Eyre[1], Andy Willaert[2], Paul J. Coucke[2]. [1]Department of Orthopaedics and Sports Medicine, University of Washington, United States, [2]Center for Medical Genetics Ghent, Ghent University, Belgium, [3]Department of Genetics, Harvard Medical School, United States

Objective: The brittle bone disease osteogenesis imperfecta (OI) is a rare congenital disorder, mainly caused by defects related to type I collagen, which forms the structural protein scaffold of the bone extracellular matrix. Clinically, OI is characterized by a broad disease spectrum, ranging from mild forms with minimal fractures to severely deforming or even lethal forms. The underlying genetic basis of this variability between, but also within, different genetic types of OI remains one of the most puzzling questions in the field. In this study we illustrate the potential of zebrafish as a tool to better to understand and further dissect the underlying molecular basis of this phenotypic variability in human OI. Methods: We generated a large set of zebrafish with similar mutations as human patients with different genetic forms of OI. Phenomic profiles were constructed by mapping and quantifying skeletal parameters, using a mCT-based pipeline. 1 Results: Our study revealed a remarkably high phenotypic reproducibility of the human disease features between zebrafish mutants and patients with comparable genetic forms of OI. Key features of OI, such as the occurrence of fractures, overmineralization, and bowing and kinking of the long bones, were noted in several mutant genotypes, often with variable penetrance. Summary and Conclusions: Mice models are laborious and expensive for large scale genetic studies. Additionally, bone phenotypes in mice often cause (perinatal) lethality, making them unavailable for the study of later stages. Zebrafish overcomes these challenges as a model. With our study, we demonstrate that zebrafish models are able to both genocopy and phenocopy different forms of human OI, arguing for a similar genetic basis driving pathogenesis. We therefore propose zebrafish as a new tool to investigate unknown genetic modifiers and mechanism underlying the phenotypic variability in human OI.

P24

Alterations in NFkB Signaling Contribute to the Bone Fragility in Osteogenesis Imperfecta type V. Ronit Marom*, Caressa D. Lietman, Abbhirami Rajagopal, Mahim Jain, Ming-Ming Jiang, Yuqing Chen, Elda M. Munivez, Terry K. Bertin, Brendan Lee. Baylor College of Medicine, United States

Osteogenesis Imperfecta (OI) type V is characterized by increased bone fragility, bone deformities, hyperplastic callus formation and calcification of the interosseous membranes. It is caused by a common mutation in the 5' UTR of *IFITM5* gene (c.- 14C>T), which introduces a new start codon adding 5 amino acid residues to IFITM5 protein. The purpose of this study was to identify downstream signaling cascades that may be altered by this mutant protein, which is known to have normal localization at the cell membrane. We utilized RNA sequencing and proteomic studies via reverse phase protein-array (RPPA) method in bone of mutant transgenic mice and cell culture models. We have previously described a transgenic mouse model overexpressing the OI type V mutant *Ifitm5* in bone that showed severe bone deformities and perinatal lethality. Overexpression of the mutant *Ifitm5* caused abnormal mineralization, persistence of cartilage-like matrix throughout the limb, and altered cell morphology with chondro- cyte-like cells in bone. RNA-sequencing in calvaria from transgenic mice suggested activation of NFkB signaling in the mutant model. The expression of *Ptgs2*, encoding the inflammatory mediator cycolooxygenase-2, was increased 6 fold in *Ifitm5* -mutant calvaria. In vitro mineralization assay in MC3T3 cells overexpressing mutant *Ifitm5* showed reduced alizarin red staining, and the application of an NFkB inhibitor partly rescued this phenotype. Interestingly, proteomic analysis using RPPA detected elevated levels of SOX9 in the mutant samples. NFkB signaling is reported to facilitate chondro- genic differentiation via regulation of SOX9 expression during endochondral bone ossification. Inflammation is known to negatively affect bone formation, and this effect is, at least partly mediated via NFkB pathway. We suggest that altered NFkB signaling plays a role in the pathogenesis, and contributes to the development of bone fragility in OI type V.

P25

Genetic Profiling of Decreased Bone Mineral Density in an Independent Sample of Caucasian Women. Xiangxue Xiao*, Darius Roohani, Qing Wu. University of Nevada, Las vegas, United States

Background: Genetic risk of osteoporosis and low Bone mineral density (BMD) in healthy populations is still unclear, especially in Caucasian women, the most vulnerable group. Genomic Wide Scans for Female Osteoporosis Gene Study (GWSFO) is a cohort that has never been involved in any BMD-associated Single Nucleotide Polymorphism (SNP) discovering study. Therefore, GWSFO is an ideal independent data source for examining genetic risk in a healthy sample. As the phenotypic risk factors are variable, while the genes remain constant, uncovering the underlying genetic risk of healthy individuals will help identify susceptible subjects for preventive interventions. Aims:
1) To examine the distribution of risk alleles in healthy Caucasian women; and 2) To examine the association of Genetic Risk Score (GRS) and BMD in a sample of healthy Caucasian women. Methods: Genotype data of GWSFO, which included 1209 unre- lated healthy US Caucasian women over 18 years of age, was acquired through dbGap. Genotype imputation was conducted at the Michigan Imputation Server, using HRC Reference Panel. Based on a recent well-powered, genome-wide association study (GWAS) meta-

analysis, a total of 62 BMD-associated SNPs was included for analysis. Weighted GRS of both femoral neck (FN_GRS) and lumbar spine (LS_GRS) for each individual were calculated. We examined the distribution of unweighted GRS (UW_GRS). The magnitude of association between GRS and BMD at the lumbar spine and femoral neck was assessed by multiple linear regression, with age, weight, and height as covariates. SAS 9.4 was used for data analysis. Results: The UW_GRS ranged from 27 to 56. Half of the women in this sample carried 66% risk alleles, which indicated that an apparent "healthy" population may have a substantially high genetic risk of low bone mass and thus of osteoporosis. Regression analysis indicated that for a given age and weight, higher GRS was significantly associated with decreased BMD at both the lumbar spine ($p<0.0001$) and the femoral neck ($p = 0.0046$). For a one unit increase of GRS, the BMD at the spine and the hip decreased ~0.09 g/cm2 and 0.06 g/cm2, respectively. A sensitivity analysis was conducted after excluding excessive alcohol or tobacco users, and the results were similar. Conclusions: A substantially large men have a high genetic risk of osteoporosis. In healthy Caucasian women, GRS was significantly associated with BMD.

Table. Association between Genetic Risk Score (GRS) and BMD: Results of Multiple Linear Regression Analysis

BMD sites and covariates	*Regression Coefficient (SE)*	*p*
Hip total BMD		
Age	-0.003 (0.0003)	<0.0001
Weight	0.004 (0.0003)	<0.0001
Femoral neck GRS	-0.059 (0.0206)	0.0046
Spine total BMD		
Age	-0.002 (0.0003)	<0.0001
Weight	0.003 (0.0003)	<0.0001
Height	0.002 (0.0006)	0.0016
Lumbar spine GRS	-0.091 (0.0180)	<0.0001

P26

Galectin-3 null mice are protected against cortical bone loss following gona- dectomy. Kevin Maupin*[1], Daniel Dick [2], Bart Williams[2]. [1]Indiana University School of Medicine, United States, [2]Van Andel Research e, United States

Loss of bone mass occurs following the loss of sex hormone production due to menopause or castration. Thus, there is a need to identify novel targets to improve bone mass that are independent of sex hormone status. Galectin-3 (Gal3) is a chaperone protein which functions both intracellularly via protein-protein interactions and extracellularly by binding specific glycans on glycoproteins. Gal3-null mice have no major negative health phenotypes and are protected against fibrosis. Previously we observed that female Gal3-null mice had increased cortical bone mass during aging. Because the phenotype was only weakly observed in males, we hypothesized that sex hormones influence the bone phenotype of Gal3-null mice. To test this, we performed gonadectomy (GDX) sex hormone rescue on male and female Gal3-null mice and compared them to their wild-type littermates. Following GDX, both male and female Gal3-null mice had significantly greater cortical bone mass and improved geometry (MMI) following GDX compared to wild types, as measured by mCT. Sex hormone rescue revealed that cortical bone from Gal3- null mice was unresponsive to androgen and hyper-responsive to estrogen, which likely explains the sexual dimorphism we previously observed in sex hormone replete animals. However, while estrogen was able to suppress axial expansion in wild-type mice, estro- gen only enhanced endocortical infilling in Gal3-null mice, suggesting that estrogen function on periosteal bone formation is altered in Gal3- null mice. Previously we observed that during aging, the cortical expansion in Gal3-null femurs was coupled to reduced mechanical properties as assessed by 4-point bending. Following GDX, reduced mechanical properties were again observed in male Gal3-null femurs. Interestingly, the empty pellets used as controls for sex hormone rescue did not affect bone geometry compared to GDX alone, but the pellets did rescue mechanical strength in femurs from Gal3-null males. Taken together, these results suggest that the cortical expansion in Gal3-null mice is independent of tissue quality and that the reduced mechanical strength in Gal3-null bones can be rescued. This study identifies Gal3 to have both sex hormone dependent and independent roles in regulating cortical bone mass and quality. While further experimentation is necessary, our data provide further support for the development of Gal3 targeted therapies to improve bone mass during aging and in sex hormone deficient conditions.

P27

Biglycan Deficiency Impairs Bone Toughness through Reduced Bound Water in Bone Matrix. Rui Hua*[1], Jie Bai[1], Qingwen Ni[2], Jean X. Jiang[3], Xiaodu Wang[1]. [1]University of Texas at San Antonio, United States, [2]Texas A&M International University, United States, [3]UT Health Science Center at San Antonio, United States

Proteoglycans (PGs) are one of the structural non-collagenous proteins (NCPs) in the extrafibrillar bone matrix, containing long unbranched glycosaminoglycans (GAGs) chains attached to core proteins. Previous studies show that PGs may play a pivotal role in sustaining the toughness of bone via retaining the bound water in the matrix in an in vitro model using human cadaveric bone samples. To further verify the mechanism, this study intended to examine the effect of PGs on the toughness of bone in vivo using a biglycan-deficient mouse model. Biglycan belongs to small leucine-rich proteoglycans (SLRPs) and is considered to be one of the major subtypes of PGs in bone matrix. In this study, wild-type and biglycan (Bgn) knockout (KO) mice were used and biochemical assays were performed to determine the amount and major subtype of GAGs in bone matrix. First, Bgn KO mice model were validated by immunoblotting with antibodies for Bgn and its related PGs, decorin (Dcn). In mineralized bone matrix, Bgn expression was totally abolished while the level of decorin was unaffected in the bone samples of Bgn knockout. Agarose electrophoresis showed that

chondroitin sulfate was the major subtype of GAGs. Next, the level of GAGs was determined in both mineralized and non- mineralized bones. A significant decrease of GAGs amount was observed only in the mineralized compartment, but not in the non-mineralized compartment of Bgn KO mouse bone. Moreover, results from a novel nanoscratch test showed a significant reduction in the in situ toughness of bone of Bgn KO mice compared to WT mice. In addition, low field NMR measurements exhibited that Biglycan deficiency had a significant effect on the amount of bound water in bone by an average reduction of 12.6%. Taken together, our results demonstrated that Bgn in bone matrix may play a pivotal role in retaining bound water in bone matrix, thus imparting the plasticity and toughness to bone.

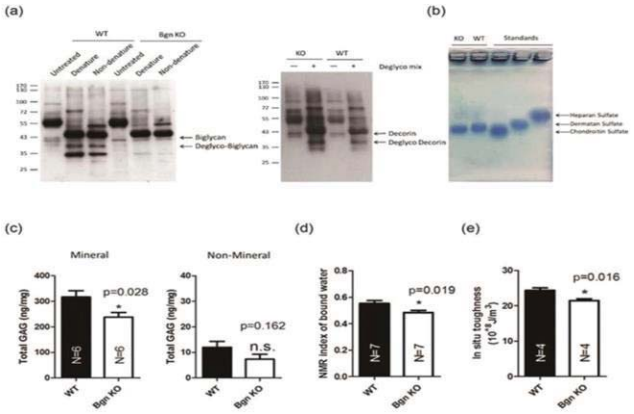

P28

Diverging Periosteal and Endosteal Modeling/Remodeling Under PTH and Mechanical Loading. Samuel Robinson*, Yizhong Hu, X. Edward Guo. Columbia University, United States

Mechanical loading and intermittent injections of parathyroid hormone (PTH) are both established stimulants of an anabolic response in bone, and have been shown to produce combined effects in some regions of both trabecular and cortical bone [1]. However, a characteristic of natural cortical bone growth is concurrent endosteal resorption and periosteal formation, a means of increasing resistance to bending without dramatically affecting total bone mass. Furthermore, bone adaptation can occur through either remodeling (resorption followed by formation) or modeling (uncoupled resorption or formation). With the possibility of both formation and resorption being affected by these treatments and adaptation occurring through either regime, we sought to more accurately characterize the response using dynamic *in vivo* morphometry. We treated C57Bl/6 mice with daily injections of PTH and uniaxial tibia loading for 3 weeks, with an additional 2 weeks of injections and regular cage activity. Weekly micro- computed tomography scans of loaded and non-loaded limbs were registered between adjacent weeks using a custom algorithm to detect the quantity and location of forma- tion and resorption events. The dynamic progression of formation/resorption at each voxel location was recorded to classify events as modeling or remodeling. On the periosteal surface, anabolic modeling was significantly increased with loading and PTH, and the two-way interaction was significant. Correspondingly, catabolic modeling was significantly suppressed. However, on the endosteal surface the effect was reversed: loading led to significantly more catabolic modeling and less anabolic modeling. Despite an early endosteal anabolic response in the loaded groups, formation slowed and then decreased to levels below non-loaded controls. In its place, a significant progression of endosteal catabolic modeling ensued, independent of PTH treatment. Formation via remodeling decreased with load on the periosteal surface, potentially a result of the response being dominated by modeling, and did not differ among groups on the endosteal surface. Therefore, in total our data demonstrate surprisingly different bone dynamics on the enodosteal and periosteal surfaces in response to load, some aspects of which are enhanced by PTH. The localized mechanical and biochemical environments that contribute to this divergence remain to be further investigated.

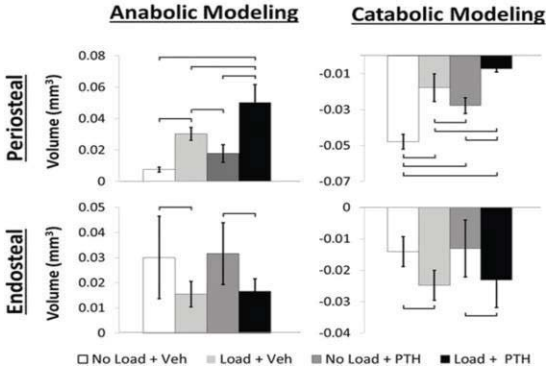

P29

Daily PTH (1-34) Administration Preserves Bone Structure and Enhances Bone Turnover after Severe Immobilization-induced Bone Loss. Lauren Harlow*[1], Karim Sahbani[1], Jeffry Nyman[2], Christopher Cardozo[1], William Bauman[1], Hesham Tawfeek[1]. [1]James J. Peters VA Medical Center, United States, [2]Vanderbilt United States

Immobilization as a result of complete spinal cord injury (SCI) is associated with rapid bone loss that progresses to severe osteoporosis. This study determined whether daily PTH administration would reduce bone loss after acute SCI. Thus, 20 week old wild type female mice underwent sham or SCI by complete spinal cord transection at thoracic segments T9-10. Human PTH (1-34) (80 mg/kg/day) or vehicle was injected subcutaneously daily starting on the day of surgery and continued for 30 days when animals were sacrificed. Tibias and femurs were isolated and examined by micro- computed tomography scanning (micro-CT) and histology; serum markers of bone turnover were measured using biochemical assays. Micro-CT analysis of proximal tibial metaphysis revealed that the SCI/vehicle animals exhibited 49% and 18% reduc- tion in trabecular bone volume/total volume and trabecular thickness, respectively, compared to sham/vehicle controls. Furthermore, analysis of femoral mid-shaft region showed that the SCI/vehicle group had 15% lower cortical thickness and 16% higher cortical porosity than sham/vehicle counterparts. Interestingly, PTH administration to SCI animals improved bone structure and architecture by restoring 78% of fractional bone volume, increasing connectivity to 366%, and lowering structure model index (higher plate/rod structure ratio) by 10% compared to sham/vehicle animals. PTH favorable effects were also evident on the cortical bone of the SCI animals by attenuating cortical bone loss to only 5% and completely preventing the SCI-associated increase in cortical porosity. Dynamic and static histomorphometry evaluation of femurs of immo- bilized SCI/vehicle animals demonstrated a marked 49% and 38% decline in osteoblast and osteoclast number/tissue area, respectively, and 35% reduction in bone formation rate. In contrast, PTH treatment of SCI animals preserved osteoblast and osteoclast number and enhanced bone formation rate (P=0.003) to levels that were similar to or higher than sham/vehicle able-bodied animals. Furthermore, PTH-treated SCI animals had higher levels of both bone formation (P=0.0001) and resorption markers (P=0.01) than either SCI or sham/vehicle groups. In summary, daily PTH administration improves bone structure and promotes bone turnover in severely immobilized SCI animals. These findings suggest that intermittent PTH receptor activation is an effective therapeutic approach to preserve bone integrity after severe immobilization.

P30

Loss of GORAB Leads to an Impaired Anabolic Cortical and Cancellous Bone Response to Mechanical Loading. Haisheng Yang*[1], Anne Seliger[2], Wing-Lee Chan[2], Michael Thelen[2], Uwe Kornak[2], Bettina Willie[3]. [1]Beijing University of Technology, China, [2]Charité-Universitätsmedizin Berlin, Germany, [3]Shriners Hospital for Children-Canada, McGill University, Canada

Gerodermia osteodysplastica (GO) is a segmental progeroid disorder caused by loss- of-function mutations in the GORAB gene, associated with early onset osteoporosis and bone fragility [1]. A mouse model of GO (*Gorab*^{Prx1}) was generated wherein the Gorab gene was deleted in long bones. We observed an abnormal osteocyte morphology and a reduced and disrupted canalicular network in *Gorab*^{Prx1} mice [2]. Given the crucial role of osteocytes in sensing mechanical signals and orchestrating adaptive bone remodeling, we hypothesized loss of Gorab would lead to an impaired anabolic response of cortical and cancellous bone to loading. In vivo cyclic compressive loading was applied to left tibiae of 10-week-old *Gorab*^{Prx1} and littermate control (LC) mice for 2 weeks (+1200 mE at midshaft determined by strain gauging, 216 cycles/day at 4 Hz) and right tibiae served as internal controls. Load-induced changes in bone formation and resorption were quantified for both midshaft cortical and metaphyseal cancellous bone using in vivo microCT-based 3D time-lapse morphometry [3] and fluorochrome-based 2D histomor- phometry. In LC mice, loading significantly enhanced bone formation responses, with the loaded limb having increased volume and surface area of newly formed bone compared to the control limb for the midshaft cortical ($MV/BV_{day0\text{-}15}$: +741%, $MS/BS_{day0\text{-}15}$: +174%) and metaphyseal cancellous bone ($MV/BV_{day0\text{-}15}$: +189%, $MS/BS_{day0\text{-}15}$: +82%)(Fig. 1). Loading significantly reduced resorbed bone volume and surface for metaphyseal cancellous bone in LC mice ($EV/BV_{day0\text{-}15}$: -22%, $ES/BS_{day0\text{-}15}$: -27%). Dynamic histomorphometry confirmed that both endocortical and periosteal bone formation rates increased with loading at the tibial midshaft in LC mice (Ec.BFR/BS: +240%, Ps.BFR/BS: +725%). In *Gorab*^{Prx1} mice all bone formation and resorption parameters were not significantly different between the loaded and control limbs (Fig. 1). These results show that loss of Gorab leads to a complete absence of bone formation and resorption responses to mechanical loading for both cortical or cancellous bone. These data suggest the low bone mass phenotype of *Gorab*^{Prx1} mice could be attributable in part to a loss in skeletal mechanoresponsiveness. Future strategies to treat GO disease could consider therapies to restore or enhance adaptive bone formation. References: [1] Hennies et al, 2008 *Nat Genet*, [2] Steiner et al. 2015 *JBMR* 28 (Suppl 1), [3] Birkhold 14*Bone*.

P31

Combining fractal- and entropy-based bone texture analysis for the prediction of Osteoarthritis: data from the Multicenter Osteoarthritis study (MOST). Zsolt Bertalan*[1], Richard Ljuhar[1], Stefan Nehrer[2], Dayul Ljuhar[3], Astrid Fahrleitner-Pammer[4], Hans-Peter Dimai[4]. [1]ImageBiopsy Lab, Austria, [2]Danube University Krems, Austria, [3]Braincon Technologies Research, Austria, [4]Medical University Graz, Austria

INTRODUCTION: Osteoarthritis (OA) is one of the leading causes of long-term pain and disabilities associated with musculoskeletal disorders. Effective treatment and disease-progression slowdown depend on early detection and quantification of risk. However, current disease parameters, like joint space width (JSW), have proven to be insufficient for the prediction of OA. The purpose of the present study was to investigate if combining fractal- and entropy-based bone texture analyses with joint space width (JSW) and joint space area (JSA) may improve prediction of OA. METHODS:

Conventional posterior-anterior (PA) knee radiographs of men and women were obtained from the Multicenter Osteoarthritis Study (MOST) database, which provides valuable information to identify and define modifiable biomechanical, bone and struc- tural, nutritional, and other risk factors for new disease and progression of existing disease (1) Oriented fractal- and entropy based texture algorithms were developed, using state-of-the-art computer hardware and software as well as specific machine-learning algorithms. The selected subchondral area used for textural analyses included 4 regions of interest (ROI) in the proximal tibia and one on each condyle of the distal femur (Figure 1). Furthermore, JSW and JSA were assessed using newly developed and fully automated software. RESULTS: 1092 conventional knee radiographs obtained from one study center were screened for eligibility. Of these, a total of 574 radiographs (230 women, 344 men) met the inclusion criteria, i.e. Kellgren & Lawrence (KL) score of 0 at baseline. At month 84, 41 female and 79 male patients had developed KL 1, and 189 female and 265 male patients remained at KL0. Area-Under-the-Curve (AUC) for incident OA using JSW/ JSA and clinical features was 0.67 0.08 for women, and 0.61 0.1 for men. In contrast, combining fractal/entropy-based texture, JSW/A and clinical features resulted in sig- nificantly improved AUC for women and men (0.80 0.07 for women and 0.69 0.1 for men, respectively). To test whether these differences in predicting incident-OA were significant, we performed classifier comparison: $t = 3.84$; $p < 10\text{-}3$ for women, and $t = 3.38$; $p < 10\text{-}3$ for men. CONCLUSION: This study provides strong evidence, that a combination of fractal- and entropy- based textural analyses of plain subchondral bone radiographs together with JSW/A and clinical features is superior to JSW/A and clinical features alone in predicting incident OA in men and women.

1) http://most.ucsf.edu/studyoverview.asp

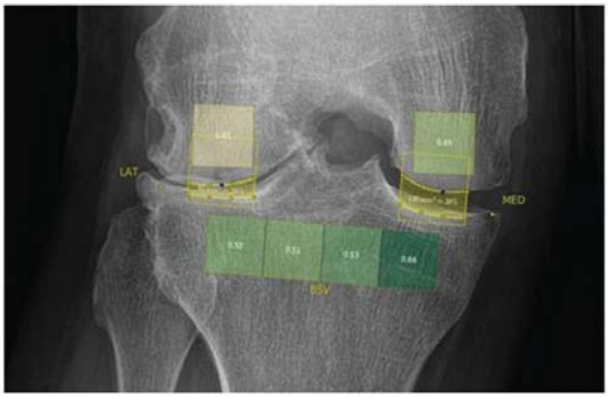

P32

Bisphosphonate inhibits bone resorption by blocking autophagy in osteoclasts. Sol Kim*[1], Vadim A. Goldshteyn [1], Atsushi Arai[2], No-Hee Park[1], Reuben Kim[1]. [1]UCLA School of Dentistry, United States, [2]Matsumoto Dental University, Japan

Bisphosphonates (BPs), pharmacological agents for the treatment of bone-related diseases such as osteoporosis or cancer metastasis. Although BP is known to target osteoclasts (OCs) to inhibit bone resorption, the underlying molecular mechanism remain unclear. Matured OCs release a variety of proteases including cathepsin K (CtsK), TRAP, or metalloproteases (MMPs) in order to degrade bone matrixes, and these proteases are required for further processing to be cleaved within a lysoosome to achieve its active form. Here, we investigated the effect of BP on processing of proteases during osteoclastogenesis. Bone marrow-derived macrophages (BMMs) were treated with M-CSF and RANKL to induce osteoclastic differentiation in the presence or absence of zoledronic acid (ZOL). We found that ZOL suppressed not only maturation and activity of bone- degrading protease but resorptive functions of osteoclasts in vitro. During osteoclsto- genesis, RANKL-induced OCs diminished in protein expression of autophagy related (Atg) such as Atg4, 7, beclin1 or p62, whereas ZOL caused a delay in diminished expression of Atg proteins, suggesting an accumulation of non-degradative autophago- somes. Similar to ZOL treated OCs, the accumulation of Atg proteins was observed in autophagy inhibitor, bafilomycin A, treated osteoclast. Furthermore, the maturation of proteases was also blocked by autophagy inhibitor. At the molecular level, BPs block the mevalonate pathway that leads to target protein prenylation including farnesylation and geranylgeranylation. Mechanistic studies revealed that BP inhibits osteoclastogenesis by interfering prenylation with small GTP- binding proteins of Rab family, specifically Rab7, and we confirmed that Rab7 is required for osteoclast differentiation in vitro. Conditional Rab7 knock-out mice which is specific Rab7-deficient in mature osteoclast displayed osteopetrotic phenotype by the failure of osteoclasts to resorb bone, and this impairment caused a significant inhibition of bone resorption in vitro. Taken together, our study demonstrates that BPs inhibit bone-resorptive function of osteoclast by suppressing the maturation of bone-de to secret into the ruffled border by interfering autophagy processing.

P33

Anti-Siglec-15 antibody inhibits bone-resorbing activity of osteoclasts and stimulates osteoblast differentiation. Nobuyuki Udagawa*[1], Shunsuke Uehara[1], Masanori Koide[2], Atsushi Arai[2], Toshihide Mizoguchi[2], Midori Nakamura[1], Yasuhiro Kobayashi[2], Naoyuki Takahashi[2], Chie Fukuda[3], Eisuke Tsuda[3]. [1]Department of Biochemistry, Institute for Oral Science, Matsumoto Dental University, Japan, [2]Institute for Oral Science, Matsumoto Dental University, Japan, [3]Rare Disease & LCM Laboratories, , Daiichi Sankyo Co., Ltd., Japan

We previously identified sialic acid-binding immunoglobulin-like lectin 15 (Siglec- 15) as a gene product expressed in giant cell tumor of bone. The expression of Siglec-15 was increased with osteoclast formation in mouse bone marrow (BM) cultures. Treatment of BM macrophage cultures with anti-Siglec-15 antibody (Siglec-15 Ab) inhibited TRAP-positive multinucleated cell formation induced by RANKL and M- CSF. However, Siglec-15 Ab failed to suppress TRAP-positive mononuclear cell (mono- nuclear osteoclast) differentiation. We then examined the effects of Siglec-15 Ab on the appearance of osteoclast precursors, which express RANK and c-Fms but not TRAP, in mouse co-cultures of osteoblasts and BM cells. Siglec-15 Ab showed no effects on the appearance of osteoclast precursors in the co-culture. Osteoclasts prepared from mouse co-cultures were further cultured on dentin slices in the presence or absence of Siglec-15 Ab. Pit-forming activity of osteoclasts was inhibited by Siglec-15 Ab. The actin rings in osteoclasts on dentin slices almost disappeared within 3 hours in the presence of Siglec- 15 Ab. Finally, we examined effects of Siglec-15 Ab on osteoblast differentiation associated with osteoclast differentiation in whole BM cultures treated with RANKL and M-CSF. Siglec-15 Ab suppressed TRAP-positive multinucleated cell formation, but not TRAP-positive mononuclear cell differentiation. Interestingly, Siglec-15 Ab treat- ment stimulated the appearance of alkaline phosphatase-positive osteoblasts in those cultures. Siglec-15 Ab failed to stimulate osteoblast differentiation in the whole BM cultures treated without RANKL and M- CSF. Our findings suggest that Siglec-15 plays important roles in the induction of both bone-resorbing activity of mature osteoclasts and osteoblast differentiation, and that mononuclear osteocla ts may play an important role in the coupling between bone resorption and formation.

P34

Sclerostin-Neutralizing Antibody Treatment Increases Serpinf1(PEDF) Expression In Mice Tibiae Independent of Mechanical Loading. Tobias Thiele*[1], Catherine Julien[2], Anne Seliger[1], Annette Birkhold[3], Michael Thelen[1], François Lefebvre[4], Martin Pellicelli[2], René St-Arnaud[2], Michael Ominsky[5], Georg Duda[1], Uwe Kornak[6], Sara Checa[1], Bettina M. Willie[2]. [1]Julius Wolff Institute, Universitätsmedizin Charité, Germany, [2]Shriners Hospital for Children, Canada, [3]University of Stuttgart, Germany, [4]Canadian Centre for Computational Genomics, Canada, [5]Amgen, United States, [6]Institute for Medical Genetics and Human Genetics, Charité- Universitätsmedizin, Germany

Bone adapts to mechanical stimuli to maintain an optimized structure. Mechanical loading causes decreased expression of sclerostin, an osteocyte-specific secreted glyco- protein encoded by the Sost gene, known to inhibit Wnt-ß-catenin signaling. However, it appears that load-induced formation can occur independent of sclerostin. Previous microCT analyses (1) of 78 wk old mice treated with sclerostin neutralizing antibody (Scl-Ab) and loaded for 2 wks showed a bone formation response to Scl-Ab and loading. Recent analyses of these data using time-lapse microCT registration (2) showed an additive formation response to loading and Scl- Ab. We aimed to examine the effect of load on gene expression after acute sclerostin inhibition. We performed a single bout of in vivo cyclic compressive loading to the left tibia of thirty,78 wk old female C57Bl/6J mice, half of which were treated with 25 mg/kg of Scl-Ab, twice weekly for 2 weeks prior to loading (n=5/treatment/time point). The right limb was a nonloaded internal control.

Mice were dissected at 1, 8 or 24 hours after loading and bone marrow was flushed. RNA was extracted, reverse-transcribed, and analyzed by microarray/qPCR. Serpinf1 was found to be in the top ten regulated genes following Scl-Ab treatment (Fig 1A). Serpinf1 expression levels were highly upregulated independent of loading. Sost, Dkk1, Wif1 (Fig 1 B) were also highly upregulated in response to Scl-Ab, independent of loading. Results were validated by IHC in 2 wk loaded mice, which had higher sclerostin and serpinf1 levels in osteocytes after Scl-Ab treatment. Osteocytic-like cell lines were also used to confirm the effect of Scl-Ab on Wnt inhibitors expression. Unpublished data shows Serpinf1 is upregulated in Sost KO mice compared to littermates. Other recent studies have shown Scl-Ab treatment causes activation of Wnt target genes (3,4). Serpinf1 and/ or other Wnt pathway inhibitors might be responding to decreased tissue level strains due to increased bone mass. Serpinf1 may also be upregulated due to increased mineralization (5), although we saw unchanged serpinf1 expression after 2wks of load-induced bone formation in vehicle treated group. These data provide a possible explanation for the diminished bone formation response to Scl-Ab after longer-term treatment (6). (1) Pflanz et al. ASBMR 2012, (2) Birkhold et al. Bone 2014, (3) Nioi et al.JBMR 2015, (4) Taylor et al. Bone, 2016 (5) Rajagopal et al. MGM, 2016 (6) McClung et al. NEJM 2014

P35

miR-145 overexpression impairs osteocytes structure and function in Adolescent Idiopathic Scoliosis , Wayne Yuk-wai Lee*[1], Jiajun Zhang[1], Yujia Wang[1], Ross KK Leung[2], Tsz-ping Lam[1], Yong Qiu[3], Jack Chun-yiu Cheng[1]. [1]Department of Orthopaedics and Traumatology, SH Ho Scoliosis Research Laboratory, The Chinese University of Hong Kong, Shatin, NT, Hong Kong SAR, China, Hong Kong, [2]School of Public Health, The University of Hong Kong, Hong Kong SAR, China, Hong Kong, [3]Spine Surgery, Nanjing Drum Tower Hospital, Nanjing University, Nanjing, a, China

Adolescent Idiopathic Scoliosis (AIS) is a three-dimensional spinal deformity of unclear etiopathogenesis with the prevalence of 1-4% worldwide. Systemic low bone mineral density (BMD) was found to be one of the significant prognostic factors for curve progression. Better understanding of how bone quality is affected will help to advance prognosis and therapeutic strategies as current treatment regime is mainly targeting on the anatomical abnormality. Osteocytes are specialised cell type for mechanosensing and orchestrating bone metabolism. We have reported abnormal osteocytes structure in AIS bone biopsies (Fig. 1a). This work investigated further the underlying mechanism and explored the potential clinical implication. In this case-control study, iliac crest trabecular bone biopsies were harvested intrao- peratively from 9 AIS patients undergoing posterior spinal fusion and from 5 age- matched control subjects undergoing respective orthopaedic surgery requiring iliac crest autografts with informed consent and then divided for microRNA microarray for identification of miR candidates and osteoblasts isolation. Osteocyte culture was derived from primary osteoblasts seeding in type I collagen gel and validated by co- immunostaining of osteocyte markers (sclerostin and E11) and secreted sclerostin in conditioned medium. The biological roles of the identified miR target on osteocyte differentiation were evaluated with loss-of-function test. The serum levels of osteocyte secreted cytokines and the miR target in another cohort of 100 subjects were measured with Multiplex and qPCR. Mann-Whitney test and Spearman's rank correlation were used for statistical analysis. Compared with the control, primary AIS osteocytes (Fig. 1b) was found to have significantly lower transcriptional level of osteocytic markers (*E11, Fgf23 and Sost*) and cell gap junction protein (Connexin 43, *Gja1*), and secreted less sclerostin. Microarray and miRWalk analysis identified miR-145-5p as a potential upstream regulator via b-catenin signalling pathway. miR-145-5p expression was significantly and positively correlated with *Ctnnb1*. Knockdown of miR-145-5p could significantly down-regulate active b-catenin expression in AIS osteoblasts, up-regulate *E11 and Sost* mRNA expres- sion and rescue sclerostin secretion. Correlation analysis showed a negative correlation between miR-145-5p and sclerostin in AIS which was absent in the control. This study provided new evidence of structural and functional abnormalities of osteocyte, and its link to aberrant miR-145-5p/b-catenin signalling in the pathogenesis of AIS. Our findings shed light on the potential role of epigenetic-related factors like the etiopathogenesis of AIS and the development of circulating miRNAs as potential biomarkers.

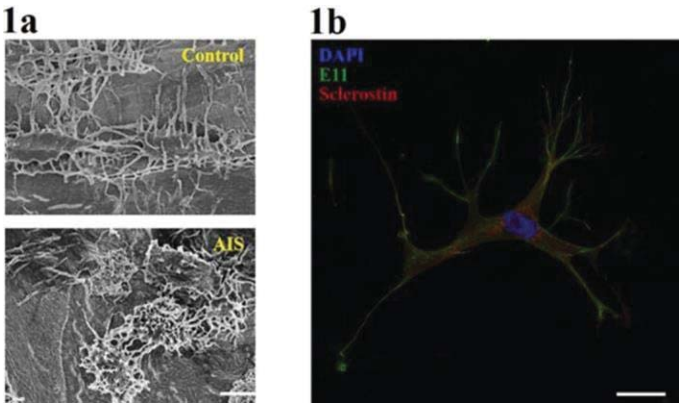

Figure 1: Abnormal osteocytes structure in AIS by SEM and Confocal image of primary osteocytes.

P36

Profiling the composition of osteocyte pericellular matrix (PCM) in vivo and in vitro. Jerahme Martinez*[1] Shaopeng Pei[1], Shubo Wang[1], Ashutosh Parajuli[1], Mary Farach-Carson[2]. [1]University of Delaware, United States, [2]The University of Texas Health Science Center at Houston School of Dentistry, United States

Osteocytes comprise the overwhelming majority of the cells in bone and play a crucial role in maintaining bone homeostasis and orchestrating bone's responses to mechanical loading. Increasing evidence indicates that the proteoglycan-rich osteocyte pericellular matrix (PCM) functions as a mechanical sensor to detect external loading signals. Previously, we identified perlecan/HSPG2, a large heparan sulfate proteoglycan, as a key component of the osteocyte PCM and demonstrated its importance for *in vivo* loading and unloading. In those studies, we used a perlecan-deficient mouse that mimics the human skeletal dysplasia Schwartz-Jampel Syndrome (SJS), which develops both osteoarthritis and osteoporosis. We hypothesize that perlecan is part of a mechan- osensitive tethering complex in the osteocyte PCM that is disrupted in SJS. To test this hypothesis in vivo and in vitro, we first examined the tissue PCM composition, using a mass spectrometry-based glycoproteomic analysis of bone tissue extracts from both wild-type and perlecan-deficient mice. For comparison, we investigated the PCM pro- duced by commonly used osteocyte cell lines, MLO-Y4 and IDG-SW3. To enrich PCM constituents prior to mass spectroscopy analysis, we metabolically labeled osteocyte- secreted sialylated glycoproteins using an azide-modified sugar, then isolated labeled products using dibenzocyclooctyl (DBCO) copper-free click chemistry. The results provide a comprehensive expression profile of native actively produced osteocyte PCM glycoconjugates, among which are novel candidate targets that, alone or in complex with perlecan, may be key components of the osteocyte's mechanosensing complex. This novel strategy provides a powerful launchpad from which to dissect the structure-function relationships of the glycoconjugate components of the load detecting complexes in osteocyte-rich bone.

P37

Deletion of RANKL from Osteoblasts and Osteocytes in Osteogenesis Imperfecta Mice (oim) Increases Bone Mass but Does Not Rescue Bone Fragility or High Bone Turnover. Sarah Zimmerman*, Melissa Heard- Lipsmeyer, Milena Dimori, Charles O'Brien, Roy Morello. University of Arkansas for Medical Sciences, United States

Osteogenesis imperfecta (OI) is characterized by osteopenia and bone fragility, and OI patients and animal models of OI often exhibit high bone turnover with the net result of low bone mass. The mechanisms driving this high bone turnover are unknown, although recent evidence shows that osteocytes can secrete many cytokines/factors that are able to regulate bone turnover under normal physiological conditions. Importantly, osteocytes have been shown to be the main source of Rankl for osteoclast formation in cancellous bone in adult mice. Therefore, we hypothesized that Rankl from osteocytes contributes to the increased osteoclast number and bone resorption in OI. To test this, we deleted Rankl from osteoblasts and osteocytes in a murine model of osteogenesis imperfecta (oim mice). This was accomplished by crossing mice carrying a floxed Rankl gene, a Cre transgene under the control of the Dmp1 promoter, and oim mice. This produced mice with the genotype Col1a2oim/oim; RanklFl/Fl; Dmp1-Cre (also called "oim-Rankl-cKO"). Compared to Col1a2oim/oim; RanklFl/Fl controls (which are not distinguishable from oim mice), oim-Rankl- cKO mice were similar in body weight and femoral biomechanical properties but had increased trabecular bone volume, trabecular number and trabecular thickness in the femur. Cortical thickness was also increased in the spine. Strikingly, serum CTX levels remained high in the oim- Rankl-cKO mice despite the deletion of Rankl in mature osteoblasts and osteocytes. This indicates that Rankl produced by osteocytes is not the main driver of the high bone turnover seen in oim mice, and that a likely cause may be Rankl produced by other cell types or perhaps the influence of other cytokines.

P38

Diagnostic Error Rates of Bone Mineral Density and Other Proxies for Bone Strength. Lyn Bowman*, Gabriel C. Hausfeld, Emily R. Ellerbrock, Jennifer M. Neumeyer, Tyler C. Beck, Maureen A. Dean, McKenzie L. Nelson, Anne B. Loucks. Ohio University, United States

Purpose. Osteoporosis is characterized by a decline in bone strength, but a patient's bone strength cannot be measured directly. So, osteoporosis is diagnosed in patients with T-scores of bone mineral density (BMD) below a threshold of -2.5. However, most such patients do not fracture, and most fractures occur in patients diagnosed as not osteo- porotic. These unexpected outcomes drive healthcare costs. The purpose of this study was to assess the extent to which unexpected outcomes of osteoporosis treatment might be explained by the imperfect correlation of bone strength and BMD, and whether such outcomes might be reduced by other diagnostic methods. Methods. When classifying bivariate observations of any Y and X relative to thresh- old values, imperfect correlation introduces false positive and false negative errors (See Figure). We defined the proportion of these errors in a population whose bone strength Y is predicted by proxy X as the Diagnostic Error Rate (DER) of that proxy. By statistical theory, geometry and algebra, we derived that, for any diagnostic threshold values, DER = SEE/(Y(Xmax) – Y(Xmin)), where SEE = the standard error of the estimate in the regression of Y on X, and Y(Xmax) and Y(Xmin) are the predicted values of the maximum and minimum values of X, respectively. We then searched the literature for regressions of human bone strength on BMD and other proxies. Because bones break as structures not materials, we considered only structural tests of bone strength measured directly by quasistatic mechanical testing (QMT). We also measured the bending strength, cortical porosity (CP), and bending stiffness (EI) of ulna bones in 35 cadaveric human arms from men and women ranging widely in age (17-99 yrs) and body mass index (BMI) (13-40 kg/m2). Results. We found the following DER values: BMD = 15-24%, bone mineral content = 11-28%, quantitative computed tomography (QCT) with finite element analysis = 11-13%, peripheral QCT = 12-17%, reference point indentation = 36-42%, BMI = 28%, CP = 34-44%, EI = 5-8% by QMT and 7% noninvasively by cortical bone mechanics technology (CBMT). If only the lower half of the

population (BMD T-scores <0) is considered for treatment, DER doubles. If only T<-1 is considered, DER is multiplied by 6. Conclusions. Misallocation of patients to treatment by BMD is sufficient to account d outcomes of osteoporosis treatment. CBMT may have the greatest potential for reducing these outcomes.

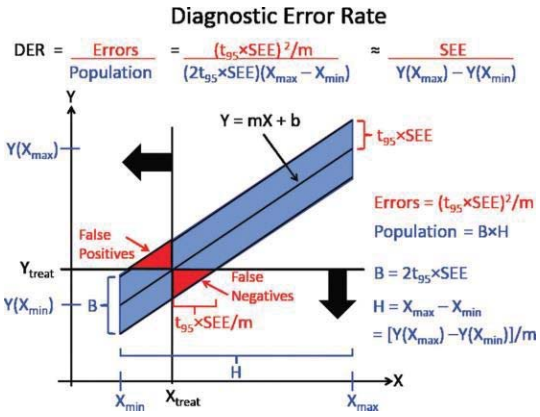

P39

Comparison of Metaphyseal and Diaphyseal Microstructure of the Tibia in Elderly Men Measured by HR-pQCT. Andrew Burgahrdt*[1], Andrew Yu[1], Sharmila Majumdar[1], Dennis Black[1], Eric Orwoll[2]. [1]University of California, San Francisco, United States, [2]Oregon Health & Science University, United States

The most recent iteration of HR-pQCT (XtremeCT II, Scanco Medical) can image more proximal regions of the extremities, including the tibial diaphysis, and achieve a higher nominal resolution of 61mm. These advances make direct measurement of micro- structural features of metaphyseal and diaphyseal cortical bone structure possible (Figure 1). Our objective was to (1) adapt a cortical bone analysis pipeline to measure the 30% diaphyseal tibia from second generation HR-pQCT images; and (2) evaluate the relationship to cortical bone measured at the standard distal metaphyseal position. We used data from a cohort of elderly men who attended the fourth visit of the Osteoporotic Fractures in Men (MrOS) study and had acceptable quality HR-pQCT scans of the distal and diaphyseal tibia. Associations between measures of bone density, geometry, structure, and mFEA estimates of strength were evaluated using Pearson correlations across the entire cohort, and within tibial length quintiles. Of the subjects studied with both distal and diaphyseal scans (N=1561), 98% had acceptable distal scans, 96% acceptable diaphyseal scans, and 95% had both (N=1475). A custom automated QA procedure determined segmentation error rates < 2% for the optimized diaphyseal tibia analysis pipeline. Cortical BMD was significantly higher at the diaphsyeal site (Table 1). Porosity was approximately half at the diaphyseal site: the number of pores was lower, but pore diameter was not different. The correlation between metaphyseal and diaphy- seal bone was moderate for integral BMD, total area, and cortical thickness (r2=0.31- 0.49, p<0.0001), and poor for porosity-related measures (r2<0.10, p<0.0001). Inter-site correlations for To.Ar, Ct.Th, and Ct.Ar were minimally different when determined for tibial-length quintiles (data not shown), suggesting site-wise variance is not due to scan positioning variability associated with limb- length. This indicates that unique biological variability can be assessed by measuring both distal and diaphyseal sites. In conclusion, measurement of bone at the 30% diaphysis by second generation HR-pQCT likely provides complimentary information about skeletal status to traditional distal metaphy- seal scan positions.

Figure 1. Scout view image illustrating the metaphyseal and 30% diaphyseal scan regions measured in the tibia by second generation HR-pQCT.

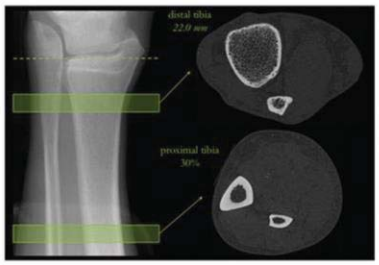

Table 1. Mean and standard deviations for bone measures at the standard distal metaphysis, 30% diaphysis, and the Pearson correlation coefficient between sites.

		Diaphyseal [mean (SD)]	Distal [mean (SD)]	r²
BMD	[mg/cm³]	730.6 (78.3)	283.1 (55.2)	0.48
Ct.BMD	[mg/cm³]	995.5 (35.2)	781.5 (79.8)	0.14
To.Ar	[mm²]	440.4 (52.1)	881.2 (130.7)	0.42
Ct.Ar	[mm²]	312.9 (40.4)	139.5 (31.5)	0.30
Tb.Ar	[mm²]	132.0 (40.7)	747.8 (139.2)	0.25
Ct.Th	[mm]	6.2 (0.9)	1.5 (0.3)	0.31
Ct.Po	[%]	2.1% (1.2%)	4.3% 1.7%	0.06
Po.Dm	[mm]	0.26 (0.0)	0.24 (0.0)	0.04
Stiffness	[kN/mm]	326 (57.4)	215 (50.1)	0.46
App.Mod	[MPa]	8098 (673.9)	2191 (526.1)	0.11

Figure 1 and Table 1

P40

Spatial Assessment of Bone Microarchitecture in Postmenopausal Women With a Recent Colles' Fracture. Andrew Burghardt*[1], Sundeep Khosla[2], Julio Carballido-Gamio[3]. [1]University of California, San Francisco, United States, [2]Mayo Clinic, United States, [3]University of Colorado Denver, United States

The spatial assessment of bone with data-driven image analysis techniques, including statistical parametric mapping (SPM), could identify biologically-relevant regions and bone features that distinguish clinical populations. We applied SPM to a case-control study of forearm fracture. The forearms of postmenopausal women with (N=84) and without (N=98) recent Colles' fractures were imaged using HR-pQCT. The distal radius was segmented and spatially normalized to a template effectively aligning corresponding anatomical regions across the study population. These transformations were applied to voxel-based maps of local bone volume fraction (BV/TV), homogenized volumetric bone mineral density (vBMD), strain energy density (SED) from mFEA, and inter- trabecular distances (Tb(1/N)). Surface-based maps of cortical thickness (Ct.Th), Ct. vBMD, and Ct.SED were used to study the cortex, in whole and in three laminar zones: sub-periosteal, central, and endocortical. Voxel/vertex-wise comparisons between cases and controls were performed in the space of the template using general linear models with the bone features as dependent variables, group membership (case or control) as the independent variable, and age, height, weight and the first 5 principal scores of shape as covariates. These comparisons yielded Student's t-test statistical maps (T-Maps), which were corrected for multiple comparisons using the false discovery rate approach (q=0.05). Voxel comparisons indicated that the central medullary space, medial cortex, and more proximal slices were different between populations (Figure 1). The fracture group had reduced SED in the central medullary region near the proximal boundary, but high SED in the palmar cortex near the distal boundary, suggesting impaired load distribution. Although global Ct.Th and Ct.vBMD were significantly different ($p<0.05$), vertex comparisons yielded only small regions of significant difference in the sub-periosteal zone after correction for shape (Figure 2a). Shape was a significant covariate (Figure 2b). Our results indicate a non-uniform spatial association between bone quality features, shape, and fracture status, highlighting t e value spatialassessments bring to understanding the structural basis of fracture risk.

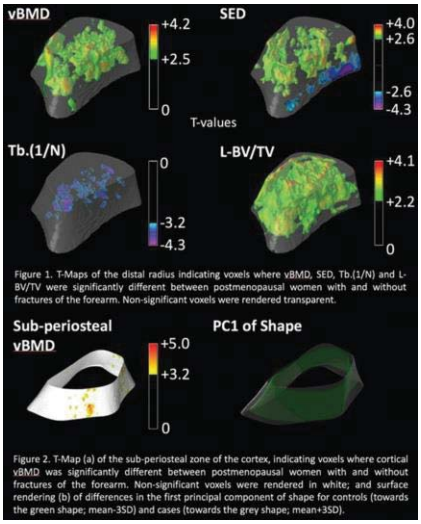

Figure 1 and 2

P41

Inter-scanner Agreement of Trabecular Bone Score Data in Pre-peak Bone Mass Females, Compared to Intra-scanner Data Variability from Pre/peri/ post-menopausal Adults. Jodi Dowthwaite*[1], Renaud Winzenrieth[2], Kristen Dunsmore[3], Tamara Scerpella[4]. [1]SUNY Upstate Medical University, United States, [2]Med-Imaps, France, [3]Syracuse University, United States, [4]University of Wisconsin- Madison, United States

Introduction: Lumbar spine trabecular bone score (TBS) estimates trabecular microarch- itectural traits using gray scale variation in postero-anterior DXA scans (TBS iNsight software, Med-Imaps, France). As scanner models may change during growth monitoring, we sought to evaluate how TBS assessments vary between DXA scanner models in maturing girls (pre- peak bone mass, PREPBM), relative to intra-scanner variation in adult women. Methods: In a sample of PREPBM females, 7.8 to 23.9 years of age (mean 13.4, sd 4.9), we evaluated inter-scanner TBS variation using same-day, lumbar spine scans performed on two cross-calibrated DXA scanners (Hologic QDR 4500W and Discovery A, Waltham, MA). Intra-scanner variation was assessed using same-day, repositioned, dupli- cate Discovery A scans of 28 female ADULTS, 37.5 to 57.8 years of age (mean 45.9, 4.7: pre/peri/post-menopause). PREPBM TBS was determined for vertebrae L1-L4 using Med-Imaps custom software incorporating a pediatric soft tissue thickness correction. Root Mean Square Error coefficients of variation (RMSECV) were calculated in ADULTS (intra-scanner) and PREPBM subjects; the latter were subdivided into children (age 8 to 12) and adolescents (age 13 to 24). PREPBM inter-scanner agreement was evaluated using a Bland-Altman plot. Deming regression generated a reversible equation for PREPBM data conversion between scanners. Results: For PREPBM participants, on both scanners, TBS minima and maxima were 1.15 and 1.67, respectively. QDR scans subtly, consistently and

systematically overestimated TBS relative to Discovery A data, yielding a conversion equation with r2= 0.94 (Discovery A= -0.0137963 + 0.993763 x TBS QDR). ADULT minimum and maximum TBS were 1.10 and 1.61, respectively; variability was almost as high as that observed across children, adolescents and young women of near-peak bone mass. The PREPBM inter-scanner RMSECV (1.95%) was lower than the ADULT intra-scanner RMSECV (2.08%); the ADOLESCENT RMSECV (1.34%) was particularly low com- pared to CHILDHOOD (2.31%). This finding is striking, because for all other standard DXA variables, we have reported ADULT RMSECV lower than PREPBM RMSECV in these same study participants (Dowthwaite et al. JCD 2017). Conclusion: For TBS, in growing girls, inter-scanner hardware disparities are addres- sable using a conversion equation. TBS may vary more than other bone outcomes across peri-menopause, providing a more sensitive indicator of trabecular deterioration.

Bland-Altman Plot:

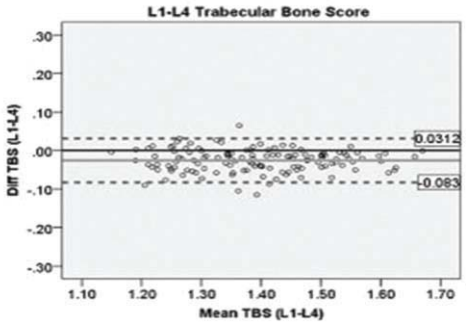

P42

Determination of Risk Threshold for Osteoporosis Therapy: A Decision Curve Analysis Approach. Thao P. Ho-Le*[1], Jackie R. Center[2], John A. Eisman[3], Hung T. Nguyen[4], Tuan V. Nguyen[5]. [1]Centre of Health Technologies, FEIT, University of Technology Sydney, Australia, [2]Bone Biology Division, Garvan Institute of Medical Research; St Vincent Clinical School, UNSW, Australia, Australia, [3]Bone Biology Division, Garvan Institute of Medical Research, NSW; St Vincent Clinical School, UNSW, Australia; School of Medicine, Sydney University of Notre Dame, Australia, Australia, [4]Centre of Health Technologies, Faculty of Engineering and Information Technology, University of Technology, Sydn, Australia, [5]University of Technology, Sydney; Bone Biology Division, Garvan Institute of Medical Research, NSW; St Vincent Clinical School, UNSW; School of Public Health and Community Medicine, UNSW; School of Medicine, Sydney University of Norte Dame, Australia

Aim: Although predictive models are available for fracture risk assessment, there is no scientifically derived threshold of fracture risk for the identification of “high risk” individuals. In this study, we employed a decision curve analysis (DCA) approach to determine the risk of fracture that is optimally suitable for the treatment of osteoporosis. Method: The study was part of the Dubbo Osteoporosis Epidemiology Study that involved 2188 women and 1324 men aged 60 years and above who have been followed up to 20 years. At baseline, bone mineral density (BMD) and clinical risk factors were obtained. During the follow-up period, the incidence of fractures and mortality was ascertained. Three mortality-adjusted models for predicting fracture risk were consid- ered:
(1) Model I included age and femoral neck BMD; (2) Model II included age, femoral neck BMD, history of fracture and falls; (3) Model III had factors in Model II plus lumbar spine BMD. The mortality-adjusted fracture risks were corrected for potential over-fitting by using a 10-fold cross-validation analysis. For each model and each predicted probability of fracture, the clinical net benefit was assessed as the benefits (true positives) over the harms (false positives), with weights assigning to true positives and false positives are derived from the threshold probability of the outcome. The optimal threshold was defined as the point that yields the highest net benefit. Results: In women, compared with the strategy of treating everyone, treating those with 5-yr predicted total fracture risk >20% yielded the greatest benefit (Model III). However, women with 10-yr predicted fracture risk >28% can also be beneficial from a treatment. For hip fracture, Models II and III showed that treating women with 5-yr risk of 4% or 10-yr risk of 6% will yield the greatest benefit. In men, the greatest benefit was achieved at the threshold of 10% for 5-year risk of total fracture or 15% for 10-yr risk. For hip fracture in men, model II showed the best benefit at 2% and 3% for 5-yr risk and 10-yr risk, respectively. Conclusion: Thus, we propose that individuals with 5-yr fracture risk of greater than 10% (for men) and greater than 20% (for women) be considered “high risk” and may be indicated for treatment. For 10-yr prediction, the optimal threshold of fracture risks for treatment indication are >15% for men and >28% for women.

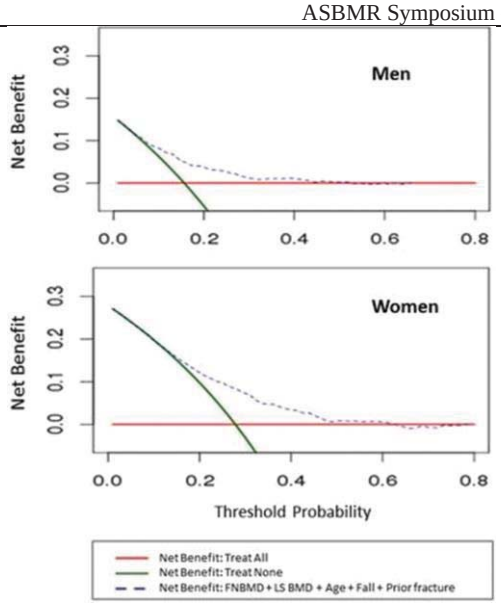

Decision curves for Model III to predict 10-year fracture risk in the elderly

P43

Prediction of Hip Fracture in Post-menopausal Women using Artificial Neural Network Approach. Thao P. Ho-Le*[1], Jackie R. Center[2], John A. Eisman[3], Hung T. Nguyen[1], Tuan V. Nguyen[4]. [1]Centre of Health Technologies, FEIT, University of Technology Sydney, Australia, [2]Bone Biology Division, Garvan Institute of Medical Research; St Vincent Clinical School, UNSW, Australia, Australia, [3]Bone Biology Division, Garvan Institute of Medical Research; St Vincent Clinical School, UNSW, Australia; School of Medicine, Sydney University of Notre Dame, Australia, [4]University of Technology, Sydney; Bone Biology Division, Garvan Institute of Medical Research, NSW; St Vincent Clinical School, UNSW; School of Public Health and Community Medicine, UNSW; School of Medicine, Sydney University of Notre Dame, Australia

Introduction: Hip fracture among post-menopausal women is one of the most serious heath problems worldwide. It is very difficult to predict hip fracture because its risk is affected by multiple interactive risk factors. Although a number of statistical models have been available for predicting hip fracture risk, the level of discrimination is ranging from modest to good. In this study, we trained an artificial neural network (ANN) to predict ten-year hip fracture risk in women using clinical information in one cohort, and validated its predictive performance in another cohort. Methods: This study involved 1167 women aged 60 years and above who were participants of the Dubbo Osteoporosis Epidemiology Study (DOES), which was designed as a prospective cohort study. The data for training (60%) and validation (40%) included age, bone mineral density (BMD), clinical factors, and lifestyle factors which had been obtained at entry time. The women had been followed up for up to 20 years, and during the period, the incidence of new hip fractures was ascertained from X-ray report. We built the muti-layer feed-forward neural networks in the training dataset using 5-fold cross-validation. The performance of model was then assessed in the test set, from which the sensitivity and specificity were evaluated and compared with other common machine learning approaches: k-nearest neighbours (KNN) and Support Vector Machine (SVM). Results: The accuracy of model I (which included only lumbar spine and femoral neck BMD) with 7 hidden nodes yielded an accuracy rate of 79% in the training dataset, and 81% in the test dataset. The AUC for model I was 0.87. Model II (which included only non-BMD risk factors) yielded an accuracy of 86% in the training dataset and 84% in the test dataset. The AUC for model II was 0.92, significantly better than Model I. When BMD and non-BMD risk factors were combined in Model III, the accuracy was 86% in the training dataset and 87% in the test dataset. Compared with Model I and Model II, Model III had the highest AUC values (0.94). The KNN and SVM had the same sensitivity as ANN (81%), but the specificity and accuracy for KNN (79%) and SVM (82%) were lower than ANN. Conclusion: These findings indicate that artificial neural network models are able to predict hip fracture more accurately than any existing statistical models, and that the model c edical decision making in the clinical setting.

P44

Age-related changes in bone strength and microstructure in Asian: the Vietnam Osteoporosis Study. Lan T Ho-Pham*[1], Tuan V. Nguyen[2]. [1]Ton Duc Thang University, Viet Nam, [2]Garvan Institute of Medical Research, Australia

Background and aim: Peripheral quantitative computed tomography (pQCT) allows the assessment of trabecular and cortical bone properties that are not possible by DXA technology. The present study sought to define the age-related changes in bone structural parameters and volumetric bone density in a Vietnamese population. Study Design and Methods: The study was part of the large project called Vietnam Osteoporosis Study (VOS) that involved 1383 women and 828 men aged 18 years and older who were

randomly recruited from the general population. pQCT measurements were performed at the distal radius and tibia using the CT bone scanner XCT 2000 (Stratec, Germany). Trabecular and cortical volumetric BMD (vBMD) were measured at the nondominant forearm at 4% and 38% point. Fracture load index, polar strength strain index (PSSI), and tibia strength strain index (SSI) were derived from the pQCT scan. Areal BMD was measured at the femoral neck and lumbar spine using a DXA system (Hologic Horizon, USA). Robust multiple linear regression was used to determine the rate of age-related changes in vBMD and aBMD. Results: The relationship between age and vBMD largely followed a quadratic function, with peak level being reached at the age of 20-30 yr The decline of vBMD started from the age of 50, with women having higher rate of loss than men. At the radius, the rate of loss in trabecular vBMD was 1.1%/yr in women which was signifi- cantly greater than that in men (0.2%/yr); the rate of loss in cortical vBMD was 0.3%/yr compared with 0.1%/yr in men. Similar trends were also observed at the tibia. As expected, PSSI, SSI, and fracture load indices in men were greater than women, but the relative rate of decline in fracture load was not significantly different between men and women. The correlation between DXA aBMD and pQCT vBMD ranged between 0.10 and 0.35. Conclusion: In normal individuals, vBMD reaches its peak at the age group of 20-30 yr, and starts declining at the age of 50. The rate of decline in trabecular vBMD was greater than cortical bone vBMD, and women have a greater rate of loss than men. The modest correlation between aBMD and vBMD suggests that vBMD can be a useful complementary tool for the assessment of bone health

P45

Quantification of Age-Related Changes in Whole-Skeleton Bone Metabolism using ^{18}F-NaF PET/CT. Alyssa Johncola*,

Jonathan Guntin, Christian McHugh, Austin Alecxih, Sun Kim, Rishika Sharma, Shivali Patel, Sheenali Patel, Thomas Werner, Poul Flemming, Abass Alavi, Chamith Rajapakse. University of Pennsylvania, United States

NaF Positron Emission Tomography/Computer Tomography, or PET/CT, is a rec developed imaging tool capable of detecting bone turnover in human subjects. While conventional bone imaging modalities such as DXA and HR-pQCT can detect structural changes in bone, NaF PET/CT can provide functional information about bone sooner than any structural manifestations of bone disease or in response to therapy. The goal of this study was to explore the use of Standard Uptake Value (SUV) of NaF PET/CT in subjects lacking skeletal abnormalities, other than age related metabolic bone diseases such as osteoporosis. Most metabolic bone diseases are characterized by an imbalance of bone forming osteoblastic activity and bone reabsorbing osteoclastic activity, leading to osseous degeneration. The relationship between osteoblastic and osteoclastic activity can be determined by incorporation, or uptake of ^{18}F-NaF into the the bone matrix. NaF passes extracellular fluid and is absorbed onto hydroxyapatite and exchanges rapidly for OH, which is on the surface of the hydroxyapatite matrix. The SUV, or NaF uptake value, can be detected and anatomically localized through PET/CT. This study included 68 female and 71 male subjects (age 21-75 years, BMI 18-43 kg/ m^2). The subjects were scanned using NaF PET/CT at 90 minutes after NaF injection. Image analysis was completed using Pmod software (PMOD Technologies LLC, Switzerland). First, the whole skeleton was segmented from the CT image using Hounsfield value 100 as the lower threshold. Then, the PET and CT images were fused to calculate the SUV at each voxel in the segmented region (outlined in green, in Figure 1) and the average SUV for the whole skeleton was recorded. The completely automatic image analysis approach result in perfect inter-operator reproducibility (i.e., intra-class correlation coefficient = 1). Average SUV decreased with age across females (p=0.01) and males (p=0.04), indicating approximately 3.8% and 2.3% decrease in bone metabolism per decade after 30 years of age, for females and males, respectively. NaF PET/CT has the potential to be complementary to structural imaging modal- ities for the management of metabolic bone diseases.

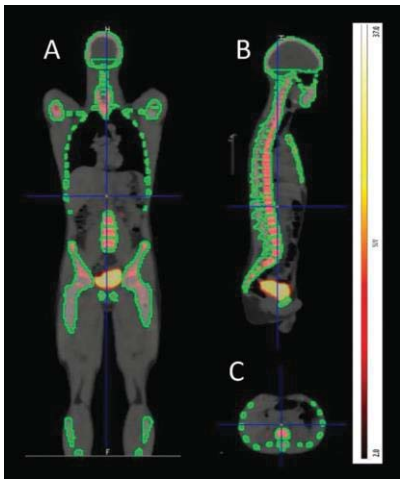

P46

Densitometric lateral spine screening to detect vertebral fractures predicts incident osteoporotic fractures in elderly women in addition to bone density. Richard L. Prince*[1], Joshua R. Lewis[2], Wai H. Lim[3], Germaine Wong[2], Kevin E. Wilson[4], Ben C. Khoo[5], Kun Zhu[1], Douglas P. Kiel[6], John T. Schousboe[7]. [1]University of Western Australia, School of Medicine and Pharmacology, Australia, [2]Centre for Kidney Research, Children's Hospital at Westmead School of Public Health, Sydney Medical School, Australia, [3]Department of Renal Medicine, Sir Charles Gairdner Hospital, Australia, [4]Skeletal Health, Hologic, Inc., United States, [5]Medical Technology & Physics, Sir Charles Gairdner Hospital, Australia, [6]Institute for Aging Research, Hebrew Senior Life, Department of Medicine, Beth Israel Deaconess Medical Center, Harvard Medical School, United States, [7]Park Nicollet Osteoporosis Center and Health Partners Institute, United States

Vertebral fractures identified on lateral spine radiographs predict subsequent fractures independent of bone mineral density (BMD). However the use of low radiation lateral spine images (LSI) by bone densitometers at the time of areal bone density (aBMD) testing has not been established. To estimate the associations between prevalent vertebral fractures identified on densitometric LSI with incident fractures a prospective 14.5 year cohort study of 1,084 community dwelling women mean age 75 (SD 3) years living in Perth, Western Australia was completed. Baseline DXA imaging for hip aBMD and LSI was undertaken (Hologic, Marlborough, MA). The LSI scans were assessed for the presence of fracture by a single experienced clinician (JTS) blinded to the outcomes. Complete fracture ascertainment over the subsequent 14.5 yrs. was obtained from Health Department of WA hospital discharge records for hip and all fracture hospitalizations; clinical spine fractures were assessed by patient self-report and verified by x-ray report. At baseline 100 women (9.2%) had a vertebral fracture (VF) identified on densito- metric LSI. Incident clinical VF occurred in 73 (7%) of women; incident low-trauma hip fractures hospitalization occurred in 121 (11%) and all osteoporotic fracture hospitalization occurred in 305 (28%). Compared to those without baseline LSI VF, women with VF had higher risks of incident clinical VF of 19% vs 5.5% (RR 3.5, CI 2.2 – 5.6); hip fracture hospitalization of 18% vs 10.5 % (RR 1.7, CI 1.1 – 1.8,) and all osteoporotic fracture hospitalization of 38% vs 27% (RR 1.4, CI 1.1 – 1.8). Amongst those with femoral neck T score -1 to -2.5, who often do not meet criteria for pharmaceutical intervention, compared to those without baseline LSI VF those individuals with LSI VF were at higher absolute risk for incident clinical VF 21% vs 6% (RR 3.9 CI 2.2 – 6.9) and for all fracture hospitalizations 46% vs 29% (RR 1.6, CI 1.2 – 2.1) but not hip fracture hospitalization. Women aged 70 years and older undergoing bone densitometry can receive addi- tional information on future fracture risk by capturing densitometric lateral spine images at the time of aBMD measurement. Because pharmacologic therapy substantially n individuals with these fractures the identification of such individuals may lead to improved patient management.

P47

Relationship between Bone Structural Variables from bone biopsy and Bone Mineral Density (BMD) in Patients on long term Bisphosphonate (BP) Therapy. Christopher Little*[1], Elizabeth Warner[2], Mahalakshmi Honasoge[2], Loren Safta[3], Shiri Levy[2], Sudhaker Rao[2], Saroj Palnitkar[2], Pooja Kulkarni[2]. [1]Wayne State University School of Medicine, United States, [2]Henry Ford Hospital, United States, [3]High School Student, United States

BMD is a 2D measurement of a 3D structure that has been the cornerstone to diagnose osteoporosis, monitor progression, and response to therapy. Bone volume in biopsy is also a 3D estimate of a 2D measurement. Intuitively it is expected to correlate with each other. A few studies showed significant correlations between bone biopsy and BMD variables in a group of patients with various metabolic bone diseases. However, the strengths of correlations were modest or not significant in a more homogenous subset. Our aim was to understand if there were correlations between the bone structural variables and BMD in a group of post- menopausal women on long-term BP therapy. Methods: Trans-Iliac bone biopsies were obtained from 25 postmenopausal women (mean age 66.8 6.6y) treated with BP for 6.1 4.3 y. Using standard methods cortical bone volume, mean cortical thickness, trabecular bone volume, and trabecular thickness were measured. BMD of both proximal femurs (femoral neck, total hip, and trochanter) was measured by DEXA about 1-2 months before biopsy. Correlations among proximal femur measures and among biopsy variables, as well as between BMD and biopsy structural variables were performed using SigmaPlot. Results: Mean right and left femoral neck BMDs were 0.636 0.068 and 0.637 0.072 with highly significant correlation between the sides ($r=0.77$; $P<0.0001$). As expected, there were statistically significant correlations among various BMD para- meters ($r=0.46$ to 0.87; $p=0.02$ to $<.0001$) with much stronger relationship between the sides (left Vs. right; $r=0.62$ to 0.84; $p<0.001$ for all). In contrast, bone structural measurements showed variable correlations ranging from strongest correlation between trabecular thickness and volume ($r=0.83$; $p<0.001$) to lack of correlation between cortical and trabecular bone volumes. There was a trend for a relationship between cortical thickness and trabecular bone volume ($r=0.36$; $p=0.06$). Finally, there were very few, if any, correlations between BMD and bone structural measurements. Conclusion: We confirmed strong correlation between the right and left femoral neck, trochanter, and total hip BMDs. However, weak to poor correlation between BMD and bone structural measurements implies that the two methods assess different aspects of bone biology. Alternatively, BPs may have differential effects on BMD and bone structure. Further research i needed to elucidate underlying pathophysiologic mechanism for these observations.

P48

Urinary N-telopeptide and rate of decline in femoral neck strength across the menopause transition: Results from the Study of Women's Health Across the Nation (SWAN). Albert Shieh*[1], Shinya Ishii[2], Gail Greendale[1], Jane Cauley[3], Arun Karlamangla[1]. [1]UCLA, United States, [2]University of Tokyo, United States, [3]University of Pittsburgh, United States

The bone resorption marker, urinary N-telopeptide (U-NTX), measured in women during their 40s, can be used to gauge the rate of areal bone mineral density (aBMD) decline over the menopause transition (MT) in the lumbar spine (LS) but not in the femoral neck (FN). One possible explanation is that the FN is composed mostly of cortical bone, and aBMD measurements by DXA do not adequately capture the effects of increased endocortical bone resorption on the cortical compartment. One such effect is the compensatory increase in bone formation at the periosteal surface, and the corresponding increase in bone size. In contrast to aBMD, composite indices of FN strength combine DXA-based measurements of FN aBMD and FN size with body size, and are independently associated with fracture risk. They also decline over the MT: indices of FN strength in compression (CSI) and impact (ISI) failure modes begin to decrease rapidly ~1 year prior to the final menstrual period (FMP), and continue to decline at a rapid rate for 3-4 years. We hypothesized that U-NTX, measured in pre- or early perimenopause, would predict the rate of FN strength decline during its rapid phase of MT-related loss. U-NTX was measured in 42-52 year-old, pre- or early perimenopausal women at the baseline visit of the Study of Women's Health Across the Nation (SWAN). FN aBMD was measured by DXA (Hologic) at baseline and annually thereafter. CSI and ISI were calculated from FN aBMD, FN size, and body size. A total of 696 women had measurements of both U-NTX and CSI or ISI decline over the MT. Among these participants, after adjusting for relevant clinical covariates (MT stage at baseline, age, body mass index, race/ethnicity, SWAN study site) in multivariable linear regression, every standard deviation (SD) increase in U-NTX was associated with 0.34% (p=0.02) and 0.36% (p=0.01) per year faster declines over the MT in CSI and ISI, respectively. We conclude that U-NTX, measured during pre- and early perimenopause, is strongly associated with rate of CSI and ISI decline during their rapid phase of MT-related loss, and may aid early identification of women who will experience the greatest loss in femoral neck strength during this critical period.

P49

Characteristics and Consequences of Hip Fracture in an Elderly Irish Population. James Mahon 1 Oisin Hannigan[1], Georgina Steen[1],Nessa Fallon[1], Niamh Maher[1], Aoife Dillon[1], Geraldine McMahon[2], Alison Reynolds[3], Thomas McCarthy[3], Irina Tomita[1], Laura Clowry[1], Ronan O'Toole[1], MC Casey[1], JB Walsh[1], Kevin McCarroll[1]. [1]Osteoporosis and Bone Health Unit, St James's Hospital, Dublin 8, Ireland, [2]Department of Emergency Medicine, St James's Hospital, Dublin 8, Ireland, [3]Department of Orthopaedic Surgery, St James's Hospital, Dublin 8, Ireland

Purpose: Osteoporosis prevalence increases with age and is responsible for significant morbid- ity and mortality in the elderly populations due to hip, vertebral and wrist fractures. We aimed to define the baseline characteristics of patients attending out University Hospital admitted with hip fracture and determine their length of hospital stay and mortality. Methods We performed a prospective longitudinal observational study of patients admitted to our hospital with a diagnosis of fragility fracture of the hip from January 2014 to March 2015. Patients over 65 years of age were eligible for inclusion. We collected cross- sectional data on basic demographics, functional status and serum vitamin D levels at time of admission and followed patients up for a 12-month period after their initial fracture. Results: 199 patients admitted with hip fracture; 161 patients recruited for follow-up. Mean age 80.5 years (SD 12.3); 108 female, 53 male. 96.3% of participants were community- dwelling and 3.7% were nursing home-dwelling. Baseline BMI was 22.7kg/m2. Mean serum vitamin D 58.3 nmol/litre (SD 34.1); mean estimated glomerular filtration rate (eGFR) 63.2 ml/min (SD 12.1). 10.6% had a prior diagnosis of osteoporosis and 76.4% of these patients were on treatment with an antiresorptive agent at the time of presentation. 22.3% of the entire cohort were on vitamin D supplements at the time of presentation. 3.1% of participants had a prior history hip fracture; 5.8% had a prior history of vertebral fracture and 13.1% had a prior history of wrist fracture. 51% had a history of falls in the previous 12 months and the median Rockwood Clinical Frailty Score was 5/9 (mildly frail). Median length of stay in hospital was 13 days (range 3-146 days); inpatient mortality was 1.84%. 12-month mortality was 22%. Conclusions: Patients presenting with hip fracture were a relatively elderly and frail population and had a significant length of hospital stay, which could increase the chances of complications such as hospital acquired pneumonia. In keeping with other studies, perioperative mortality following hip fracture was low, but one-year mortality is relatively high, highlighting the importance of osteoporosis screening and treatment in elderly frail patients. This is especially important in the context of the fact that a minority of participants had a prior diagnosis of osteoporosis before presentation with their fracture, implying a missed opportunity for

P50

Older Men with Decreasing Hemoglobin Have a Higher Risk of Future Hip Fracture: The Cardiovascular Health Study. Rodrigo J. Valderrabano*[1], Petra Buzkova[2], Po-Yin Chang[3], Neil A. Zakai[4], Howard A. Fink[5], John A. Robbins[3], Joy Y. Wu[1], Jennifer S. Lee[6]. [1]Division of Endocrinology, Stanford University School of Medicine, United States, [2]University of Washington, United States, [3]University of California, Davis, United States, [4]Department of Medicine and Department of Pathology and Laboratory Medicine, University of Vermont, United States, [5]GRECC, Veteran Affairs Health Care System, United States, [6]Division of Endocrinology, Stanford University School of Medicine and Palo Alto Veteran Affairs Health Care System, United States

Purpose: Hematopoiesis and bone health are linked. We previously found that anemia in older men is associated with increased risk of non-spine fracture (Fx) inde- pendent of BMD. We hypothesized that lower hemoglobin (Hgb) levels are associated with an increased risk of hip Fx in both older men and women. Methods: The Cardiovascular Health Study is a prospective longitudinal cohort of 5,888 non-institutionalized, non-wheelchair bound men and women aged >65 years recruited during 1989-90 (first visit).

We used data from 4,670 participants with available Hgb levels in the first visit and 1992-93 (second visit). Anemia at the second visit was defined as <13 g/dL for men and <12 g/dL for women (WHO criteria). Hgb change was annualized and divided into sex- specific quartiles. Incident hip Fxs were ascertained every 6 months after the second visit from self-reports and hospitalization records, and defined by ICD-9 codes. Cox proportional hazards modeling estimated the hazard ratios (HR) and 95% confidence intervals (CI) for incident hip Fx. Unadjusted; age, sex and race-adjusted; and fully adjusted (age, sex, race, height, weight, smoking, alcohol, bone medication, steroids, physical activity score, self-reported health, heart disease) models were performed for participants with anemia (vs. without) and for participants in the quartile with the greatest Hgb loss (vs. others). Results: 12.5% of women and 14.6% of men had anemia at the second visit. During a median follow-up of 12 years, men with anemia had higher hazards of hip Fx in the unadjusted model (HR 1.76; 95% CI 1.17-2.65); however, risk was attenuated in the fully adjusted model (HR 1.58; 95% CI 0.98-2.54). Men in the quartile with the greatest annualized Hgb loss (>0.36 g/dL) had higher fully adjusted hazards of hip Fx (HR 1.59; 95% CI 1.10-2.31) than other men. Associations were not observed in women except for black women, in whom those with anemia had higher fully adjusted hazards of hip Fx (HR 4.38; 95% CI 1.41-13.55) than those without. Conclusions: In this older cohort, men with the greatest Hgb loss had a 59% higher risk of subsequent hip Fx. Men with anemia had a similar higher risk of hip Fx, but the association was not statistically significant. Results were consistent with past work evaluating nonspine Fx. Decreasing Hgb may be an earlier marker of skeletal fragility than anemia. Study findings support further r search evaluating the utility of Hgb measurement in sex-specific Fx risk assessment.

P51

Cross-Sectional Association of BMAT Unsaturation Index (UI) with QCT Measures of Bone Density and Strength. Gina Woods*[1], Kaipin Xu[2], Sigurdur Siggurdsson[3], Susan Ewing[2], Deborah Kado[1], Thomas Lang[2], Thomas Link[2], Gudny Eiriksdottir[3], Trisha Hue[2], Eric Vittinghoff[2], Tamara Harris[4], Clifford Rosen[5], Vilmundur Gudnason[6], Ann Schwartz[2], Xiaojuan Li[2]. [1]University of California, San Diego, United States, [2]University of California, San Francisco, United States, [3]Icelandic Heart Association, Iceland, [4]National Institute on Aging, NIH, United States, [5]Maine Medical Center Research Institute, United States, [6]University of Iceland, Iceland

Higher levels of bone marrow adipose tissue (BMAT) are associated with lower BMD and prevalent vertebral fracture (PVF) in older adults. The composition of BMAT, in addition to the amount, may also influence bone. Lipid composition can be evaluated with magnetic resonance spectroscopy (MRS). We hypothesize that a higher proportion of unsaturated lipid within the BMAT depot is associated with higher BMD and bone strength. This study aims to investigate the association between BMAT lipid unsaturation index (UI), expressed as the ratio of unsaturated lipids to all lipids (%), QCT measures of BMD, and PVF in 288 older adults from the AGES-Reykjavik study. Participants were age 71+, not using medications known to affect BMAT or BMD. BMAT UI was measured by 1.5-T H1-MRS. BMD was assessed by QCT, and PVF by DXA VFA. Multivariable linear models were used to determine the association between average UI (L1-L4) and PVF or log-transformed QCT BMD. Participants were 78.8 (SD 3.5) years, with mean BMI of 27.3 (SD 3.7) kg/m2, mean trabecular spine BMD of 0.066 (SD 0.029) g/cm3, and mean vertebral (L1-L4) BMAT content of 55.0 8.3%. 19.2% (n=55) of participants had one or more prevalent vertebral fractures. The average lipid UI was 4.5 1.3%. Lipid UI at the individual vertebral level increased from 3.9% at L1 to 4.7% at L4 (p for trend <0.0001). Higher UI was associated with younger age (r=-0.19, p=0.002), and higher BMAT content (r=0.17, p=0.003), but not with BMI (r=-0.004, p=0.95). Average UI was higher in men than women, but was not statistically significant (4.6% vs. 4.3%, p = 0.06). Average UI was no different in those with vs. without PVF (4.5% vs. 4.5%, p=0.95), in fully adjusted models including age, gender, calendar time, trabecular spine BMD, diabetes status, and total BMAT content. However, per SD increase in UI, spine integral BMD was 5.2% higher (p=<0.0001), femoral neck integral BMD was 3.0% higher (p=0.02) and total hip integral BMD was 4.1% higher (p=0.0009) in fully adjusted models (Table 1). Spine trabecular BMD, spine compressive strength, femoral neck cortical BMD and total hip trabecular and cortical BMD were also higher in those with higher UI. In conclusion our study showed that older adults with higher proportion of unsaturated lipids in BMAT have higher trabecu ensity, independent of the total amount of BMAT.

Percent Difference in Bone Density and Strength (QCT) per SD Increase in BMAT UI (n=288)

	% Difference in Bone Measurement (95% CI)	P-value
Spine		
Trabecular BMD	**10.0 (3.7, 16.8)**	**0.002**
Integral BMD	**5.2 (2.7, 7.8)**	**<0.0001**
Compressive Strength	**16.8 (8.6, 25.6)**	**<0.0001**
Femoral Neck		
Trabecular BMD	1.5 (-3.0, 6.2)	0.52
Cortical BMD	**1.5 (0.3, 2.7)**	**0.02**
Integral BMD	**3.0 (0.6, 5.6)**	**0.02**
Total Hip		
Trabecular BMD	**3.1 (0.1, 6.3)**	**0.04**
Cortical BMD	**1.4 (0.4, 2.3)**	**0.004**
Integral BMD	**4.1 (1.7, 6.6)**	**0.0009**

Adjusted for age, gender, BMI, calendar time, diabetes and total BMAT content

P52

Trends in Mean Femoral Neck Bone Mineral Density Among Individuals Aged 30 or Older in the United States, 2005-2006 through 2013-2014. Yingke Xu*[1], William Donald Leslie[2], Qing Wu[1]. [1]University of Las Vegas, Nevada, United States, [2]University of Manitoba, Canada

Background: Bone mineral density (BMD) is a major predictor of osteoporotic fracture. Data from the National Health and Nutritional Examination Survey (NHANES) has shown that osteoporosis prevalence in the US declined between 1988- 1994 and 2005-2006. As well, US Medicare data indicates that a declining trend in hip fracture may have plateaued in 2013-2014. However, whether there has been a corre- sponding change in BMD trajectory for the US population in recent years is unknown. Therefore, we examined BMD trends among US adults from 2005-2006 to 2013-2014, overall and within sex, race and age subgroups. Methods: We used femur neck BMD data from the last four NHANES cycles (2005-2006 to 2013-2014) in subjects aged 30 or older. Although the densitometers and software of BMD measures were updated during its history, the update has no impact on femoral neck BMD measures. Mean BMD was estimated for each survey year, overall and by sex, age and race subgroup. Sample weights, which account for the unequal selection probabilities, were used for all analyses. Standard errors employed to construct confidence intervals were estimated using Taylor series linearization. Orthogonal contrasts were used to test for significant between-group differences, with Bonferroni adjustment for multiple comparisons. SAS version 9.3 (SAS Institute Inc) was used for analyses. Results: Overall mean BMD for the first three NHANES cycles was stable (p>0.25), but significantly decreased in 2013-2014, from 0.821 g/cm2 to 0.788 g/cm2 (p<0.0001). Although mean BMD in men was higher than in women in each survey cycle, similar BMD trends were observed for both sexes and only declined in the last cycle, from 0.862 g/cm2 to 0.816 g/cm2 for men (p<0.0001), and from 0.794 g/cm2 to 0.761 g/cm2 for women (p=0.0005). Non-Hispanic Blacks had the highest mean BMD within each age and sex subgroup, and no significant change was observed in mean BMD across the four survey cycles in Non-Hispanic Black men or women. Stable mean BMD for the first three cycles with a significant decline in 2013-2014 was seen in all other race subgroups, in all age subgroups in men, and in women aged 50-69 years. Summary: Mean femoral neck BMD in US men and women was stable from 2005-2006 to 2009-2010,but declined in 2013-2014, overall and within most subgroups. Further studies are warranted to explain this recent BMD decline.

Table. Mean Femoral Neck BMD Among Individuals Aged 30 or Older in the United States, 2005-2006 through 2013-2014

Mean BMD(g/cm²)	2005-2006	2007-2008	2009-2010	2013-2014	p-value [b]
Overall	0.821(0.811-0.830)	0.825(0.817-0.833)	0.827(0.820-0.833)	0.788(0.779-0.796)	<0.0001
Men	0.853(0.845-0.862)	0.857(0.850-0.865)	0.862(0.853-0.870)	0.816(0.803-0.830)	<0.0001
Age group					
30-49	0.890(0.877-0.903)	0.887(0.874-0.900)	0.895(0.884-0.906)	0.852(0.832-0.871)	0.002
50-69	0.822(0.805-0.839)	0.829(0.818-0.841)	0.826(0.811-0.841)	0.797(0.780-0.815)	0.03
≥70	0.756(0.724-0.789)	0.771(0.754-0.789)	0.771(0.752-0.791)	0.717(0.697-0.738)	0.05
Race					
Hispanic*	0.869(0.853-0.887)	0.885(0.869-0.901)	0.877(0.862-0.892)	0.843(0.827-0.859)	0.01
NH-White	0.841(0.831-0.852)	0.846(0.836-0.855)	0.851(0.840-0.862)	0.799(0.781-0.818)	0.0002
NH-Black	0.934(0.919-0.949)	0.919(0.894-0.944)	0.949(0.928-0.971)	0.905(0.884-0.927)	0.15
NH-Other	0.843(0.799-0.888)	0.832(0.803-0.862)	0.811(0.784-0.838)	0.797(0.775-0.820)	0.04
Women	0.789(0.777-0.799)	0.795(0.786-0.805)	0.794(0.786-0.802)	0.761(0.750-0.772)	0.0005
Age group					
30-49	0.842(0.832-0.853)	0.843(0.828-0.858)	0.848(0.838-0.857)	0.825(0.811-0.839)	0.08
50-69	0.749(0.735-0.763)	0.755(0.744-0.767)	0.741(0.730-0.753)	0.728(0.713-0.745)	0.02
≥70	0.644(0.631-0.658)	0.685(0.669-0.702)	0.674(0.654-0.693)	0.644(0.618-0.670)	0.78
Race					
Hispanic*	0.831(0.815-0.847)	0.820(0.795-0.845)	0.819(0.807-0.833)	0.780(0.757-0.803)	<0.0005
NH-White	0.773(0.762-0.783)	0.782(0.774-0.791)	0.776(0.766-0.786)	0.744(0.727-0.762)	0.0037
NH-Black	0.866(0.849-0.884)	0.873(0.857-0.889)	0.898(0.873-0.923)	0.856(0.838-0.873)	0.85
NH-Other	0.786(0.764-0.807)	0.762(0.737-0.787)	0.761(0.729-0.793)	0.724(0.699-0.750)	0.0023

*Hispanic includes Mexican American and Other Hispanic

[b] p-values were calculated by orthogonal contrasts

Table for Trends in Mean Femoral Neck Bone Mineral Density Among Individuals Aged 30 or Older in the

P53

Opportunistic Identification of Vertebral Fractures from Cross-Sectional Imaging and Impact on Fracture Liaison Services. Emily Russell*1, Emma Fower2, Kassim Javaid2. 1Oxford Medical School, United Kingdom, 2Oxford University Hospitals, United Kingdom

Up to 75% of vertebral fractures do not reach clinical attention. Identification of vertebral fractures is critical for effective secondary fracture prevention as they are associated with a 2.3x increase in future hip fracture. CT scans are a common investigation performed for a variety of clinical indications and provide an ideal platform for opportunistic identification. We tested the screening of CT scans in patients over the age of 50 for vertebral fractures. Methods: 16,935 CT scans were performed in a UK region (population 620,000) over one year, in patients over the age of 50. We retrospectively analysed a representative sample of 321 scans for moderate or severe vertebral fractures using Optasia medical's ASPIRETM service. This uses machine-learning to flag scans, with all images then over-read by an Optasia radiologist to confirm the presence of fracture. Where fractures were identified, radiologist reports were examined to look for mention of the fracture and suggestion of referral for further management. Patients were cross referenced with the local Fracture Liaison Service (FLS) to see how many patients were already known to services. Results: Of the 321 scans analysed, 53 (16.5%) moderate/ severe vertebral fractures were found by the ASPIRE system. 63% had been reported by the radiologists, although none recommended further secondary fracture prevention. The ASPIRE service identi- fied 20 patients with previously undiagnosed vertebral fractures. The rate was higher in women (8.6%) vs men (4.1%). Of the newly identified vertebral fracture patients, 3 were already known to the FLS. If all new, unknown patients found by the ASPIRE service were appropriate for referral, this could mean an initial extra 886 patient referrals per year to the FLS in comparison to the 620 hip fractures seen by the FLS per year. Conclusion: Computer driven services have the potential to identify vertebral fractures with a greater sensitivity than

radiologists when used opportunistically on CT scans taken for a variety of clinical indications. However, to reduce the burden of fractures, substantial service planning is required to account for the increase in referrals for secondary fracture prevention of at least 1.4 times the number of hip fractures in this locality.

P54

High Dairy Protein Intake is Associated with Greater Bone Strength Parameters at the Distal Radius and Tibia in Older Men: A Cross-sectional Study. Lisa Langsetmo*[1], James Shikany[2], Andrew Burghardt[3], Peggy Cawthon[3], Jane Cauley[4], Eric Orwoll[5], Douglas Bauer[3], John Schousboe[6], Brent Taylor[7], Tien Vo[1], Elizabeth Barrett-Connor[8], Kristine Ensrud[7]. [1]University of Minnesota, United States, [2]University of Alabama, United States, [3]University of California, San Francisco, United States, [4]University of Pittsburgh, United States, [5]Oregon Health and Science University, United States, [6]Park Nicollet Clinic and Health Partners Institute, United States, [7]University of Minnesota and VA Health Care System, United States, [8]University of California, San Diego, United States

Previous studies have reported that the association between protein intake and fracture depends on the source (dairy, non-dairy animal, plant). Experimental studies have indicated that protein source has differential effects on markers of bone mineral metabolism, but the consequence for bone strength and effects on cortical vs. trabecular bone are unknown. Our objective was to determine the association of protein intake by source (dairy, non-dairy animal, plant) with bone strength and trabecular and cortical bone microarchitecture at weight bearing (tibia) and non-weight bearing (radius) skele- tal sites among older men. We used data from 1016 men (mean 84.3 years) who attended the Year 14 exam of the Osteoporotic Fractures in Men (MrOS) study, completed a food frequency questionnaire (500-5000 kcal), were not taking androgen or androgen agonists and had high resolution peripheral quantitative computed tomography (HRpQCT) scans of the distal radius and/or distal tibia. Protein was expressed as % of total energy intake (TEI); mean SD for TEI=1548 607 kcal and for total protein=16.2 2.9%TEI. We used linear regression with standardized HRpQCT parameters as dependent vari- ables and adjusted for age, height, center, education, race/ethnicity, marital status, smoking, alcohol intake, physical activity level, corticosteroids use, supplement use (calcium and vitamin D), and osteoporosis medications. Increased dairy protein intake was associated with higher estimated failure load at the distal radius and tibia, as well as higher cortical and trabecular BMD, higher cortical thickness and area (but not cortical porosity) and lower total area (Table 1). Non-dairy animal protein was associated with higher cortical thickness, cortical area, and cortical BMD, and total BMD at the radius, but the remaining associations at the radius (including failure load) and those with all parameters at the tibia were not significant. Plant protein intake was not associated with any bone strength parameter. In conclusion, increased dairy protein intake was asso- ciated with higher failure load at both weight bearing and non-weight bearing sites and these associations were consistent with both cortical and trabecular bone strength parameters. In contrast, there was a more limited association between non-dairy animal protein and bone strength parameters. These results support a link between dairy protein intake and skeletal health but an intervention study is needed to evaluate causality.

Table 1: The Association* between Protein Intake by Source (Dairy, Non-dairy Animal, Plant) and High Resolution Peripheral Quantitative Computed Tomography Bone Strength Parameters

Effect size (95% CI)	Dairy protein	Non-dairy Animal Protein	Plant protein
Distal Radius			
Failure load	**0.16 (0.07, 0.26)**	0.06 (−0.01, 0.13)	0.02 (−0.09, 0.13)
Area	**−0.10 (−0.19, −0.01)**	−0.04 (−0.10, 0.02)	−0.09 (−0.20, 0.01)
BMD	**0.20 (0.10, 0.30)**	**0.07 (0.00, 0.14)**	0.04 (−0.07, 0.15)
Trabecular BMD	**0.13 (0.03, 0.23)**	0.03 (−0.03, 0.10)	0.05 (−0.07, 0.16)
Cortical BMD	**0.19 (0.10, 0.29)**	**0.07 (0.01, 0.14)**	0.07 (−0.04, 0.18)
Cortical Thickness	**0.17 (0.07, 0.27)**	**0.08 (0.01, 0.15)**	−0.02 (−0.13, 0.09)
Cortical Area	**0.17 (0.07, 0.27)**	**0.08 (0.01, 0.15)**	−0.05 (−0.16, 0.06)
Cortical Porosity	−0.04 (−0.14, 0.07)	−0.02 (−0.09, 0.05)	−0.03 (−0.15, 0.09)
Distal Tibia			
Failure load	**0.12 (0.02, 0.21)**	−0.01 (−0.07, 0.06)	−0.01 (−0.12, 0.10)
Area	**−0.11 (−0.19, −0.03)**	−0.04 (−0.10, 0.01)	−0.06 (−0.15, 0.03)
BMD	**0.18 (0.08, 0.28)**	0.01 (−0.06, 0.07)	0.02 (−0.10, 0.13)
Trabecular BMD	**0.13 (0.03, 0.23)**	−0.01 (−0.08, 0.06)	0.08 (−0.03, 0.19)
Cortical BMD	**0.13 (0.04, 0.23)**	0.04 (−0.02, 0.11)	−0.02 (−0.13, 0.09)
Cortical Thickness	**0.14 (0.05, 0.24)**	0.00 (−0.06, 0.07)	−0.05 (−0.16, 0.06)
Cortical Area	**0.14 (0.04, 0.24)**	0.00 (−0.07, 0.07)	−0.08 (−0.20, 0.03)
Cortical Porosity	−0.01 (−0.11, 0.10)	−0.03 (−0.10, 0.04)	0.06 (−0.06, 0.18)

*Effect size (beta coefficient with unit=SD) adjusted for age, height, center, education, race/ethnicity, marital status, smoking, alcohol intake, physical activity level, corticosteroids use, supplement use (calcium and vitamin D), and osteoporosis medications. Protein measured as percentage of total energy intake (TEI), SD=2.9% TEI.
Note: data in **bold** = p<0.05

P55

Baseline Characteristics of the VITamin D and OmegA-3 TriaL (VITAL): Effects on Bone Structure and Architecture.

Catherine Donlon*[1], Sharon Chou[2], Nancy Cook[3], Trisha Copeland[4], JoAnn Manson[3], Julie Buring[3], Meryl LeBoff[5]. [1]Brigham and Women's Hospital, Endocrinology, Diabetes and Hypertension Division, United States, [2]Brigham and Women's Hospital, Endocrinology, Diabetes and Hypertension Division, Instructor in Medicine, Harvard Medical School, United States, [3]Brigham and Women's Hospital, Division of Preventive Medicine, Professor of Medicine, Harvard Medical School, United States, [4]Brigham and Women's Hospital, Division of Preventive Medicine, United States, [5]Brigham and Women's Hospital, Endocrinology, Diabetes and Hypertension Division, Professor of Medicine, Harvard Medical School, United States

Vitamin D is widely used to support bone health, although effects of supplemental vitamin D alone on bone are inconsistent. While most previous randomized control trials (RCTs) have tested low doses of supplemental vitamin D (1000 IU/day) or vitamin D plus calcium, this ancillary study to the *VITamin D and OmegA-3 TriaL* (VITAL) aims to determine whether high-dose vitamin D3 (2000 IU/d) affects bone health and body composition. The parent VITAL study is a 2x2 factorial designed RCT investigating effects of supplemental cholecalciferol and/or omega (!)-3 fatty acids (1 g/d) for the primary prevention of cancer and cardiovascular disease. The study has a median of 5-yrs of treatment in 25,874 US men 50 yrs and women 55 yrs. Participants were enrolled in VITAL between Nov 2011 and Mar 2014. The intervention phase is

slated to end on Dec 31, 2017, with an additional 2 yrs of post-intervention follow-up. In our ancillary study, *VITAL: Effects on Bone Structure and Architecture*,1 in-person assessments were completed at baseline and 2-yrs post- randomization in a subcohort of 773 participants (46.8% women, 53.2% men). Medical histories were obtained by annual questionnaires. Body composition (fat and lean tissue) and bone mineral density (BMD) were determined by dual- energy X-ray absorptiometry. Baseline bone structure measures included Trabecular Bone Score and peripheral quantitative computed tomo- graphy. Physical performance was tested using grip strength and the Short Physical Performance Battery (SPPB; gait speed, standing balance, and chair stands). At baseline, participants had a mean age of 63.8 6.1 yrs and body mass index (BMI) of 28.31 5.14 kg/m2 ; 30% were obese. Mean BMD was greater in men than women at the spine (1.08 0.16 vs. 0.96 0.15 g/cm2), femoral neck (0.82 0.13 vs. 0.72 0.11 g/cm2), and whole body (1.23 0.13 vs.1 .08
0.10 g/cm2). Among participants, 25% had low muscle mass by appendicular lean mass/BMI (defined as men <0.789, women <0.512).2 Few participants had sarcopenia by functional measures, including grip strength2 and the SPPB. Most baseline characteristics were evenly distributed among treatment groups, suggesting that unidentified confounders will be similarly distributed. Sex differences among variables are being determined. At VITAL study completion, 2 -yr follow-up data analyses will advance clinical and public health recommendations regarding the role of supplemental vitamin D3 and/or !-3 fatty acids on musculoskeletal outcomes.

References:

1. LeBoff MS, et al. Contemp Clin Trials. 2015;41:259-68.
2. Studenski SA, et al. J Gerontol A Biol Sci Med Sci. 2014;69(5): 547-558.

P56

Type 2 Diabetes Impairs Insulin-Stimulated Blood Flow in Femur and Lumbar Vertebra of Hyperphagic OLETF Rats.

Pamela Hinton*, Rebecca Dirkes, T. Dylan Olver. University of Missouri, United States

Recently, impaired bone vascular function represents a possible mechanism for the increased bone fragility and fracture risk associated with Type 2 diabetes (T2D). Impaired insulin-induced vasodilation, referred to as microvascular insulin resistance, in skeletal muscle and nervous tissue is associated with hallmark features of T2D including decreased skeletal muscle glucose uptake and neuropathy, respectively. Whether microvascular insulin resistance manifests in the bone vasculature, and con- tributes to increased bone fragility in the setting of T2D remains unknown. This study tested the hypothesis that T2D is associated with bone microvascular insulin resistance, indicated by decreased insulin-stimulated vasodilation and blood flow in the femur and lumbar vertebra. Four-week old, male Otsuka Long-Evans Tokushima Fatty (hyper- phagic model of T2D) rats were randomized to either T2D (ad lib access to a chow diet) or CON (fed 70% of T2D intake) until sacrifice at 40 weeks of age. Blood flow to the femoral proximal epiphysis, distal epiphysis, diaphysis and marrow and to vertebrae (L4) was measured before (at 0 min) and during (at 60 min) a euglycemic hyperinsuli- nemic clamp (EHC) via infusion of fluorescent microspheres. The effects of T2D on insulin- stimulated blood flow were evaluated using a RM ANOVA with post hoc paired and independent sample t-tests; group differences in %? blood flow were evaluated using Mann-Whitney U test. As expected, the hyperphagic T2D rats had significantly greater body weight, body fat and fasting glucose than CON. T2D rats had reduced whole body insulin sensitivity compared to CON, indicated by a lower glucose infusion rate required to maintain euglycemia during the EHC. Basal regional femoral and vertebral blood flow were similar among groups, but the blood flow response to insulin stimulation was depressed in the T2D compared to CON in the proximal and distal epiphyses and lumbar vertebra. Mean arterial pressure (MAP) was greater in T2D compared to CON and was reduced after insulin stimulation in both groups. However, the percent increases in vascular conductance (VC; blood flow/MAP) in the proximal and distal epiphyses were decreased in T2D compared to CON. Thus, attenuated insulin-stimu- lated increases in VC in T2D likely accounted for reduced blood flow relative to CON. In summary, the results of this study suggest t lin resistance might play a causal role in diabetic bone fragility.

P57

Renin-angiotensin system inhibition ameliorates bone fragility due to altered material properties in uremic rats with secondary hyperparathyroidism.

Suguru Yamamoto*[1], Takuya Wakamatsu[1], Yoshiko Iwasaki[2], Akemi Ito[3], Ichiei Narita[1], Masafumi Fukagawa[4], Junichiro Kazama[5]. [1]Division of Clinical Nephrology and Rheumatology Niigata University Graduate School of Medical and Dental Sciences, Japan, [2]Department of Health Sciences, Oita University of Nursing and Health Sciences, Japan, [3]Ito Bone Histomorphometry Institute, Japan, [4]Tokai University, Japan, [5]Fukushima Medical University, Japan

Background: Chronic kidney disease (CKD) patients are at an extremely high risk of bone fracture, for which altered material properties has recently been considered to be a major mechanism besides the decrease of bone mineral density. Although we have recently reported that pharmacological use of renin-angiotensin system (RAS) inhibitors is asso- ciated with incident of fracture in hemodialysis patients, especially those with moderate secondary hyperparathyroidism (SHPT), the underlying mechanisms remain unknown. Methods: Male Sprague-Dawley rats were divided into two groups, comprising only 5/6 nephrectomy (CKD with high turnover bone, HTB) or subtotal nephrectomy plus parathyroidectomy (CKD with low turnover bone, LTB) at 13 weeks of age. Each group was treated either bu olmesartan (HTB-O and LTB-O) or hydralazine (HTB-H and LTB-H) to maintain comparable blood pressure for 6 weeks. Storage modulus by dynamic mechanical analysis and confocal raman spectroscopy in femoral bone were measured. Empty lacunae in cancellous bone was measured to detect apoptosis of osteocytes.Results: Comparable levels of kidney dysfunction, blood pressure and serum para- thyroid hormone (PTH) level (HTB-O 907.6 414.1 pg/mL vs HTB-H 668.6 156.1 pg/ mL, p= 0.14) were observed in the HTB-O and HTB-H rats. HTB-O showed higher bone elasticity (storage modulus; 3.01 109 1.00

109 Pa vs HTB-H 1.19 109 0.79 109 Pa, p=0.046), lower pentosidine-to-matrix ratio and higher crystallinity as compare to HTB-H. HTB-O also showed less osteocyte apoptosis (empty lacunae; 36.6 12.2N/mm2 vs Nx-H 67.9 13.6 N/mm2, p<0.01) in cancellous bone.In low turnover bone model, low serum PTH level was found both in LTB-O and LTB-H (LTB-O 53.9 38.9 pg/mL vs LTB-H 22.1 4.2 pg/mL, p= 0.20). LTB-O showed decrease of pentosidine-to-matrix ratio (0.41 0.07 vs LTB-H 0.75 0.24, p=0.03) while there were no significant difference between LTB-O and LTB-H in bone elasticity, as well as bone crystallinity. Conclusion: Angiotensin II receptor blockade modulated physical property of bone mainly owing to improvement of material property in uremic rats with secondary hyperparathyroidism. The effect was disappeared in those with parathyroidectomy. Ihibitor reduces fragility fracture risk specifically in CKD patients with secondary hyperparathyroidism.

P58

Severity of chronic obstructive pulmonary disease is associated with low muscle mass, osteoporosis and fragility fractures.
Roberta Graumam*, Marcelo Pinheiro, Vera Szejnfeld, Aurora Cabral, Luis Eduardo Nery, Charlles Castro. Universidade Federal de São Paulo - Escola Paulista de Medicina, Brazil

Background/purpose: Chronic Obstructive Pulmonary Disease (COPD) has been associated with different co-morbidities. The use of glucocorticoid and vertebral osteo- porotic fractures in these patients may further impair respiratory function and impact negatively on prognosis. In the present study we assess the prevalence of osteoporosis and fragility fractures in patients with COPD as compared to healthy controls. Potential associations between bone fragility outcomes with clinical, demographic and epidemio- logical parameters were also investigated. Methods: A total of 97 patients with COPD answered a structured clinical questionnaire detailing disease variables and underwent bone densitometry (DXA), radiographic survey for morphometric vertebral fractures, pulmonary function and laboratorial tests. Patients with other comorbidities and med- ications (other than glucocorticoid) that could affect bone metabolism were excluded. Results: A total of 47 men (65 8 years old) and 52 women (64 10 years old) with COPD and 67 healthy controls matched by gender were included. Previous diagnosis of osteo- porosis was reported in only 6.3% of the patients while densitometric osteoporosis and osteopenia was detected in 40.2% and 39.2%, respectively, and fragility fractures (ver- tebral and non-vertebral) were observed in about 23.7% of them. Only 5 patients (5.15%) were receiving treatment for osteoporosis. COPD severity measured by pulmonary function test was associated with worse bone outcomes: FEV1 and BMD were correlated in both men (total femur: r=0.451; p=0.004) and women (spine: r=0.561; p<0.001 and total femur: r=0.622; p<0.001). As compared to healthy controls, severe COPD (FEV1<50%) was associated with lower total skeletal lean mass (p=0,002), skeletal lean mass index (p=0,005) and lower BMD at spine and proximal femur (p=0,001 for all sites). Multivariate linear regression analyzes demonstrated that FEV1 was signifi- cantly associated with BMD at the lumbar spine, femoral neck and total femur either for men or women (p<0,05). Conclusion: Osteoporosis and fragility fractures are highly prevalent in patients with COPD. Severity of the disease as measured by spirometry (FEV1) correlates significantly with bone mass and body composition parameters. These findings suggest that higher surveillance for osteoporosis is required in COPD patients, especially in those with severe disease.

P59

17 Patients with Monoclonal Gammopathy of Undetermined Significance (MGUS) Presenting with Symptomatic Vertebral Compression Fractures (SVCF).
Michael Lovy*[1], Jack Hodgkins[1], Nir Ben-Shlomo[2], Brian Hodgkins[1]. [1]Desert Oasis Healthcare, United States, [2]Ben-Gurion Medical School, Israel

Background: The presence of MGUS has been associated with vertebral fracture (1), is more prevalent among patients with SVCF (2), and is associated with an increased risk of fracture (3). Changes in cytokine profiles and bone microarchitecture that may explain this risk have been found and the skeletal signifcance of MGUS has been emphasized (4). Clinical description of patients with MGUS and SVCF is lacking. Purpose: To describe the clinical details and circumstances of fracture in a cohort of patients with MGUS who presented with SVCF and compare that to patients with SVCF and no MGUS. Methods: 17 patients with MGUS were identified among 150 patients presenting with SVCF in our community based outpatient fracture clinic. All patients had a complete history and physical, review of past medical records and radiographs, CBC, sedimentation rate, chemistry profile, TSH, urinalysis, vitamin B12, PTH, 25-OH vitamin D, and serum protein electrophoresis. We performed testosterone level and immunofixation of serum and urine in select patients. Results: There were 9 females and 8 males ranging in age from 70-94 (mean 80.5 years), with a BMI of 20-32 (mean 26.4) and an average of 1.23 comorbid conditions. 3 patients were on steroids. 9 fractures occurred after falling, 5 spontaneously, 2 while lifting and 1 with bending. 1 patient each with Schnitzler, CAPS, Kaposi sarcoma, pernicious anemia, and hepatitis C were diagnosed at the time of presentation. 9 patients had peripheral neuro- pathy. There were a total of 22 fractures including 5 patients with 2 fractures-12 thoracic and 10 lumbar. 59% of fractures were distributed from T10-L2. M-spike ranged from 0.1-1.6% comprised of IgG 72%, IgM 22% and IgA 6% and kappa and lambda light chains each 50%. Vitamin D insufficiency and deficiency were each present in 2 patients. There were more men (p=0.081) and fewer falls (p=0.067) among the MGUS patients but these and all other clinical comparisons did not reach statistical significance. Conclusion: The circumstances of fracture and patient characteristics of this cohort of MGUS patients with SVCF did not differ from those with SVCF and no MGUS. Even with the understanding of the deleterious effect of MGUS on bone, the fact that MGUS is asymptomatic makes preemptive therapeutic intervention a challenge. 1) Bida, et al, Mayo Clin Proc. 2009;84:685-693, 2) Golombick, et al, Acta Hematol. 2008;120:87-90, 3) Melton, e ;19:25-30, 4) Drake, J Bone Miner Res. 2014;2929-2533.

P60

Long-term effects of bisphosphonate therapy: perforations, microcracks and mechanical properties. Shaocheng Ma*, Ulrich Hansen, Justin Cobb, Richard Abel. Imperial College, United Kingdom

Bisphosphonates (BP) are the frontline therapy for osteoporosis, which act by redu- cing bone remodeling to prevent bone loss, thinning of trabeculae and perforations caused by hyperactive osteoclasts; thereby maintaining microstructure. However, there is growing concern that BP may over suppress remodeling resulting in the accumulation of microcracks.This paper aims to investigate the effect of BP on microstructure and mechanical properties.Trabecular bone samples were harvested from femoral heads of 3 cohorts: a BP treated (alendronate 70mg/weekly) fracture group (n=8), untreated fracture controls (n=8) and healthy ageing non- fracture controls (n=5). Mean ages respectively 79.3 6.4, 77.8 3.4 and 77.8 4.9 years were comparable (ANOVA F=0.523, p=0.644). Assessment of microdamage was performed using a particle accelerator synchrotron micro-CT system (Diamond Light Source, UK). Cylindrical cores (h 10 and d 7 mm) were drilled from the trabecular chiasma. The density and volume of both perforations and microcracks were measured at the center of the cores (away from drilling damage) using image analysis software (VG StudioMAX). Mechanical uniaxial tensile tests were carried out using standard rectangular samples (11 x 2.8 x 1 mm) sectioned from the region immediately inferior to the cores. Stress-strain curves were examined to calculate the ultimate tensile strength and Young's Modulus, which were normalized according to trabecular bone volume. Microstructural and mechanical data were analyzed using non-parametric statistics i.e. Kruskal-Wallis. Trabecular bone volume fraction in the non-fracture group (0.34 0.03) was sig- nificantly higher (p=0.001) than the untreated fracture group (0.24 0.03) but not the BP-treated fracture group (0.29 0.07). BP patients exhibited a significantly lower density (p=0.040) and smaller volume (p=0.030) of perforations than fracture controls, but significantly higher density and larger volume than non-fracture controls. BP patients exhibited a significantly higher density of microcracks (p=0.010) and larger microcrack volume (p=0.001) than both fracture and non-fracture controls. BP patients exhibited significantly lower normalized tensile strength (p=0.001) and Young's Modulus (p=0.030) than both fracture and non-fracture controls. BP therapy seems effective at reducing perforations but may also cause microcrack accumulation, leading to a loss of microstructural integrity and consequently reduced mechanical strength.

P61

Denosumab Reduced Bone Remodeling, Eroded Surface, and Erosion Depth in Cortical Bone of Iliac Crest Biopsies From Postmenopausal Women in the FREEDOM Trial. Roland Chapurlat*[1], Nathalie Portero-Muzy[1], Jean-Paul Roux[1], Stephane Horlait[2], David Dempster[3], Andrea Wang[2], Rachel Wagman[2], Pascale Chavassieux[1]. [1]INSERM UMR 1033, Université de Lyon, France, [2]Amgen Inc., United States, [3]Columbia University, United States

Denosumab (DMAb), a RANKL inhibitor, reduced the risk of vertebral, hip, and nonvertebral fractures in the FREEDOM trial of postmenopausal women with osteo- porosis compared with placebo (PBO).1 Bone histomorphometry of iliac crest bone biopsies collected during FREEDOM showed that DMAb reduced trabecular remodel- ing parameters, including eroded surface per bone surface (ES/BS).2 We now report the effects of DMAb vs PBO on cortical bone histomorphometry from iliac crest bone biopsies obtained during FREEDOM. A total of 112 biopsies were evaluable for cortical bone histomorphometry, including 67 obtained at month 24 (37 PBO, 30 DMAb) and 45 at month 36 (25 PBO, 20 DMAb). Both cortices were analyzed, if available. Endocortical (Ec) ES/BS, osteoclast surface (Oc.S/BS) and erosion depth (E.De) were assessed by an automatic-interactive method.3 Cortical porosity and Ec wall thickness (W.Th) were measured. Dynamic remodeling parameters were assessed for Ec, periosteal, and intracortical envelopes. The Ec structural variables, Oc.S/BS, ES/BS, and mean and maximal E.De, were significantly lower in the DMAb group vs PBO at months 24 and 36 (Table). There were no significant differences between DMAb and PBO groups for W.Th, cortical porosity, or cortical thickness. No extensive search for cortical fluorochrome labels was done, unlike prior trabecular analyses,2 and cortical labels in at least one cortical envelope were observed in 13 (43%) and 10 (50%) of DMAb biopsies at months 24 and 36, respectively. Though envelope-specific dynamic bone formation and remodeling para- meters could not be reliably assessed, the overall labeling findings indicate that DMAb markedly reduced cortical bone turnover. These data are consistent with the mechanism of action of DMAb, which inhibits osteoclasts throughout the skeleton. Lower Ec eroded surfaces with DMAb may reflect inhibited bone resorption and refilling of resorption spaces. Reduced cortical labeling and bone formation indices with DMAb may reflect refilling of resorption spaces that were present before fluorochromes were administered, and reduced activation of new remodeling sites. Reduced E.De is a novel finding for DMAb that may contribute to increased bone strength by reducing Ec bone loss and structural vulnerabilities asso- ciated with deep resorption cavities.Cummings SR, et al. N Engl J Med. 2009;361:756. Reid IR, et al. Bone Miner Res. 2010;25:2256. Roux C, et al. Bone. 1995;17:153.

P62

QCT Demonstrates Long-Term Proximal Femur Trabecular Density Increases in Osteoporotic Women Following Treatment with a Minimally-Invasive Local Osteo-Enhancement Procedure Involving Injection of a Resorbable, Triphasic Calcium-Based Implant Material. Klaus Engelke*[1], Dominique Favell[2], Ronald Hill[2], Thomas Fuerst[3], Bryan Huber[4], James Howe[2], Harry Genant[5]. [1]Bioclinica Germany, Germany, [2]AgNovos Healthcare, United States, [3]Bioclinica, United States, [4]Copley Hospital, United States, [5]Bioclinica; University of California, San Francisco, United States

Fragility hip fractures significantly impact quality of life and are associated with high mortality rates. These fractures often occur due to failure of trabecular bone in the proximal femur. Individuals with osteoporosis have reduced trabecular density in the proximal femur, resulting in reduced structural integrity and bone strength. A new investigational treatment uses a minimally-invasive local osteo-enhancement procedure (LOEP) to inject a unique, resorbable triphasic calcium sulfate/calcium phosphate implant material (AGN1) into the proximal femur to rebuild lost trabecular bone and increase bone strength. In canine studies, AGN1 was resorbed and replaced with integrated bone with normal humeral bone strength. In this IRB- approved clinical study, 12 postmenopausal women (age range 56-89; T-score (mean sd) left hip -3.1 0.5; right hip 3.0 0.7) underwent AGN1 LOEP on left proximal femurs; the right served as an untreated control. Total hip integral BMD (intBMD), trabecular (trBMD) and implant volume were measured by QCT (MIAF, U. of Erlangen) pre- LOEP, 12 and 24 weeks and 5-7 years (average 315 weeks) post LOEP in 10 of 12 patients. The initial implant volume (estimated 15.3 4.9 cm3) was 78%, 95% and 100% resorbed at 12, 24 and 315 weeks, respectively. Compromised bone strength before AGN1 LOEP was confirmed in all femurs by their low trBMD (Table) and was lowest in the implant area. IntBMD and trBMD increased significantly in treated femurs at all timepoints (Table). These increases were due to changes in the implant area as trBMD surrounding the implant area was not increased at 315 weeks compared to control (data not shown). Similar to pre-clinical observations, qualitative evaluation showed that bone formed in the implant area was integrated with surrounding bone. In conclusion, AGN1 LOEP significantly increased trBMD in the implant area, resulting in rapid and durable increases in proximal femur BMD. By increasing proximal femur BMD in osteoporotic femurs, it would be expected that bone strength improves, increasing fracture resistance.

Total Hip (TH) BMD: Integral and Trabecular Density[1] (mg/cm³)

		TH intBMD		TH trBMD		BMD Implant Area
Week	N	Control	Treated	Control	Treated	Treated
0	10	177±35	176±32	21±20	22±21	7±38
12	10	172±28	290±35*	21±18	217±56*	525±79
24	8[2]	174±33	257±21*	22±20	161±18*	418±50
315	10	169±28	235±33*	17±15	121±37*	536±78

[1]excludes femoral head [2]two subjects missing axial reconstructions *p<0.001 by paired t-test vs. control

P63

FEA-Estimated Proximal Femur Strength Increases Through 5-7 Year Follow- up in Osteoporotic Women Treated with a Local Osteo-Enhancement Procedure Involving Injection of a Resorbable, Triphasic Calcium-based Implant Material. Tony Keaveny*[1], David Lee[2], Dominique Favell[3], Ronald Hill[3], James Howe[3], Bryan Huber[4], Mary Bouxsein[5]. [1]University of California, Berkeley, United States, [2]O.N. Diagnostics LLC, United States, [3]AgNovos Healthcare, United States, [4]Copley Hospital, United States, [5]Harvard University, United States

Hip fragility fractures are catastrophic, costly, and are associated with high mortality rates. One new investigational treatment to lower hip fracture risk uses a minimally- invasive local osteo-enhancement procedure (LOEP) to inject a unique, resorbable, triphasic calcium sulfate/calcium phosphate implant material (AGN1) into the proximal femur with the intent of increasing femoral strength by regenerating bone lost due to osteoporosis. An IRB-approved clinical study was conducted to evaluate the biomecha- nical performance of the injected proximal femurs of 12 post-menopausal osteoporotic women (age range 56-89; right/left hip BMD T-scores: -3.0 0.7 and -3.1 0.5; mean SD). For each patient, the left femur was injected and the right served as an untreated control. Hip CT scans were taken pre-operatively and at 12 and 24 weeks, and for 10 patients at 5–7 years. The CT scans were used to conduct patient-specific, non- linear Finite Element Analysis (FEA) to non-invasively estimate hip strength in simu- lated sideways fall and stance loading conditions (O.N. Diagnostics, Berkeley, CA). For the newly regenerated bone tissue in the implant area, we applied a scale factor assuming either 100% (a =1.0) or, more conservatively, 30% (a =0.30) of the new tissue performed as normal load-bearing bone. Regardless of assumed scale factor, femoral strength in sideways fall was substantially higher in treated than control femurs at all follow-up visits (Figure). At 5–7 years, the treatment effect persisted as the treated femurs showed a 36.5 14.5% (a =1.0, $p < 0.001$) and 23.1 14.6% (a =0.30, $p < 0.01$) increase in sideways-fall strength relative to control femurs. The effects were smaller for stance loading and were statistically significant when all new tissue was assumed to be normal load-bearing bone (a =1.0). Mechanistically, at early time points newly formed bone adjacent to the implant area provided additional pathways through

which load was transferred. As a result, there appeared to be newly generated integrated load-bearing bone tissue within the original implant area through the 5–7 year follow up. These results suggest that local osteo-enhancement of the proximal femur using AGN1 in osteoporotic women can substantially increase proximal femoral strength for a side- fall and that this benefit is apparent soon after treatment and persists for at least 5–7 years.

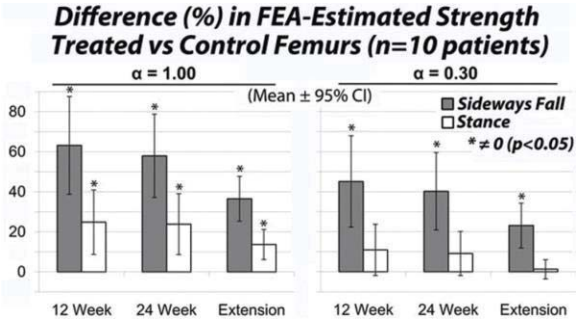

P64

Characterization of > 100 Patients with Atypical Femur Fractures: The Quebec Atypical Femur Fracture Registry. Suzanne Morin*[1], Michelle Wall[2], Etienne Belzile[3], Laetitia Michou[4], Louis-Georges Ste-Marie[5], Edward Harvey[1], Prism Schneider[6], Sonia Jean[7], Jacques Brown[3]. [1]McGill University, Canada, [2]Research Institute of the McGill University Health Center, Canada, [3]Laval University, Canada, [4]Centre de Recherche du CHU de Quebec, Canada, [5]University de Montreal, Canada, [6]University of Calgary, Canada, [7]Institut national de santé publique du Quebec, Canada

Background: Atypical femur fractures (AFF) are a rare subset of atraumatic sub- trochanteric and diaphyseal fractures associated with prolonged use of antiresorptive agents. Their pathophysiology remains unclear. Methods: Since 2012, a collaborative network of Quebec (Canada) clinicians identify and refer consenting men and women, 45 years and older, with AFF to the Quebec AFF Registry for clinical and radiographic data collection. In addition, 2D-3D X-Ray EOS scans for femur geometry assessment were done in a subset of subjects. Descriptive statistics are presented and compared to data from reference populations: 1) men and women with femur fractures in Quebec; 2005-2008 and 2) for geometric parameters, data from Chaibi, Y. 2011 and Than, P. 2012. Results: We have registered 102 participants (women 93%) with AFF (Table). Most were Caucasian (95%) and 69.5 [9.3] years at the time of AFF. All were exposed to BPs with an average cumulative duration of 10.4 [4.5] years. There were 154 fractures (77 complete) among the 102 participants; 71% experienced prodromal pain. Fifty-two participants had bilateral fractures, of which 87% were documented to be at concordant sites on the femora. AFF were more common in the diaphysis (68%) than at the subtrochanteric site. Use of proton pump inhibitors (52%), hormone therapy (9%) and raloxifene (6%) was higher than in the Quebec population. In women (N=37) who underwent EOS scans femoral neck shaft angle (125.9 [5.2] o), varus deformity at the knee (-2.2 [4.2] o), femur bowing (-3. 6 [3.49] o) and hip knee shaft angle (7.98 [2.3] o) confirmed varus anatomy at the hip and accentuated bowing of the femur compared to reference data. Forty-five participants used teriparatide post-AFF. In patients who underwent surgery (N= 85), subtrochanteric AFF were most often treated with long cephalomedullary nails, whereas diaphyseal AFF treatment was variable. Patients with unilateral complete AFF showed greater improvement in functional performance 6 months post-surgical fixation compared to patients with unilateral incomplete AFF without surgical fixation. Conclusions: Significant differences are apparent in AFF subjects compared to reference populations. Furthermore, variance amongst orthopedic and medical practices may impact functional recovery in these patients. Through comprehensive data collec- tion (including saliva specimens) the Quebec AF Registry aims to provide new data towards the understanding of AFF pathogenesis.

Table Clinical Characteristics of Participants in Quebec Registry AFF

Characteristics		AFF N=102
Age *years (SD)*		69.5 (9.3)
Women *n (%)*		94 (93)
Height (cm) *mean (SD)*		157.7 (7.6)
Weight (kg) *mean (SD)*		68.3 (12.5)
BMI (kg/m²) mean *(SD)*		27.4 (4.5)
Race/Ethnicity *n (%)*		
Caucasian		97 (95)
Asian		5 (5)
Previous Fragility Fracture *n (%)*		58 (57)
Family History *n (%)*		
Osteoporosis		43 (42)
Parental hip fracture		17 (17)
Other family member hip fracture		15 (15)
Supplement Dosage *mean (SD)*		
Vitamin D (UI/d)		1087 (997)
Calcium (mg/d)		779 (334)
Biochemistry Serum *mean (SD)*	*n*	
PTH *(pmol/L)*	73	7.4 (6.9)
Alkaline Phosphatase *(U/L)*	85	69.8 (29.6)
Osteocalcin *(µg/L)*	50	11.1 (5.5)
TSH *(mIU/L)*	67	2.19 (1.84)
C-telopeptide *(µg/L)*	60	0.211 (0.127)
25-OH Vitamin D *(nmol/L)*	88	81.6 (26.1)
Bone Mineral Density *mean (SD)*	*n*	
Femoral Neck (g/cm²)	81	0.768
T-score	87	-1.6
Lumbar Spine (g/cm²)	83	0.965
T-score	88	-1.6
Mechanism of Injury *n (%)*		
Bone broke without fall		67 (66)
Fall from standing height		33 (32)
Prodromal Pain		
Present *n (%)*		72 (71)
Length of time (months) *mean (SD)*		10.3 (13.4)
Fractures *n (%)*		
Total		154
Bilateral		52 (51)
Complete		77 (50)
Incomplete		77 (50)

P65

The effect of teriparatide on fracture healing of vertebral compression fracture in post menopausal women. Seung Woo Suh*[1], Si Young Park[2], Jae Young Hong[1], Tae Wook Kang[1]. [1]Korea Univeresity Hospital, Korea, Republic of, [2]Korea University Hospital, Korea, Republic of, University Hospital, Korea, Republic of

Introduction: Acute vertebral compression fractures cause severe back pain and need long time to heal. The progression of fracture or nonunion is not rare. The teriparatide is a synthetic parathyroid hormone which has been used as anabolic agent and treatment of osteoporosis. It also can be used for promoting fracture healing in special condition. Periodic infusion of teriparatide enhances bone formation and increases bone strength. We evaluated the effect of periodic teriparatide infusion on fracture healing of acute vertebral compression fractures Methods: A prospective study consisting of a review of case report form. We prospectively enrolled 84 postmenopausal women who had one or two acute painful vertebral compression fractures confirmed by MRI. All patients were treated conserva- tively. Among them, 32 patients were treated conservatively with teriparatide for at least 6 months (group I), and 52 were treated with antiresorptive agent (group II). VAS and ODI scores were assessed at each follow up until 1 year after trauma. We also measured radiographic changes, the degree of collapse progression. Results: The progression of fractured vertebral body collapse was shown in both groups, but the degree of progression was significantly lower in group I than in group II. At the last follow-up, mean increments of kyphosis and wedge angle were significantly lower in group I. Clinical outcome measures were closely related with vertebral body collapse. Conclusion: Periodic infusion of teriparatide might have many beneficial effect on acute vertebral compression fractures in postmenopausal women. Patients using teri- paratide showed quicker symptomatic improvement and less collapsed vertebral body 1 year after trauma compared to patients using anti-resorptive agent.

P66

Prevalence of severe suppression of bone turnover (SSBT) in patients on long- term bisphosphonate (BP) therapy. Shijing Qiu*, Elizabeth Warner, Pooja Kulkarni, Mahalakshi Honasoge, Arti Bhan, Shiri Levy, George Divine, D. Sudhaker Rao. Henry Ford Hospital, United States

In vivo tetracycline labeling of bone is a gold standard maker to determine the rate of bone turnover (or bone remodeling). Severe suppression of bone turnover (SSBT) is commonly defined as complete absence of tetracycline labeling in cancellous bone. However, it is inappropriate to assume that bone with tetracycline labeling, no matter how little, as having normal bone turnover. In the current study, we developed reference range for bone turnover based on the results from healthy premenopausal women, the lower limit of which as the cutoff to define SSBT. The bone turnover-related variables, including mineralizing surface (MS/BS, %), mineral apposition rate (MAR, mm/day), bone formation rate (BFR/BS, mm3/mm2/ year) and activation frequency (Ac.f, /year), were determined in iliac bone biopsies obtained from 43 healthy premenopausal white women. The reference range was defined as a 95% interval with 2.5% of the values less than the lower limit and 2.5% were more than the upper limit. SSBT was defined when BFR/BS and/or Ac.f fell below the lower limit. The same measurements were performed on iliac bone biopsies from postmeno- pausal healthy women and from patients on long-term BP therapy (all postmenopausal) with and without atypical femur fracture (AFF). The results are shown in Table 1. Since wall thickness to calculate Ac.f may not be detected in some patients with BP exposure, we suggest BFR/BS as more appropriate variable to define bone turnover. In postme- nopausal women, the prevalence of SSBT was < 5% in cancellous bone, and none in whole biopsy. In contrast, the prevalence of SSBT increased to approximately 60% in cancellous bone and 30% in whole biopsy in BP-treated patients, both of which were significantly higher than those in postmenopausal women. However, there was no significant difference in the prevalence of SSBT between BP treated patients with and without AFF. In conclusion, this study confirms that BP exposure can significantly increase the risk of SSBT in postmenopausal women. Although the prevalence of SSBT was similar in BP-treated patients with and without AFF, a higher trend was seen in patients with AFF.

Table 1. The difference in SSBT prevalence among healthy postmenopausal women and BP treated patients with and without atypical femur fracture

	MS/BS	MAR	BFR	Ac.f
	%	μm	$\mu m^3/\mu m^2$/year	/year
Reference Range (Premenopausal Women n = 43)				
Cancellous Surface	0.881 - 14.2	0.107 - 0.791	0.628 - 26.9	0.016 - 0.751
Combined Surface	1.41 - 12.5	0.107 - 0.847	0.689 - 29.8	0.019 - 0.727
Cancellous Surface				
HPMW	4/66 (6.06)	1/66 (1.52)	3/66 (4.55)	2/66 (3.03)
Patients with BP exposure	35/54 (64.8)	24/54 (44.4)	32/54 (59.3)	29/51 (56.9)
no AFF	22/34 (64.7)	14/34 (41.2)	19/34 (55.9)	19/34 (55.9)
with AFF	13/20 (65.0)	10/20 (50.0)	13/20 (65.0)	10/17 (58.8)
Combined Surface				
HPMW	1/66 (1.52)	0/66 (0)	0/66 (0)	0/66 (0)
Patients with BP exposure	28/54 (51.9)	12/54 (22.2)	16/54 (29.6)	13/48 (27.1)
no AFF	15/34 (44.1)	6/34 (17.6)	9/34 (26.5)	8/33 (24.2)
with AFF	13/20 (65.0)	6/20 (30.0)	7/20 (35.0)	5/15 (33.3)

HPMW: Healthy postmenopausal women. All variable rates in HPMW were significantly lower than those in patients with BP exposure

P67

Vertebral and Nonvertebral Fracture Risk in Subgroups of Patients Receiving Teriparatide in Real-World Clinical Practice: Integrated Analysis of Four Prospective Observational Studies. Stuart Silverman*[1], Bente Langdahl[2], Saeko Fujiwara[3], Kenneth Saag[4], Nicola Napoli[5], Satoshi Soen[6], Damon Disch[7], Fernando Marin[8], Hiroyuki Enomoto[9], John Krege[10]. [1]Cedars-Sinai/UCLA Medical Center and OMC Clinical Research Center, United States, [2]Arhus University Hospital, Denmark, [3]Health Management and Promotion Center, Japan, [4]University of Alabama at Birmingham, United States, [5]University Campus Bio-Medico, Italy, [6]Department of Orthopaedic Surgery and Rheumatology, Kindai University Nara Hospital, Japan, [7]Eli Lilly and Company, United States, [8]Lilly Research Centre, United Kingdom, [9]Eli Lilly Japan K.K., Japan, [10]Elli Lilly and Company, United States

Purpose: Although the phase 3 teriparatide (TPTD) fracture prevention trial showed significant reductions in clinical vertebral fracture (CVF) and nonvertebral fracture (NVF), real-world evidence regarding the effects of TPTD in subgroups of patients is limited. Our goal was to report the rate of CVF and NVF with TPTD in subsets of patients from four integrated real-world observational studies. Methods: Data from DANCE (USA), EFOS and EXFOS (Europe), and JFOS (Japan) prospective, observational studies of ambulatory women (n=8117) and men (n=710; no response=1) with osteoporosis receiving subcutaneous TPTD 20 mg/day for 18 to 24 months (mo) as prescribed during real-world practice were integrated. During treatment with TPTD, CVF and NVF fracture rates at 0–6 months (a reference period) were compared to 6-mo to end of dosing (>6 mo). Subgroups were diabetes, glucocorticoids, rheumatoid arthritis, previous bisphosphonates, previous hip fracture, previous vertebral fracture, female gender, and age 75 yrs, and comparison was to those patients not in these subsets using a piecewise exponential model for the first occurrence of fracture to evaluate rates. Results: Data for 8828 patients with 1 assessment on treatment showed that 92% were women, mean age was 71 years, and median treatment with TPTD was 1.6 years. For the full cohort, NVF, CVF, and clinical and hip fractures, per 100 patient-years were significantly lower in the >6 mo vs 0–6 mo reference period by 50, 43, 62, and 56%, respectively. The effects of TPTD on CVF and NVF over time were statistically consistent in all subgroups; age interaction P=.07 for CVF where patients in both age groups had significantly reduced CVF over time and for all other interactions P>.11. Regardless of the time period, patients in the glucocorticoid and previous vertebral fracture subgroups had significantly higher risk of CVF, and patients in the rheumatoid arthritis, previous hip fracture, previous vertebral fracture, and female subgroups had significantly higher risk of NVF; age, diabetes, and previous bisphosphonate showed no significant effect on CVF or NVF. In all analyses, fracture risk significantly decreased from 0–6 to >6 mo (except NVF by gender where only women had a significant reduction). Conclusions: The present integrated posthoc results show a statistically consistent decrease in clinical vertebral and nonvertebral fracture risk during teriparatide treatment in important subgroups of real-world patients.

P68

Clinical efficacy and safety of bazedoxifene(Viviant®) in postmenopausal women with osteoporosis and osteopenia. Hee-Dong Chae*, Ji-Won Song, Sung-Hoon Kim, Chung-Hoon Kim, Byung-Moon Kang. Asan medical center, Korea, Republic of

Objective : Bazedoxifene is a selective estrogen receptor modulator that decreases fracture risk and bone turnover in postmenopausal women. The objective of this study was to evaluate the efficacy and safety of bazedoxifene in women with postmenopausal osteoporosis or osteopenia. Materials and Methods : A prospective pilot study was performed in Asan Medical Center from 2014 to 2016 and the eligible patients were followed up for up to 15 months. Patients were screened and women with osteoporosis or osteopenia were included. Subjects received bazedoxifene 20 mg per day, followed by visits at months 1, 3, 9, and 15. Bone mineral density (BMD) of lumbar spine and hip was measured using DXA (Dual X-ray absorptiometry) at months -24 and -12, at the start of the study, and at month 12. Safety and tolerability evaluations included adverse event reports, physical examinations and clinical laboratory tests, including chemical and lipid assessments. Other safety monitoring included breast examination, mammography, and gynecologic ultrasound. Results : Sixty-seven patients were enrolled, and 65 patients completed the study in 15 months. Five patients (8%) showed significant improvement in lumbar spine BMD at month 12 ($p<0.03$), however total hip BMD showed no statistically significant improve- ment. Fourty of the 65 patients(61%) maintained the lumbar spine BMD, and 50 patients(78%) had no significant change in femur BMD. Fifteen patients(23%) showing a decrease in lumbar spine BMD and 5 patients (8%) showing a decrease in femur BMD prior to administration of bazedoxifene obtained sustained BMD after medication. Ten of the 65 patients(15%) complained of dyspepsia, the other 10 patients(15%) showed an increase in liver enzymes, and 5 patients (8%) had shoulder pain, but these events did not lead to discontinuation of medication. There were no serious adverse events including venous thromboembolism, coronary heart disease, cerebrovascular accidents, breast cancer, or endometrial carcinoma. Conclusions: Treatment with bazedoxifene prevented bone loss and reduced bone turnover and was generally safe and well tolerated in postmenopausal women with osteoporosis or osteopenia.

P69

Strontium treatment has synergistic effects with PTH as evaluated in OVX rats. Patrick Ammann*. Division of Bone Diseases, Switzerland

Most of the anti-fracture efficacy of strontium treatment is related to an improve- ment of bone material level properties. Strontium is also known to stimulate bone formation during skeletal growth and bone healing process. An obvious question is to understand if strontium could improve bone material level properties under PTH treat- ment and influence the PTH stimulating effect on bone formation. The aims of this study are (i) to evaluate whether the association of stontium with PTH or Alendronate can be synergistic and able to better prevent the decrease of bone strength in OVX rats than either drug administered alone and (ii) to investigate

whether its potential synergistic effects are dependent on the in vivo stimulation of new bone formation. OVX rats were treated with strontium ranelate (SR, 625 mg/kg day po) alone, with a stimulator of bone formation (PTH 8 microg/kg*day SC) or treatment decreasing bone remodeling, i.e. formation, (Alendronate 18 microg/kg twice a week, SC) with or without strontium ranelate (625 mg/kg day po). Seven groups of 12 rats (SHAM, OVX, SR, PTH, Alendronate, SR-PTH, SR-Alendronate) received treatments or respective vehicles for 8 weeks. At the end of the experiment, vertebrae where removed for biomechanics, microCT and nanoindentation testing. A curative protocol was also performed. PTH and Alendronate, but not strontium, fully prevent the deleterious effect of OVX on bone strength; values obtained under PTH are significantly higher as compared to SHAM. This was associated with the preservation of bone volume in Alendronate treated animals but not in strontium treated rats, and further significant increment under PTH as compared to SHAM. Combined therapy with strontium resulted in a further significant increase of maximum load as compared with PTH treatment alone. The addition of strontium improved intrinsic bone tissue quality In SR- PTH treated rats and corrected the impaired intrinsic tissue quality observed under PTH treatment. Furthermore it resulted in a significant increment of trabecular thickness reflecting the positive influence of strontium on bone formation. No effect was observed in the case of the association with Alendronate. Similar effects were observed in a curative protocol. Together, these data suggest that strontium treatment maximizes the in vivo effect of PTH by improving the intrinsic bone quality of the new formed bone and potentially by a synergistic effect on bone formation.

P70

Addition of Diabetes Agravates Deleterious Effects of Metabolic Syndrome on Bone. Cedo Bagi*, Edwin Berryman, Kristin Edwards, David Zakur, Chang-Ning Liu. Pfizer, Inc, United States

Rationale. Metabolic syndrome (MSy) and osteoporosis share the same risk factors. Patients with type 1 and 2 diabetes, have a higher risk of osteoporosis and fractures. Occurrence of diabetes in patients with MSy signals the point at which time the disease follows an increasingly malignant path with the worsening of symptoms caused by liver failure. Nonalcoholic fatty liver disease (NAFLD), and its more serious form nonalco- holic steatohepatitis (NASH), are known manifestations of obesity and MSy. To deter- mine the long-term influence of a westernized diet on bone we combined streptozotocin treatment with this westernized diet to create a rat model of human MSy. Methods. Mature male rats were fed and watered with either standard chow and RO water (controls), or a high fat, high cholesterol diet and sugar water containing 55% fructose and 45% glucose (HFTFX). A third group of rats also received the HFTFX diet and a single dose of streptozotocin (30 mg/kg; ip) to induce diabetes (HFTFX STZ). Body weight was done twice weekly. Glucose tolerance tests were conducted several times during the course of the study. Serum chemistry, liver enzymes and biomarkers of bone metabolism were evaluated at 10 and 28 weeks. Sheer wave elastography (SWE) was deployed to assess liver fibrosis. The liver and pancreas were evaluated by histology. Cancellous bone was evaluated by mCT, and cortical bone by pQCT and by 3-point bending method. Results. Body mass and fat was significantly greater in HFTFX and HFTFX STZ rats compared to Controls. Rats in both HFTFX and the HFTFX STZ group showed clear signs of NASH. The HFTFX STZ rats were insulin resistant at 10 and 28 weeks, although the insulin resistance diminished over time. Both HFTFX and HFTFX STZ rats exhibited deterioration of cancellous bone at the proximal tibia, however the change was more dramatic in HFTFX STZ rats. Despite the fact that obese rats had somewhat larger bones the cortical bone thickness was diminished and contributed to significant deterioration of bone strength. Diminished cortical bone strength in HFTFX fed rats was further aggravated by diabetes. Conclusion. The HFTFX and HFTFX STZ rats provide pre-clinical modelsof NAFLD and NASH and can be easily manipulated to mimic various aspects of MSy in humans. The addition of diabetes even at a very mild form significantly aggravates the symptoms of MSy and tes to the deterioration of bone structure and strength.

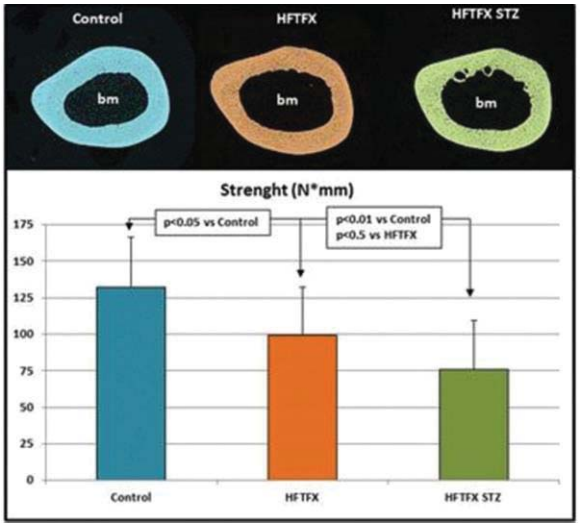

P71

Abaloparatide Increased Bone Mass in a Rabbit Glucocorticoid-Induced Osteopenia Model. Heidi Chandler*, Allen Pierce, Jeffery Brown, Michael Ominsky, Gary Hattersley. Radius Health Inc, United States

Estrogen deficiency and glucocorticoid (GC) therapy are the main causes of postme- nopausal and secondary osteoporosis, respectively. Abaloparatide (ABL), a selective PTH1 receptor agonist, increased BMD and bone formation in estrogen-deficient ovar- iectomized (OVX) animals and in postmenopausal women with osteoporosis, with limited increases in bone resorption indices. The ability of ABL to reverse established bone loss caused by glucocorticoid excess was studied in New Zealand White rabbits. Forty rabbits underwent OVX (n=32) or sham surgery (n=8) at ~6 months of age, with 24 OVX rabbits receiving GC methylprednisolone (OVX + GC) for 6 weeks post-surgery. After a 6-week bone depletion period, the OVX + GC rabbits continued to receive GC and treatment was initiated with ABL at 5 or 25 mg/kg (n=8/group) or vehicle (Veh) sc once daily, while the other OVX (n = 8) and sham groups received Veh sc. GC treatment resulted in robust bone loss at the end of the bone depletion period in OVX rabbits, with lumbar spine DXA BMD that was 28% lower in the Veh-treated OVX+GC group compared to OVX controls at week 0 ($p<0.05$), an effect which persisted through the treatment period. After 8 weeks of ABL, bone mass was dose-dependently increased in OVX+GC rabbits, with 35% greater lumbar spine BMD in the ABL-25 mg/kg group compared with OVX+GC Veh ($p<0.05$). The GC-mediated loss of lumbar spine BMD in OVX rabbits was predominantly restored in the ABL-25 mg/kg group, which had a similar mean BMD to that of the OVX control group at week 8. These preclinical findings demonstrate that ABL increases bone mass in a glucocorticoid-induced osteopenia model.

P72

Abaloparatide-SC Improved Cortical Bridging and Increased Callus Mass and Strength in a Rat Closed Femur Fracture Model. Heidi Chandler*, Allen Pierce, Jeffery Brown, Michael Ominsky, Gary Hattersley. Radius Health Inc, United States

Healing of long bone fractures involves endochondral and intramembranous bone formation, which together form a callus that achieves union, stabilization, and gradual recovery of bone strength. Endogenous PTHrP activates PTH1 receptors (PTH1R) at fracture sites to promote endochondral and intramembranous ossification, and exogen- ous PTH1R agonists including PTHrP have been shown to enhance fracture healing in animal models. We therefore studied the effects of abaloparatide (ABL), a selective PTH1R agonist, in a rat femur fracture model. Ninety-six 12-week-old male SD rats underwent a closed, internally stabilized fracture of the right femur. Treatment began the next day with daily sc ABL at 5 or 25 mg/kg/d (ABL5 and ABL25, n = 32/dose level) or with daily sc saline (VEH, n = 32). Sixteen rats from each group were necropsied after 4 and 6 weeks of healing, with 12 fractured femurs per group used for micro-CT and biomechanical testing and the other 4 femurs used for micro-CT and histology. Semi- quantitative histologic scoring of cortical bridging across the fracture gap showed significantly greater bridging in the ABL5 and ABL25 groups at week 4 compared with VEH controls. Histomorphometry at week 4 indicated significantly greater callus area in the ABL5 and ABL25 groups, which persisted at week 6 for the ABL25 group, compared to VEH. Micro-CT of fracture calluses showed that the ABL5 and ABL25 groups had significantly greater callus bone volume, bone volume fraction, and BMC at weeks 4 and 6, compared to VEH. Three-point bending tests at week 4 indicated that callus stiffness was 60% and 96% higher in the ABL5 and ABL25 groups, respectively (both $p<0.05$ vs VEH). At week 6, callus stiffness was 112% higher in the ABL5 group ($p<0.05$ vs VEH). Callus peak load was 77% higher in the ABL25 group at week 4 ($p<0.05$ vs VEH), and remained numerically higher in both ABL groups at week 6 compared with VEH. Together these data suggest systemically administered ABL can enhance local healing in a rat closed femur fracture model.

P73

Abaloparatide, a Selective PTH1 Receptor Agonist, Reversed Bone Loss and Improved Trabecular Architecture in Orchiectomized Rats. Heidi Chandler*[12], Tara Mullarkey[12], Rachel Stewart[3], Gary Hattersley[12]. [1]Radius Health Inc, United States, [2]Radius Health inc, United States, [3]inviCRO, United States

Androgens promote the acquisition and maintenance of bone mass. Hypogonadism and androgen deprivation therapy for prostate cancer contribute to bone loss and increased fracture risk in men. Anabolic therapy with PTH(1-34) can increase bone mineral density (BMD) in men with low bone mass, but concomitant stimulation of bone resorption with PTH(1-34) may limit its bone- building potential. Abaloparatide (ABL) is a selective PTH1 receptor agonist that increases bone formation and BMD with limited increases in bone resorption indices, suggesting potential for increasing BMD in states of androgen deficiency. ABL was therefore tested in castrated (orchiectomized; ORX) rats, an androgen deficiency model that may recapitulate some of the deleterious skeletal changes seen in men with androgen deficiency. Male Sprague-Dawley rats underwent ORX or sham surgery at ~3 months of age. After a 4-week bone depletion period, ORX rats were then treated by daily sc injection for 4 weeks with ABL (20 mg/kg/ d, n = 8) or vehicle (Veh, n = 8). Sham controls (n = 8) received daily Veh sc. The 4th lumbar vertebra (L4) was collected at necropsy for micro-CT evaluation. After 8 total weeks of androgen deficiency, the ORX group had 13.2% lower L4 BMD ($p < 0.005$ vs sham) and 17.3% lower trabecular bone volume fraction (BVF; $p = 0.067$) compared with sham controls. Trabecular thickness (Tb.Th) was similar in the ORX and sham controls, but the ORX group showed a significant 133% increase vs sham controls for trabecular pattern factor (TPF), a morphometric index that is inversely related the extent of trabecular disconnections and perforations. After 4 weeks of treatment, starting 4 weeks post-surgery, the ABL group had 16.6% greater L4 BMD, 50.2% greater BVF, and 32.6% greater Tb.Th compared with ORX controls (all $p <$ group showed a 39.3% lower TBF compared with ORX controls ($p < 0.05$) suggesting more robust and better-connected trabecular architecture. The ABL group also had 24.2% greater BFV and 29.0% greater Tb.Th compared with sham controls (both $p < 0.01$). These data indicate that ABL reversed vertebral bone loss and trabecular

microarchi- tectural deterioration in ORX rats by increasing trabecular bone volume and thickness, with preliminary evidence that ABL may reduce the extent of trabecular perforations and disconnections.

P74

Chronic kidney disease and aging diminish both whole bone and microscale bone quality. Chelsea Heveran*[1], Adam Rauff[2], Eric Livingston[3], Ted Bateman[3], Moshe Levi[4], Dana Carpenter[3], Karen King[5], Virginia Ferguson[3]. [1]Department of Mechanical Engineering, University of Colorado, United States, [2]Department of Bioengineering, United States, [3]Department of Mechanical Engineering, United States, [4]Department of Medicine, Division of Renal Diseases and Hypertension, University of Colorado School of Medicine, United States, [5]Department of Orthopaedics, University of Colorado School of Medicine, United States

Chronic Kidney Disease (CKD) increases the prevalence of bone fracture, yet the combined effects of aging and CKD on bone are unknown. The purpose of this study was to evaluate how whole bone and microscale bone quality are detrimentally affected with aging and CKD. Male C57Bl/6 mice aged 3 mo (young), 15 mo (middle-age) and 21 mo (old) under- went 5/6th nephrectomy to establish CKD or sham surgeries (N=48, n=6-10 per age/ treatment group). Mice were aged three months and euthanized. MicroCT evaluated microarchitecture of the cortical femur and trabecular tibia. Femurs were broken *via* three-point bending then dehydrated, embedded, sectioned at the mid-diaphysis, and polished. Microscale mineral:matrix (v1PO4:amide III) and modulus (*E*) were mapped across the cortical thickness with site-matched Raman spectroscopy and nanoindenta- tion. Mature enzymatic crosslinks (HP and LP) and pentosidine were evaluated for the humerus using high-performance liquid chromatography. Osteocyte lacunae were imaged *via* confocal microscopy from fuchsin-stained tibias and reconstructed in 3D to evaluate lacunar geometries. CKD was confirmed with increased serum BUN ($p<0.001$). At the whole bone scale, bone quality was lower with both aging and CKD and most diminished in old mice with CKD. Age and CKD decreased cortical (*e.g*, thickness, tissue mineral density (Ct.TMD)) and trabecular (*e.g*, thickness (Tb.Th)) microarchitecture ($p<0.05$). Age and CKD also decreased stiffness and max load ($p<0.05$). CKD affected skeletal cross-links, reducing LP ($p<0.05$). Further, HP and LP were -23.5% ($p=0.054$) and 13.7% ($p=0.08$) lower in old mice with CKD than sham, respectively. At the microscale, age and CKD also decreased bone quality. *E* may be reduced (-6.8%, $p=0.06$) while mineral:matrix was 18.4% higher in middle-age mice with CKD ($p<0.05$). Osteocyte lacunar geometries also showed effects of age and CKD. In sham mice, osteocyte lacunae became smaller and more spherical with advancing age ($p<0.05$). However, in CKD, lacunae had similar geometries across all ages, perhaps indicating disrupted perilacunar remodeling with kidney dysfunction. Aging and CKD together reduce both whole bone and microscale bone quality. Less mature crosslinks and lower TMD suggest that both mineral and matrix changes occur with CKD and are most pronounced with advanced age. Also, the osteocyte may be uality changes in CKD. These findings may help explain the clinically-observed bone fragility in CKD.

	Young		Middle-age		Old	
	Sham	*CKD*	*Sham*	*CKD*	*Sham*	*CKD*
Ct.Th (μm)	198.1 ± 4.2	187.7 ± 5.3	189.4 ±3.9	167.7 ± 4.7*	201.7 ±5.6	162.4 ± 4.3*
Ct.TMD (mg HG/cm³)	1044.8 ± 8.88	1015.9 ± 4.09*	1056.1 ± 6.58	1037.7 ± 6.16*	1063.1 ± 3.05	1038.7 ± 6.40*
Tb.Th (μm)	50 ±1.6	43±1.3*	49 ±1.0	45 ±1.9	45 ±1.3	40 ±1.5*
Stiffness (N/mm)	97.96 ± 4.87	88.82 ± 5.01	92.30 ± 6.12	64.62* ± 6.41	83.28 ± 7.92	57.68* ± 3.24
Ln(mineral: matrix)	2.56 ± 0.056	2.67 ± 0.057	2.68 ± 0.056	2.85 ± 0.052*	2.67 ± 0.062	2.74 ± 0.058
(E (GPa))²	735.2 ± 36.4	687.9 ± 37.5	634.0 ± 36.6	536.6 ± 34.3	506.0 ± 40.5	562.4 ± 38.1
mol LP/ mol collagen	0.27 ± 0.0079	0.23 ± 0.019	0.30 ± 0.020	0.30 ± 0.016	0.31 ± 0.015	0.26 ± 0.072*
Lacunar volume (μm³)	454.9 ± 39.2	405.4 ± 55.2	365.1 ± 66.7	256.6 ± 32.1	269.7 ± 26.2	357.5 ± 54.9

Table 1: Bone quality is diminished with age and CKD. Mean ± standard error. * = < 0.05 for CKD vs sham within the same age.

P75

Cyclic Treatment Regimen Rescues Parathyroid Hormone (PTH) Discontinuation- Induced Bone Loss and Microarchitecture Deterioration. Wei-Ju Tseng*, Hongbo Zhao, Wonsae Lee, Yang Liu, Yihan Li, Chantal de Bakkar, Ling Qin, X. Sherry Liu. University of Pennsylvania, United States

Despite the potent effect of intermittent PTH treatment on promoting new bone formation, BMD rapidly decreases upon PTH discontinuation. To uncover the mechan- isms behind this adverse phenomenon, we first examined the changes in tibial bone microarchitecture in ovariectomized (OVX) rats by *in vivo* mCT. 18 4-mo-old rats underwent OVX surgery and developed osteopenia for 4 wks (50% reduction in BV/TV). Bone loss continued in VEH-treated rats (n=9) for 12 wks. In contrast, 3-wk PTH treatment (40 mg/kg, n=9) led to 97% and 27% greater BV/TV and Tb.Th, respectively, in the PTH *vs.* VEH group. Intriguingly, 1 wk after the withdrawal (wk 4), BV/TV and Tb.Th continued to show trends of improvement. Trends of bone deterioration appeared during the 2nd and 3rd wk of PTH withdrawal (wk 5 and 6), with a 28% decrease in BV/TV at wk 6 *vs.* wk 4 (Fig 1A). Histology (n=6/group) suggested that 3-wk PTH treatment led to 117% greater osteoblast # (Ob.N/BS) and 55% and 70% lower osteoclast # (Oc.N/BS) and adipocyte # (Adi.N/Ma.Ar), respectively, than VEH group. After 1-wk withdrawal from PTH, Ob.N/BS decreased 82% but remained 36% greater than VEH, and Oc.N/BS and Adi.N/Ma.Ar continued to be suppressed. 2 wk after PTH discontinuation, there was no remaining difference in Ob.N/BS and Oc.N/BS from VEH while Adi.N/Ma.Ar was 56% lower than VEH group (Fig 1BCD). The continuous anabolic window upon early withdrawal from PTH offers a new mechanism in support of a cyclic administration regimen with repeated cycles of on and off PTH treatment. Next, 3 treatment regimens were examined in OVX rats: VEH (n=3, 18-wk saline), PTH-VEH (n=6, 9-wk PTH followed by 9-wk saline), and Cyclic PTH (n=7, 3-wk PTH followed by 3-wk saline, 3 cycles). In the PTH-VEH group, 9-wk PTH led to a 97% increase in BV/TV, followed by a 72% decrease after 9-wk discontinuation, with no difference from VEH group at wk 18. Similar trends were found for Tb.Th (Fig 2). In contrast, in the Cyclic PTH group, the first cycle of 3-wk PTH on and 3-wk off prevented reduction in BV/TV and led to a 33% increase in Tb.Th. BV/TV stabilized and Tb.Th continued to increase during the 2nd and 3rd cycles. At wk 18, BV/TV and Tb.Th in Cyclic PTH rats were greater than both PTH-VEH and VEH rats ($p<0.05$, Fig 2AB). In summary, our study discovered a continuous anabolic window upon early withdrawal from PTH which treatment regimen to maximize the total duration and efficacy of PTH treatment on bone microarchitecture.

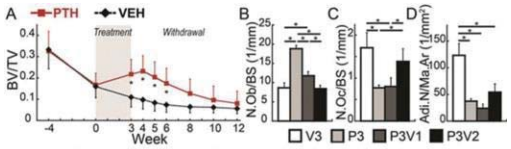

Fig 1 (A) Changes in BV/TV in 12-wk VEH treated, and 3-wk PTH followed by 9-wk VEH treated OVX rats. (B-D) Comparisons in cellular activities among rats with 3-wk VEH (V3) and PTH (P3), and 3-wk PTH followed by 1- and 2- wk VEH treatments (P3V1 and P3V2). * difference between treatment groups ($p<0.05$).

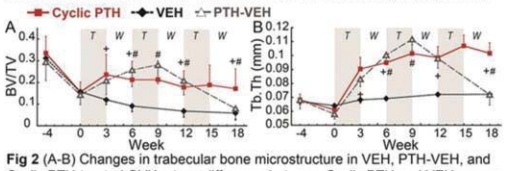

Fig 2 (A-B) Changes in trabecular bone microstructure in VEH, PTH-VEH, and Cyclic PTH-treated OVX rats. + difference between Cyclic PTH and VEH groups ($p<0.05$). # difference between Cyclic PTH and PTH-VEH groups ($p<0.05$). *T*: Treatment, *W*: Withdrawal in the Cyclic PTH group.

P76

Bone Structure and Bone Mineral Density in Growing Male Mice is Largely Unchanged when Calcium and Vitamin D is Fed at Levels Lower Than Those Present in the AIN93G Reference Diet. C. Brent Wakefield*[1], Jenalyn L. Yumol[1], Sandra M. Sacco[1], Phillip J. Sullivan[1], Elena M. Comelli[2], Wendy E. Ward[1]. [1]Brock University, Canada, [2]University of Toronto Canada

Background: Our group along with others use CD-1 mice to study the effects of nutritional interventions on bone development. While reference diets are used in these studies to ensure nutritional intake is standardized between and within research groups, there is evidence that the AIN93G reference diet contains excess calcium (Ca) and vitamin D (vit D) which may confound results. Considering males may require higher dietary Ca and vit D due to a greater rate of growth, females were studied separately. Purpose: To determine if a lower level of Ca and vit D than that in the AIN93G reference diet supports bone development in growing male CD-1 mice. Methods: Weanling male CD-1 mice were randomized to modified AIN93G diets containing either 100 IU vit D/ kg diet (trial 1) or 400 IU vit D/kg diet (trial 2) within one of three Ca levels (3.5, 3, or 2.5 g/kg diet) or the reference AIN93G diet (REF) (1000 IU vit D and 5 g Ca/kg) from weaning to 4 months of age (N = 124). At 2 and 4 months of age, BMD and structural properties of the tibia were analysed using *in vivo* microcomputed tomography (SkyScan 1176). The 4th lumbar vertebrae (L4) were scanned *ex vivo* at 4 months of age. Results: In trial 1 (100 IU vit D/kg diet), at the proximal tibia, the 2.5 g Ca/kg group had lower trabecular thickness compared to the REF group, and cortical thickness was lower in the 2.5 and 3 g Ca/kg groups at the midpoint compared to the REF group ($p<.05$). In trial 2 (400 IU vit D/kg diet), at tibia midpoint, the 2.5 g Ca/kg group had lower ($p<0.05$) cortical thickness compared to the 3.5 g Ca/kg group. There were no differences in LV or for other trabecular or cortical bone measures at the tibia in Trial 1 or 2. Conclusion: When Ca levels were lowered to 2.5 or 3 g Ca/kg some tibia but not LV outcomes were compromised. Considering

humans generally consume less Ca and vit D than what is recommended, it is possible that rodent research diets that do not contain higher levels of nutrients than needed may strengthen the extrapolation of results to the human scenario. Further research is needed to refine the level of Ca and vit D of reference diets that meets hile also allowing other food components to be tested for their role in supporting healthy bone development.

P77

Prior Focal Radiation Causes Atrophic Nonunion Healing in Mouse Long Bone Fracture. Luqiang Wang*[1], Abhishek Chandra [2], Robert Tower[1], Jaimo Ahn[1], Yejia Zhang[1], Ling Qin[1]. [1]Department of Orthopaedic Surgery, Perelman School of Medicine, University of Pennsylvania, United States, [2]Department of Physiology and Biomedical Engineering, Division of & Gerontology, Mayo Clinic, United States

Approximately 5-10% of bone fractures have delayed or nonunion healing. Among them, atrophic nonunion can be especially challenging representing a major clinical burden in skeletal trauma treatment. Cancer patients treated by radiotherapy are more prone to developing fracture nonunion within the irradiated area even several years later. To better understand the mechanism, we studied the fracture healing process in mouse long bones with prior focal radiation. Two-month-old C57BL/6 male mice received radiation at the midshaft of right tibiae (5 mm long) from a focal irradiator (SARRP, 8 Gy twice) and two weeks later, closed and transverse fractures within the irradiated area and contralateral legs. At this time point, bone marrow hematopoietic components had already recovered but the periosteal cellularity was significantly lower in the irradiated bone. Three days later, the periosteum in irradiated bones expanded significantly less compared to control at the proximal side of the fracture (the region close to the growth plate) and showed almost no notable expansion distal to the fracture site (the region close to the growth plate). Callus volume and bone volume were drastically decreased in irradiated bones at 1 and 2 weeks after fracture with virtually no bone detected distal to the fracture line. While the irradiated bones still healed through endochondral and intramembranous ossifications at the proximal side, albeit at a much less robust level compared to control, only cells with fibrotic morphology were detected at the distal side. Those cells failed to express osteogenic (osterix and osteocalcin) or chondrogenic (Sox9 and type 2 Collagen) markers. They also did not express VEGF with no vessel infiltra- tion and no osteoclasts in the area. By 4 weeks, the bony callus at the proximal side draped over the fibrotic tissue of the distal side but they never consolidated. This resulted in a nonunion in all irradiated bones (n=11 mice/group). Mechanical testing at 6 weeks confirmed a drastically decreased peak load (-86%), stiffness (-75%), and energy to failure (-73%). This location-dependent healing in irradiated bones demonstrated that both periosteum insult and the lack of surrounding vasculature are critical elements for fracture nonunion. Furthermore, we establish a highly reliable, nonsurgical, and clini- cally relevant nonunion fracture model in mice for future studies of mechanisms and treatments of this disease.

P78

Atypical femoral fracture in autosomal dominant type II osteopetrosis. Kyu Hyun Yang*, Young Chang Park, Xuan Lin Zheng, Hyun Soo Moon. Yonsei University, Korea, Republic of

Background osteopeterosis is a heterogeneous group of heritable conditions involve a defect in bone resorption by osteoclasts. We observed three cases of subtrochanteric fractures in two patients with autosomal dominant type II osteopetrosis, and treated them surgically. Although the report from ASBMR task team excluded femoral fracture in patient with metabolic bone disease in defining atypical femoral fracture (AFF), clinical and radio- graphic features of osteopetrotic subtrochanteric fractures (OSF) resemble those of AFF. Result We reviewed two OSF patients who had been transferred to our hospital with history of trivial falls. Radiographs of these patients showed generally dense, sclerotic bone features, in addition to narrow medullary canal and thickening of lateral femoral cortex. Fracture pattern was unique as it consisted of transverse fractures without comminution, and beak-like callus formation in the lateral cortex. Both patients were treated with surgical intervention according to the treatment protocol of AFF. Patient 1 (26-year-old male) diagnosed with left OSF, was treated with closed reduction and internal fixation using a femoral nail (Fig.1-a,b). Patient 2 (70-year-old female) was diagnosed with right complete OSF, as well as contralateral incomplete OSF. Both femora had grade II anterolateral femoral bowing. Prophylactic IM nailing was performed for the left side, while open reduction and internal fixation with a locking plate was needed for the right side (Fig.1-c,d). Discussion AFF has been suggested to occur due to prolonged, decreased remodeling of the bone. It is known to cause bone brittleness as well as accumulation of microfracture in the femur, especially in the lateral cortex. In the context of pathogenesis, osteopetrosis has the same pathomechanism as AFF, due to defect in osteoclast function. We treated two osteopetrosis patients according to AFF treatment protocol, and covered the full length of their femur with IM nail or plate. IM nailing was quite difficult, due to hardness of bone and narrow medullary canal. As a result, we developed a reaming technique that was useful for this situation. Deformity of medullary canal is a main contraindication of IM nailing. However, IM nailing can be a treatment of choice in special conditions, such as osteogenesis imperfecta, AFF with excessive anterolateral femoral bowing, and osteopetrosis. Conclusion We recommend including OSF in the definition of AFF and treating it accordingly.

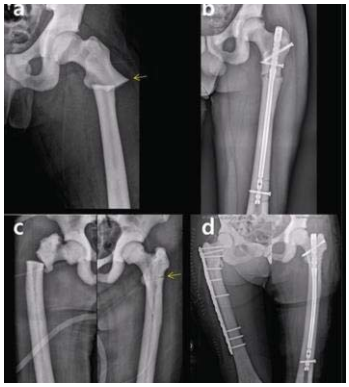

P79

Increasing Muscle Mass by GDF Ligand Trap Treatment Improves Bone Geometry in a Mouse Model of Severe Osteogenesis Imperfecta. Josephine T. Tauer*, Frank Rauch. Shriners Hospital for Children - Montreal, Canada

Objective: Osteogenesis imperfecta (OI) is mainly characterized by bone fragility but also by reduced muscle mass and function. Muscle mass and bone mass are closely linked, wherefore an intervention that increases muscle mass should also increase bone mass. Here we investigated the effect of a novel GDF ligand trap (Acceleron Pharma) on skeletal mu cle mass and bone properties in a mouse model of severe dominant OI, the Col1a1Jrt/+ Methods: Starting at an age of 8 weeks, GDF ligand trap (3 mg or 10 mg per kg body mass) or vehicle was injected subcutaneously twice per week for 4 weeks into male OI and wild-type (WT) mice.

Results: At baseline, OI mice had 20% lower body mass than control littermates. This difference persisted during the intervention as WT and OI cohorts exhibited a similar dose-dependent increase in body mass during GDF ligand trap treatment. Injections of GDF ligand trap led to a dose-dependent increase in muscle mass of quadriceps and gastrocnemius in WT and OI cohorts (Figure 1). In WT, GDF ligand trap also increased soleus weights (by 19 % and 26 %) and EDL weights (by 26 % and 73 %) in a dose- dependent manner. In OI cohorts, GDF ligand trap increased soleus and EDL weights as well, but both dosages almost to the same extent. GDF ligand trap injections had no effect on heart muscle mass or liver mass. Concerning bone unit, GDF ligand trap had no effect on femoral length in WT and OI mice but improved trabecular bone volume in the distal femoral metaphysis of WT mice (Figure 1).
However, GDF ligand trap treatment resulted in a significantly increased mid-diaphyseal periosteal diameter in OI mice only (Figure 1), leading to an improved polar moment of inertia. Conclusion: GDF ligand trap increases muscle mass and seem to improve diaphyseal bone geometry in a model of severe OI, representing a new therapy option for severe OI.

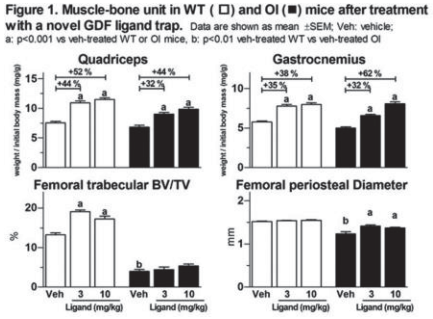

Figure 1. Muscle-bone unit in WT (□) and OI (■) mice after treatment with a novel GDF ligand trap. Data are shown as mean ±SEM; Veh: vehicle; a: p<0.001 vs veh-treated WT or OI mice, b: p<0.01 veh-treated WT vs veh-treated OI

P80

Distinctive Impact of Peak Jump Power on the 3D Geometry of the Proximal Femur assessed by Asynchronous Quantitative Computed Tomography in Elderly. Namki Hong*[1], Chang Oh Kim[2], Yoosik Youm[3], Hyeon Chang Kim[4], Yumie Rhee[1]. [1]Department of Internal Medicine, Severance Hospital, Endocrine Research Institute, Yonsei University College of Medicine, Korea, Republic of, [2]Division of Geriatrics, Department of Internal Medicine, Severance Hospital, Yonsei University College of Medicine, Korea, Republic of, [3]Department of Sociology, Yonsei University College of Social Sciences, Korea, Republic of, [4]Department of Preventive Medicine, Yonsei University College of Medicine, Korea, Republic of

Physical activity and weight-bearing exercise is associated with low hip fracture risk, affecting bone mineral density (BMD) as well as bone geometry of hip via localized bone adaptation. Countermovement jump power has emerged as a reliable assessment for muscle function, which demonstrated positive correlation with tibial bone geometry. However, it remains unclear whether the peak jump power is independently associated with BMD and geometry of the proximal femur in elderly. Among 548 participants enrolled in Korean Urban Rural Elderly cohort in 2016, 534 subjects underwent computed tomography scan at pelvis and jumping mechanography test. Peak jump power relative to body mass (W/kg), volumetric BMD (vBMD) and bone geometry parameters of proximal femur, and mid-thigh muscle cross-sectional area (CSA) were measured. Subjects who could not jump due to muscle weakness, joint pain, recent fractures or surgery were grouped as non-jumpers as the most frail group. Compared with subjects with higher jump power (N=224; sex-specific median, 27.5 W/kg for men and 20.3 W/kg for women), non-jumpers (N=86) had older age (75.6 vs. 73.4 years),

higher prevalence of women (80.2 vs. 64.3%), lower thigh muscle CSA (82.9 vs. 100.9cm2), more falls within last year (37.2 vs. 18.3%), and lower participation to moderate to vigorous physical activity (17.5 vs. 34.9%, P<0.05 for all). After adjustment for age, sex, height, and thigh muscle CSA, non-jumpers had significantly lower total hip vBMD (adjusted mean 240.8 vs. 254.1 mg/cm3), lower femur neck vBMD (252.3 vs. 266.7 mg/cm3) particularly at superior posterior quadrant (inte- gral vBMD
120.2 vs. 131.6 mg/cm3), and higher buckling ratio (BR, 14.2 vs. 12.5, P<0.05 for all) compared to high jumpers. Among subjects who jumped (N=448), higher jump power (per 1 standard deviation increase, 5.8 W/kg) was robustly associated with greater integral vBMD (b=5.38, P=0.009) and cortical thickness (b=0.06, P=0.010) at superior posterior quadrant of femur neck, whereas the association was attenuated at other quadrants after adjustment for age, sex, height, thigh muscle CSA, regular exer- cise, and serum bone turnover markers. In conclusion, peak jump power was positively associated with vBMD and cortical thickness of femur neck, particularly at superior posterior quadrant, independent of age, sex, height, and lower extremity muscle mass in community-dwelling elderly, suggesting the localized interplay between lower extremity muscle and bone.